HYDROLOGICAL MODEL STUDY IN YUVACIK DAM BASIN BY USING GIS
ANALYSIS

A THESIS SUBMITTED TO
THE GRADUATE SCHOOL OF NATURAL AND APPLIED SCIENCES
OF
MIDDLE EAST TECHNICAL UNIVERSITY

BY

FATİH KESKİN

IN PARTIAL FULFILLMENT OF THE REQUIREMENTS
FOR
THE DEGREE OF MASTER OF SCIENCE
IN
GEODETIC AND GEOGRAPHIC INFORMATION TECHNOLOGIES

FEBRUARY 2007

Approval of the Graduate School of Natural and Applied Sciences

_____

Prof. Dr. Canan Özgen
Director

I certify that this thesis satisfies all the requirements as a thesis for the degree of Master of Science.

_____

Assoc. Prof. Dr. Şebnem DÜZGÜN
Head of Department

This is to certify that we have read this thesis and that in our opinion it is fully adequate, in scope and quality, as a thesis for the degree of Master of Science.

_____   _____

Assist. Prof. Dr. Zuhal Akyürek   Prof. Dr. Ali Ünal Şorman
Co-Supervisor   Supervisor

Examining Committee Members

Prof. Dr. Vedat TOPRAK(Chairman) (METU, GEO) _____

Prof. Dr. Ali Ünal Şorman   (METU, CE) _____

Assist. Prof. Dr. Zuhal Akyürek   (METU, CE) _____

Assist. Prof. Dr. Ayşegül AKSOY   (METU, ENVE)_____

Dr. Murat A. HATİPOĞLU   (DSI, CE) _____

I hereby declare that all information in this document has been obtained and presented in accordance with academic rules and ethical conduct. I also declare that, as required by these rules and conduct, I have fully cited and referenced all material and results that are not original to this work.

Name, Last name: Fatih Keskin

Signature:

ABSTRACT

HYDROLOGICAL MODEL STUDY IN YUVACIK DAM BASIN BY USING GIS ANALYSIS

Keskin, Fatih

M. S., Geodetic and Geographic Information Technologies

Supervisor: Prof. Dr. A. Ünal ŞORMAN

Co-supervisor: Assistant Prof. Dr. Zuhal AKYÜREK

February 2007, 163 pages

In this study, semi-distributed hydrological model studies were carried out with the Mike11 model in Yuvacık dam Basin. The basin with a drainage area of 257.8 km^2 is located in 12 km South East of Izmit city in Türkiye. The basin is divided into three sub-basins named as Kirazdere, Kazandere and Serindere where each sub-basin is represented by its own characteristics. The largest peaks of inflow were observed when the storm events occur due to both snowmelt and rain. Therefore, observed flows for the period of 2001-2006 were grouped as daily and hourly storm events according to the event types such as rainfall, snowmelt or mixed events. Rainfall-Runoff Model (NAM) module of the model was used for the simulation of daily snowmelt and rain on snow events and Unit Hydrograph Method (UHM) module was used for the simulation of hourly rainfall events.

A new methodology is suggested for the determination of Curve Number (CN) of the sub-basins by using the fractional area and topographic index values combined with hourly model simulations. The resulting CN values were used in the UHM module

and the suggested CN approach has been validated with the classical SCS-CN approach with GIS analysis.

As a result of the study, the parameters of each sub-basin are calibrated with hourly and daily model simulations. The resulting flows are compared with the observed flows where model efficiency is tested with visual and statistical evaluations. The modeling studies give promising results for the computation of runoff during different seasons of a year.

Keywords: Mike11, Hydrological Model, Curve Number, Topographic Index, GIS

ÖZ

YUVACIK BARAJI HAVZASINDA CBS ANALİZİ İLE HİDROLOJİK MODEL ÇALIŞMASI

Keskin, Fatih

Yüksek Lisans, Jeodezi ve Cografi Bilgi Teknolojileri

Tez Yöneticisi: Prof. Dr. A. Ünal ŞORMAN

Ortak Tez Yöneticisi: Yrd. Doç. Dr. Zuhal AKYÜREK

Şubat 2007, 163 Sayfa

Bu çalışmada, Yuvacık baraj havzasında Mike11 modeli kullanılarak yarı dağıtımlı hidrolojik model çalışmaları yapılmıştır. Havza 257.8 km^2 dreanaj alanı ile Izmit ilinin 12 km güney doğusunda yer almaktadır. Havza Kirazdere, Kazandere ve Serindere olmak üzere herbiri kendi karakteristikleri ile temsil edilen üç ana alt havzaya bölünmüştür. Havzada kaydedilen pik akımlar hem kar erimesi, hemde yağış olaylarından oluşmuş olup, 2001-2006 yılları arasındaki gözlenen akımlar günlük ve saatlik olaylar olarak iki gruba ayrılmıştır. Günlük kar erimesi ve kar üstü yağmur olayların benzetimleri için model programının NAM modülü, saatlik yağış olaylarının benzetimleri içinse UHM modülü kullanılmıştır.

Saatlik olayların alansal katılım ve topoğrafik indeks değerlerinin birlikte kullanımı ile havzada yeni bir eğri numarası bulma yöntemi önerilmiştir. Yeni bulunan eğri numaraları birim hidrograf modülünde kullanılmış ve klasik SCS-CN metodunun CBS analizi uygulanması ile doğrulanmıştır.

Çalışma sonucunda her alt havzanın parametreleri saatlik ve günlük olay benzetimleri ile kalibre edilmiştir. Benzetim sonucunda oluşan akımlar gerçekleşen akımlarla karşılaştırılmış olup, model sonuçları görsel ve istatistiksel olarak test edilmiştir. Model çalışmaları yılın değişik mevsimlerindeki akım hesabı için iyi sonuçlar vermiştir.

Anahtar Kelimeler: Mike11, Hidrolojik Model, Eğri Numarası, Topoğrafik Indeks, CBS

To my Father: İbrahim Keskin,

My Wife: Songül,

and

My son: Eren…

ACKNOWLEDGEMENTS

TABLE OF CONTENTS

LIST OF TABLES

LIST OF FIGURES

CHAPTER 1

INTRODUCTION

1.1. Importance of the study

Importance of water is increasing due to the high population growth and global warming in the World as well in Turkey. Moreover droughts or floods are being occurred in several parts of the country where there is no such evidence in the past. Therefore, basin and river management systems including hydrological modeling has become a very important issue in Turkey.

Mathematical models are widely used in the engineering problems to reflect what is in reality and give solutions by using advanced computer technology. Because of this, modeling is the most powerful tool while solving engineering problems. Hydrological models give more realistic solutions due to the latest development in technology. Hydrological models are very benefical, however in reality most of the hydrological models have many parameters and those parameters must be adjusted for good simulation.

On the other hand another factor which affects the relation between Rainfall-Runoff (RR) is the prediction of the rainfall intensity and duration. Studies showed that the most of the observed rainfall can not be predicted correctly by current prediction models. Besides in current models, the large area and global values decrease the efficiency of the model. The application of the model to a smaller area could increase the efficiency by using special characteristics of the area. For an effective application of a hydrological model rainfall temporal and spatial information about rainfall is needed for the basin. The raingauges by recording the rainfall for an exact point can not represent the spatial distribution of rainfall. The accuracy of the data increases when the areal rainfall data accuracy increases.

1.2. Aim of the study

In this study it is aimed to determine parameters for a relationship between rainfall and runoff with help of Geographical Information Systems (GIS) and hydrological modeling software. Also a new methodology is suggested to determine the Curve Number (CN) of the basin by GIS analysis and model simulations, where CN is an important parameter to define the Rainfall-Runoff (RR) relationship.

An application of a RR model, namely Mike11 with NAM module and UHM module, are performed in Yuvacık Dam basin to determine basin parameters for the relationship between rainfall and runoff. The optimum operation of the dam reservoir is required in terms of effective usage of water, the optimum operation methodology is especially important for the periods of high (flood) and low (drought) flow conditions as the low water level was observed in 2006.

The lumped rainfall-runoff models are designed to compute values from areal averages of input data, such as areal average of rainfall. The model used in this study, NAM rainfall-runoff module of Mike11 modeling system is a deterministic, semi-distributed hydrological model of the rainfall-runoff process. It is based on both physical and semi-empirical formulations to describe the inter-relationships between surface flow, groundwater and snow storage.

In this study Yuvacık dam basin, which is in the eastern part of Marmara Region of Turkey at about 40°32´-40º41´North and 29º29´-30º08´ East and located 12 km south of Izmit city is selected. The drainage area of Yuvacık Dam basin is about 257.8 km^2. In the north of the basin exist a dam called Yuvacık dam or with its old name Kirazdere dam (DSI, 1983).Yuvacık dam which is used for domestic water supply for the Izmit city and flood control was built in 1999. Total annual water demand of the dam is about 145 million cubic meters where storage volume of the dam being 54 million cubic meters is about 1/3 of the total annual demand. Therefore the effective modeling of the runoff is needed for the optimum operation of the reservoir to provide the demand of the city when the supply is insufficient. The dam is operated

by Thames Water Turkiye (TWT) which is the branch of one of the biggest water company in United Kingdom.

1.3. Data and software used in the study

The rainfall and runoff data for the basin was obtained from TWT. Digital Elevation Model (DEM) of the study area is obtained from the 1:25.000 scaled topographic maps, which were obtained from General Directorate of State Hydraulic Works (DSI). The precipitation and temperature data in and near the basin were obtained from General Directorate of Meteorological Organization (DMI). In addition to that, data about precipitation and temperature stations operated by DSI were added to those obtained from DMI in order to include important rainfall events.

In this study, ArcGIS software of Environmental Systems Research Institute (ESRI) is used as the main GIS software. For the Hydrological modelling Mike11 Model of Danish Hydraulic Institute (DHI) with NAM and UHM module is used. Besides that, ArcGIS Hydro Data Model (ArcHydro) is used for delineation of the river network and drainage basins.

The subjects described in the following chapters are briefly reviewed below:

In Chapter 2, general information about hydrologic models with their classification and a detailed literature review are presented. Also a short summary of GIS related with hydrological applications is given.

In Chapter 3, study area with the hydrometric and meteorological data network is described. The surface characteristics (topography, vegetal cover, landuse, soil and geology) of the basin are produced. So in addition to the hydrometeorological data the surface information of the basin is obtained and determination steps of basin characteristics are given.

In Chapter 4, the detailed explanation of the hydrological model that are used in this study is given. The model extend with its calibration is identified and then the parameters of the model are presented following the input requirements of the model.

In Chapter 5, a new methodology for determining the curve number of the basin by the help of GIS analysis is suggested. The CN values found by the new methodology are tested by the CN values found with classical methods.

In Chapter 6, example model runs and their implementations on the study run are given. At the end of this chapter parameters of the basin are determined and sample graphs are given as comparison of observed with simulated hydrographs.

In the last chapter, Chapter 7, the conclusions of the study and recommendations for the future studies are given.

CHAPTER 2

LITERATURE REVIEW

2.1. General

The definition of the relationship between RR is a very important and difficult subject in hydrology. Many methods have been developed for estimating the runoff from rainfall. For the estimation of runoff at basin outlets, we have mainly three model types. These models are empirical models, conceptual models and physical models. Other then these, lumped and distributed parameter models are used to adapt these models to computerized applications with respect to lumped or distributed parameter inputs. In this chapter, short description of previously developed models related with RR relationship and integration of GIS with hydrological models is presented.

In this study a semi-distributed model, Mike 11 is used as the hydrological model. Lumped and distributed parameter models are used to represent the hydrological events with some approaches and assumptions. They are aimed to represent discharge or runoff using the parameters related with climatic, morphologic and land use situation of the corresponding basin. Both of them have certain advantages and disadvantages.

Lumped Parameter Models take the averages of the related variables over catchment areas and use them to produce the discharge or runoff, like hydrologic process occurs at one point. Distributed parameter models use spatial variability of the variables and compute the flow from one cell to another. The parameters are assumed the same in the whole basin that is in interest.

Some hydrologists applied only hydrological models for RR relationship; others applied coupled meteorological – hydrological models for RR relationship.

Einfalt et al. (2004) has installed a hydrological modeling of flood forecasting system in Turkey. The system was installed in four basins of Turkey. These are West Black Sea, Susurluk, Gediz, and Büyük Menderes Basins. The model consists of two forecasting models. One is atmospheric model and the other is the hydrological model. The atmospheric model is named as "Scout" and operates with Numerical Weather Prediction (NWP) data, radar data, and raingauge data. Mike11 is used as the hydrological model which is also the model that is used in this study. Scout makes forecast for the rainfall over each basin and hydrological model uses these rainfall forecast as an input and forecast for the runoff in the river system of each basin up to 48 hours.

Snowmelt is very important in the RR relationship especially where snow is a dominant factor in the runoff. Generally many models are good for the estimation of runoff but not for simulating the snowmelt and rain on snow events. The representation of accumulation and melting of snow is the main part of modeling. Many models were developed for the estimation of snowmelt in the models.

Luce et al. (2004) studied spatial variability in snow accumulation and melt due to topographic effects on solar radiation, drifting, air temperature, and precipitation which is the main factor for the study of RR models where snow has big effect over the study area. Distributed and lumped snow pack models were used to examine the ability of simplified representations of spatial variability in topography and drifting to estimate surface water input. They have found that in semi-arid mountainous watersheds, wind plays a large role in redistributing snow, and the spatial variability and pattern of snow water equivalent is highly dependent upon wind induced drifting. Drifting results in delayed surface water inputs and sustains melt into late spring. They also highlighted that the point that incorporating detailed drifting

information, which may be difficult to obtain, is perhaps of greater or equal importance than modeling the effects of local topography on radiation.

Kuntsmann and Stadler (2005) coupled high resolution meteorological-hydrological simulations for alpine catchment of the river Mangfall and its subcatchments. The hydrological model was calibrated to reproduce the observed runoff at the outlets of the 18 subcatchments. During this study a height dependent bias between station-based and MM5(Mesoscale Modeling 5) based simulation was observed. The MM5-based interpolation of precipitation yielded 21% less total yearly precipitation in the catchment compared to the station based-based interpolation. Even when not all details of observed runoff were met by the coupled meteorological-hydrological simulations, in general observed runoff was reproduced reasonable. The results justified that the water balance and the runoff behavior of many catchments can be described satisfactorily by coupled simulations.

Quinn et al. (2005) made a study to examine the effect of scale incompatibility between soil information and the detailed digital terrain data and remotely sensed information by comparing simulations of watershed processes based on the conventional soil map and those simulations based on detailed soil information across different simulation scales. He had studied two modeling approaches which are the lumped parameter approach and the distributed parameter approach. The study showed that operating the watershed models at scales approaching those of the soil data layers reduces bias in model predictions. The scale of the soil property data, which is often converted from polygon-model soil surveys, can be assessed using a frequency distribution of soil patches—contiguous areas of pixels sharing the same property value. Modeling at scales that are much smaller or much larger than model soil patch sizes could introduce errors due to the scale incompatibility between soil data and other detailed environmental data (such as digital terrain data and remotely sensed data). The study also showed that the distributed parameterization scheme may reduce the degree of effect on model results due to scale incompatibility between conventional soil map and other detailed environmental data layers.

However, the change in pattern of the effect across model simulation scale is very similar to that under the lumped parameterization scheme.

For the determination of the rainfall, not only the intensity and duration of the rainfall is in interest but also the spatial variability of the rainfall. The meteorological radar data is good for showing the spatial distribution of the rainfall. Radar data can be used in nowcasting purposes because the accuracy of radar data goes up to next 1 hour. In Turkey there are 4 radar stations which are located in Ankara, Balıkesir, Zonguldak and Istanbul. Many models have been applied for the use of radar data and rainfall in many regions.

Andrieu et al. (1997) studied the effect of the mountainous area in rainfall radar measurement. The data is from an experiment in the Mediterranean Sea region. In addition to radar data, some other ground measurements were recorded. These are rainfall rate from 49 network stations, drop size distribution data, temperature, pressure, humidity, and wind data from two stations. The output of the study concluded that the knowledge of topography which is taken from DEM is very useful and the use of S-Band weather radar was recommended for the accuracy of rainfall measurement, wind field measurement by means of Doppler radar could lead to an improvement.

Jensen and Pedersen (2005) have installed nine high-resolution optical rain gauges Radars grid cells of 500 by 500 m size to determining the spatial variability in the precipitation. The nine rain gauges were placed in the centre of one ninth of the grid cell. The gauges were not equipped with a heating device and are only capable of measuring precipitation in the state of water. The results of the study concluded that it is difficult to establish a relation between radar measurements and raingauge measurements. Also the study concluded that a very high density of rain gauges is required for establishing a reliable boundary condition for run-off modeling for fast response catchments.

Gorokhovich and Villarini (2005) made a study for finding the correlation between weather radar reflectivity and precipitation with a database of 82 radar stations and more than 1500 rain gauges in continental USA. Rainfall data from multiple gauges within the radar zone of 230 km were extracted and combined with corresponding reflectivity values for each time interval of the selected rain event. Statistical analysis for the potential correlation showed a strong correlation between rainfall values from rain gauges data and radar reflectivity values.

Some of the hydrological modeling and studies have been carried in the past with or without atmospheric modeling by using the same hydrological model that was used in this study..

Buffo and Gonella (1999) had used the model to simulate the flood events on the whole Piemonte region (Italy) which is about 70000 km^2 in size. They got good results for the simulation of RR in the basin. The results of this study were used for realtime flood forecasting in the basin.

Demir (2001) had applied the model in Sohu Basin (Turkey) for the simulation of RR. In his study there were no snow measurements in Sohu basin so he was not able to test the model in snowmelt conditions.

Usul et al. (2001) had used the model and its GIS module to generate the flood inundation maps in Ulus basin (Turkey). They have showed that the model can be used safely for the preparation of flood inundation maps.

In all of the above studies which were done with the same hydrological model, none of the advanced snow ablation and melting components and parameters has been used, so this study is the first one that is done to simulate especially the snowmelt and its effects on runoff in Turkey where the simulations are verified with real snow measurements.

Soil Conservation Service curve number (SCS-CN) method is another method to define the relationship between RR. It was developed by United States Soil Conservation Service (SCS, 1975) and widely used in hydrology and basin management. The Soil Conservation Service curve number (SCS-CN) method (SCS, 1956, 1964, 1971, 1985) is one of the most used methods for computing the volume of surface runoff for a given rainfall event from small agricultural, forest and urban watersheds (Mishra and Singh, 2004). It works with the characteristics of the basin of which soil types, land use and soil moisture have been defined. Several studies have been carried on the SCS Curve Number Method in the past. It is of common experience that the SCS-CN method performs best on agricultural watersheds, for which it was originally developed, and on urban watersheds; fairly on range sites; and poorly on forest sites (Hawkins and Ponce, 1996). The natural variability due to soil moisture is widely recognized through the Antecedent Moisture Condition (AMC) identified in the hydrologic literature (Jain et al, 2006).

The original model was justified by Victor Mockus, to whom the traditional SCS-CN method is largely attributed, 'on grounds that it produces rainfall–runoff curves of a type found on natural watersheds' (Rallison, 1980).

There have been many studies on SCS-CN method. For example, Hawkins and Ponce (1996) critically examined this method; clarified its conceptual and empirical basis; delineated its capabilities, limitations, and uses; and identified areas of research in the SCS-CN method (Mishra and Singh, 2004). Yu (1998) derived the SCS-CN method analytically assuming the exponential distribution for the spatial variation of the infiltration capacity and the temporal variation of the rainfall rate. Mishra and Singh (1999a) derived it from the Mockus (1949) method and Mishra and Singh (1999b) described its behavior using the initial abstraction.

Hjelmfelt (1991), Hawkins (1993) and Bonta (1997) suggested procedures to determining curve numbers using field data of storm rainfall and runoff. Grove et al.

(1998) and Moglen (2000) discussed the effect of spatial variability of CN on the computed runoff.

The formation of the Unit Hydrograph is very important where unit hydrograph is used in the hydrological simulations. The unit hydrograph theory approximates the catchment response with that of a linear system. The unit hydrograph (UH) is thus the direct runoff hydrograph resulting from a unit depth of excess rainfall at a constant rate for a given (small) time step and occurring uniformly over the catchment. Hydrographs originated from an event are obtained through the convolution of the excess rainfall hyetograph with the unit hydrograph. There are well known lumped UH models: SCS, Clark, Snyder (Chow et al., 1988).

2.2. GIS in hydrology

A hydrological model is a simplified simulation of the complex hydrological system. The major problem in modeling the hydrological processes based on their physical governing laws is the variability in space and time of the parameters that control these processes (Porter and McMahon, 1971). In the first generation of hydrological models this has been dealt with by assuming homogeneous properties for the hydrological processes over the whole catchment area or, in the best cases, for subdivisions of the catchment area (Moore et al, 1993).

Over the last twenty years the need for hydrological models has shifted from generating stream flow hydrographs into predicting the effects on water resources of the actual land use practices (Abott et al, 1986) or the need to estimate the distributed surface and subsurface flows (Moore et al, 1993). These needs require better description of the catchment topography and the distributed properties of the hydrological processes acting on it.

The emergence of remote sensing techniques as potential sources of data of the hydrological processes and the improved capabilities of generating and processing, GIS techniques have gained a prominent role in hydrological modeling. This role has

developed from the traditional use of GIS as an interface to the hydrological models for pre-processing and post processing of data into "rethinking hydrological models in spatial terms so that better GIS-based hydrological models can be created" (Maidment, 1993).

The capability of GIS has lead the modeling in hydrology to have new opportunities with the detailed information supplied by GIS analysis. Use of GIS in hydrology is a developing sector which can really help and ease the application of hydrological models. GIS in hydrology is comprehensively used to form the drainage areas from DEM or Triangular Irregular Network (TIN) for any given location. Even new GIS programs have built in components to delineate the basin and form base for further applications such as ArcHydro of ArcGIS (ESRI, 2005). Also it is possible to generate the slope, river networks, and aspect map or calculate the hydraulic length by GIS easily. Furthermore, estimation of lumped catchment characteristics with GIS by using spatial variability, dividing the basin into catchments and use of these inputs in distributed modeling can be given as an example.

As Berry and Sailor, (1987) mentioned, the new technologies do not take place of the conventional methods but they increase the precision and speed of calculations. Even they help to test every possible effect on the simulations with repeated iterative calculations.

There are many hydrological studies which use GIS analysis. Some examples from world are given below;

Maidment (1993) proposed to use the raster-based GIS to derive a spatially distributed unit hydrograph using the time-area diagram method. In the method the flow direction is defined after creating DEM. With calculating the flow velocity for each cell, travel time can be easily calculated. In one of his other study (Maidment, 1996), he tried to obtain a new hydrological model by integrating the GIS spatial data management capabilities.

Nowadays, many hydrological models use GIS techniques and RS technology to determine the parameters of the basin. The scientists must be careful when using the GIS techniques in the models. The techniques make our work so easy, but also they can make our work harder. The scientists must know the effect of the error in the application due to GIS techniques.

Wang and Yong (1998) studied the SCS-CN method by integrating the GIS Analysis by using the soil and landuse map to produce the CN map. For representation of the spatial variation of soil and landuse, he had used polygon shape files for analysis instead of raster grid. They had showed that spatial variation of the CN can be easily shown by GIS integration.

Grove et al. (1998) used CN method for predicting the runoff by GIS analysis. In this study, they had used distributed CN where area weighted average of all CN values is calculated for a basin and they had shown that significant errors in runoff estimates can occur when composite rather than distributed CN values are used.

Wang and Yin (1998) studied the comparison of drainage networks derived from digital elevation models at two different scales, using various drainage parameters common in hydrology and geomorphology. The study was applied to 20 basins in West Virginia. The study concluded the following items. It was found that the general shape and even some of the details of the 1/24000 and 1/250000 DEM-derived drainage networks seemed to match closely to the 1/100000 validation networks and the deficiencies of the 1/250000 DEM-derived networks are as a result of reduced spatial and vertical resolutions. The study indicated that the 1/250000 DEMs tended to underestimate consistently all of the gradient measures. It was suggested that the rate of improvement for the estimates from the 1/24000 DEMs was greater compared with the 1/250000 DEMs.

Raaflaub and Collins (2005) studied the effect of error in gridded digital elevation models on the estimation of topographic parameters. The DEM used in this study was taken from a series of gridded DEMs provided by the province of Alberta, Canada. Depending on the roughness of the terrain, the DEMs were originally derived from aerial photographs at spacing of 25 m, 50 m, or 100 m. The effect of both correlated and uncorrelated gridded DEM data error is investigated using Monte Carlo methods. The DEM is used in slope, aspect, topographic index generation. The results showed that both slope and aspect error sensitivity was significantly smaller in the presence of correlated DEM error than for uncorrelated DEM error. All algorithms produced slope estimates that were equally sensitive to correlated error, while the aspect error sensitivity mirrored that for uncorrelated error. The steepest neighbor principle is more dependent on the slope value. Errors in the topographic index are largest for the algorithms based on the steepest neighbor principle.

Silberstein (2006) made a study for showing the importance of collecting data. He wanted to show that as modeling power has increased there has been a concurrent reduction in "data power", particularly in the collection of hydrological data. He had discussed the growth in sophistication of hydrological modeling through the last hundred years. He had argued that modeling in the absence of adequate data is not science, unless it is to develop hypotheses that are to be tested by observation. He had concluded that modeling is an important accompaniment to measurement, but is no substitute for it; science requires observation, and without that we will cease to progress in understanding our environment, and therefore in managing it appropriately.

Several studies, recently were also, done which integrating GIS techniques with hydrological modeling in Water Resources Laboratory of Department of Civil Engineering at METU. In two of the studies, hydrological model and GIS is used together to form flood inundation maps. Another one used Watershed Modeling System (WMS) model with GIS (Şensoy et al., 2000) to model Karasu basin. Şorman (1999) applied CN method by GIS analysis in Güvenç basin.

Yener (2006) made a hydrological modeling study in Yuvacık dam basin by using HEC-HMS. As a result of modeling studies, infiltration loss and baseflow parameters of each subbasin are calibrated with both hourly and daily simulations. Observed runoffs are compared with the forecasted runoffs that are obtained using Mesoscale Modelling 5 (MM5) grid data (precipitation and temperature) in the model. He had concluded that the model can be used in real time runoff forecast studies by comparing forecasted and observed runoffs. At last, runoffs that correspond to different return periods and probable maximum precipitation are predicted using intensity-duration-frequency data as input and frequency storm method of HEC-HMS.

CHAPTER 3

STUDY AREA AND METHODOLOGY

3.1. Location of the study area

In this study Yuvacık dam basin is selected because of the data availability. Yuvacık dam basin with a drainage area of 257.8 km^2 is in the south eastern part of Marmara Region of Turkey at about 40°32´-40º41´North and 29º29´-30º08´ East and located 12 km south of İzmit city. In the north of the basin, yuvacık dam (Kirazdere dam) which was built in 1999 exists (DSI, 1983). The main objective of the reservoir operational strategy is to provide domestic water supply to the Izmit Great Municipality and to control the downstream flooding. Therefore the effective modeling of the runoff is needed for the optimum operation of the reservoir to provide the demand of the city when the supply is insufficient.

Yuvacık dam basin has four big catchments named as Kirazdere, Kazandere, Serindere and the contributing catchments. Serindere catchment has the largest area and Kazandere catchment has the smallest area. The catchments and dam lake is shown in Figure 3.1.
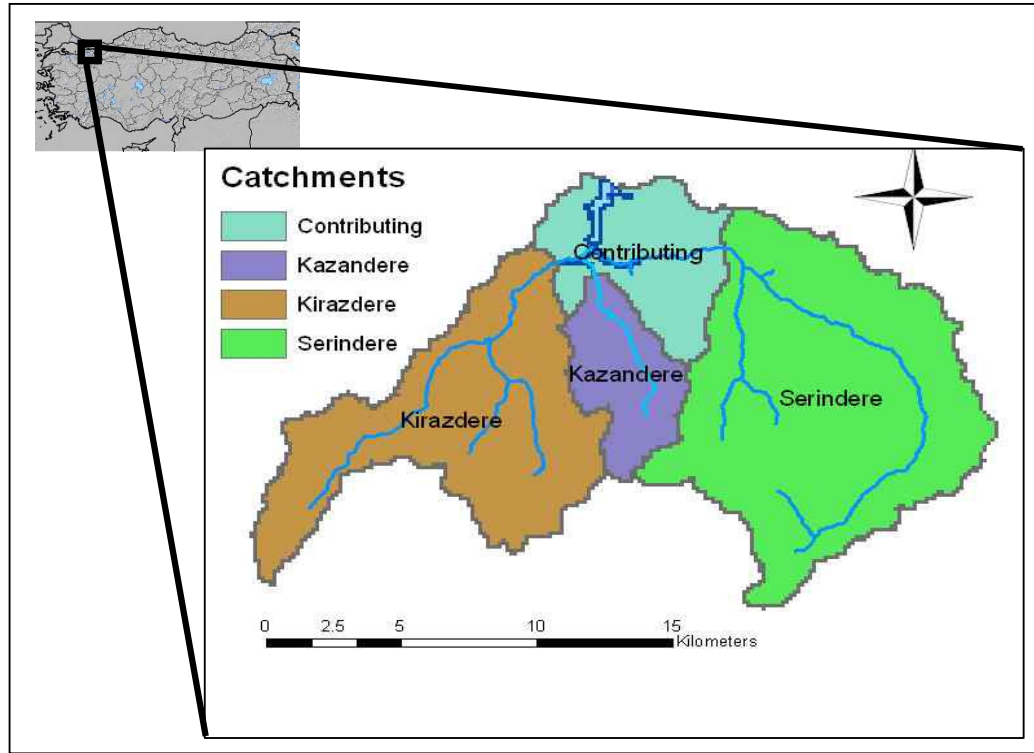
Figure 3.1. Yuvacık dam basin and its location in Turkey

3.2. Data collected for this study

Some of datasets used in this study obtained from the study of Zengin et al. (2005). Used datasets from their study are land use map, land capability map, soil map and geology map. The hydrometeorological network is shown in Figure 3.2. Most of the rainfall and discharge data are obtained from TWT. Also there are some hydrometeorological data which was obtained from DSI and DMI. The Digital Elevation Model (DEM) is produced from 1/25000 scaled topographic maps and all of the data layers are transformed into UTM-35N projection on ED-50 datum.

3.2.1. Hydrometeorological data

There are 15 meteorological stations and 4 discharge measurement stations in the basin. Some of the stations are old stations and some of them are newly installed in the basin. The old meteorological station network was not adequate to represent the spatial distribution of the rainfall over the basin because the locations of these

17

stations are very close to each other and the elevations of the available stations are limited to lower altitudes of the basin. The elevations of old rainfall measurement stations vary from 173 meters to 520 meters, the new elevation range of the upgraded network changes between 76 meters to 1487 meters which indicates a better representation of the spatial distribution of both rainfall and snowfall over the whole basin. The old six rain gages (RG1-RG6) were not equipped with any instrument to measure snow depths. Thus, new stations were recommended to be installed to measure temperature, rainfall and snow depth with new techniques and equipments. All of the available data from these stations were used in the modeling studies of the basin.

The oldest meteorological station in the area is the Kocaeli station (in operation since 1930's) which is operated by DMI. The data those are being recorded in this station are temperature, rainfall and snow depth. DSI operates a meteorological station in Hacıosman location (HO) which is in the basin and represents the basin. Rainfall and snow depth data have been recorded daily since 1980s at this station.

The discharge measurements have been done since 2001 at different locations in the basin (FP1 to FP4) in 5 minutes intervals, one of which is just at the entrance site of the reservoir lake located for the measurement of the lake level, and the other three are at the outlets of three sub-basins. Rainfall data were recorded since 2001 from different stations by TWT (RG1 to RG6) in 5 minutes intervals. Since the stations (RG1 to RG6) are recording stations and recording the data at 5 minutes time intervals, these data are converted to daily cumulative values which are used in the modeling.

Since the evaporation data were not available for the sites, the evaporation data of the nearby station were used with a proper elevation adjustment.

Table 3.1. Station information of Yuvacık basin

Organization *	Operation Start Year	Station ID	Station Name	Data Type **	Data Interval	Data Transmission ***	Elevation (m)
TWT	2001	FP1	Flow Plant 1	S	5 minutes	RF	185
TWT	2001	FP2	Flow Plant 2	S	5 minutes	RF	180
TWT	2001	FP3	Flow Plant 3	S	5 minutes	RF	200
TWT	2001	FP4	Flow Plant 4	S	5 minutes	RF	188
TWT	2001	RG1	Rain Gage 1	P	5 minutes	RF	188
TWT	2001	RG2	Rain Gage 2	P	5 minutes	RF	320
TWT	2001	RG3	Rain Gage 3	P	5 minutes	RF	460
TWT	2001	RG4	Rain Gage 4	P	5 minutes	RF	520
TWT	2001	RG5	Rain Gage 5	P	5 minutes	RF	265
TWT	2001	RG6	Rain Gage 6	P	5 minutes	RF	173
TWT	2006	RG7	Tepecik	P, SD, T, RH	5 minutes Daily	GSM	700
TWT	2006	RG8	Aytepe	P, SD, T, RH	5 minutes Daily	GSM	953
TWT	2006	RG9	Kartepe	P, SD, T, RH	5 minutes Daily	GSM	1487
TWT	2006	RG10	Çilekli	P, SD, T, RH	5 minutes Daily	GSM	805
TWT	2006	M1	Kazandere	P, SD, T, RH	5 minutes Daily	M	732
TWT	2006	M2	Menekşe Yaylası	P, SD, T, RH	5 minutes Daily	M	915
TWT	2006	M3	Arif Tarı	P, SD, T, RH	5 minutes Daily	M	546
DSI	1980s	HO	Hacıosman	P, SD	Daily	M	900
DMI	1930s	KE	Kocaeli	P, SD, T	Daily	M	76

* TWT: Thames Water Türkiye, DSI: State Hydraulic Works, DMI: State Meteorological Service
** S: streamflow depth, P: precipitation, SD: snow depth, T: temperature, RH: relative humidity
*** RF: Radio frequency, GSM: cellular phone communication network, M: Manual

At the end of 2005 seven "new stations" comprising of four "fixed" stations (RG7 to RG10) that transmit the collected data using GSM network, and three "mobile" stations (M1, M2, and M3) where the data is retrieved manually by a laptop in the field were installed. These seven stations started operation at the very beginning of 2006. In near future (at least after one water year), some of the "mobile" stations may be turned into "fixed" stations if they are found to be representative of the basin. Some of the "old stations" will be disassembled from their current places and moved out of the basin and reassembled in several of the northwest settlements like İzmit, Gölcük. These reassembled gages may be used to detect the storms coming from the

Balkans (northwest of Turkey) in order to take action before the storm reaches the basin. The location of the stations is given in Figure 3.2.
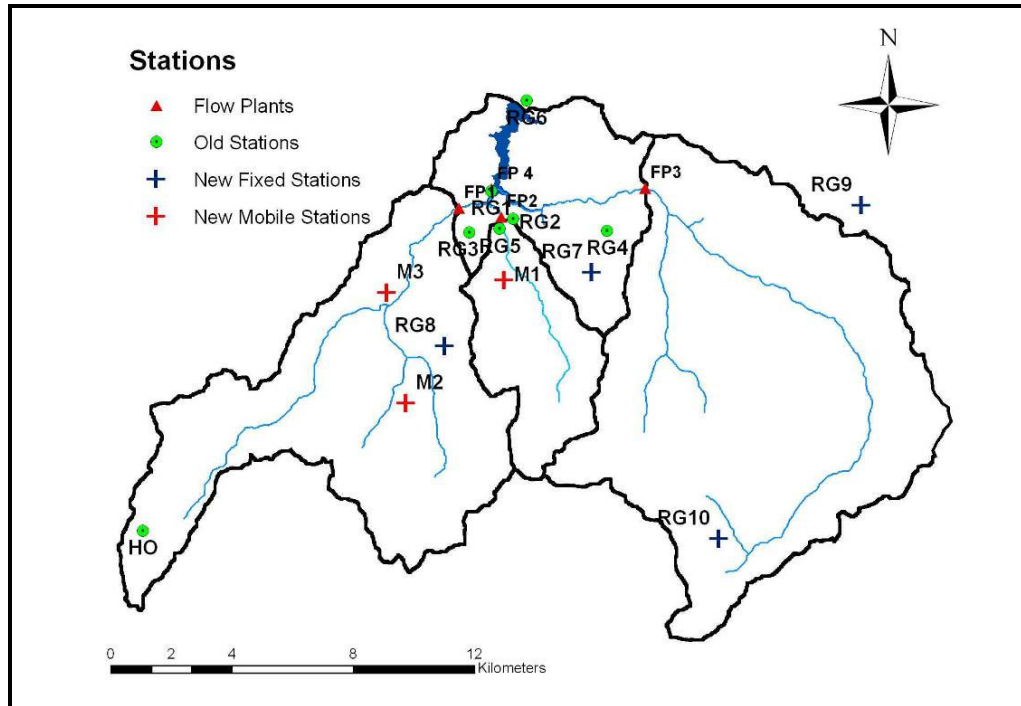
Figure 3.2. Discharge and meteorological stations in Yuvacık basin

3.2.2. Soil data

The soil map is so detailed where there is about 134 different sub-types of soil (Although their main soil type is same). Similarity analysis were tried to simplify the soil map into a more generalized one for ease of the use in the study, but the obtained results are not good. So the main soil groups are used for simplification of the soil map. The resulting map is shown in Figure 3.3. Also for the preparation of soil map 32 deep soil sample holes (max. 80 cm.) and 95 shallow soil sample holes were drilled by TWT. The soil map was formed from the information of the soil samples and from the air photos taken in 1994 with 1/35000 scale as black-white. The location of the soil samples in the basin is shown in Figure 3.4. The number of holes per catchments is shown in Table 3.2. As seen from Table 3.2, the number of holes in each catchment is changing with respect to the catchments area.

20
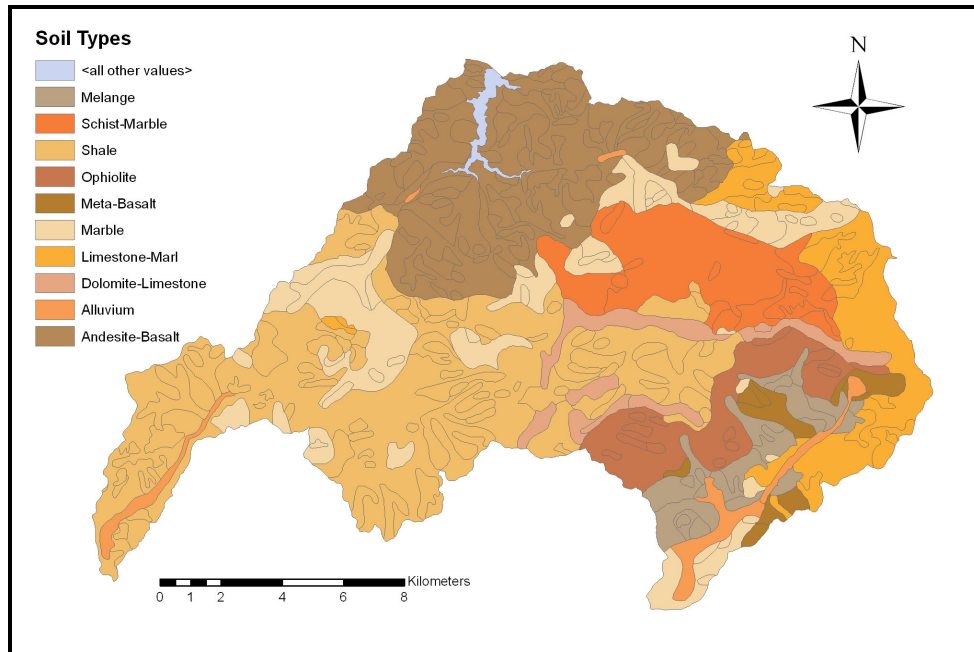
Figure 3.3. Soil map of Yuvacık basin
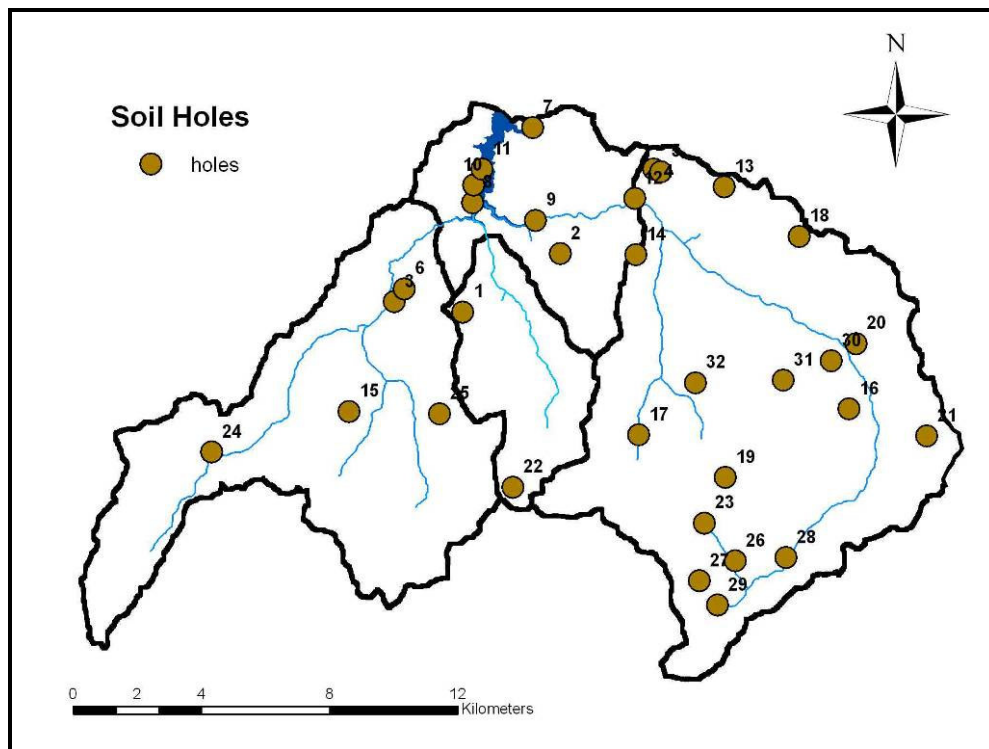
Figure 3.4. Soil sample locations in the catchments

Table 3.2. Number of drilled Soil sample holes in each catchment.

Catchment Name	Number of Holes
Kirazdere	5
Kazandere	2
Serindere	18
Contributing	7
Total	32

3.2.3. Land use data

The land use map is shown in Figure 3.5. The map is formed by the help of the air photos taken in 1994, 1970 and 1992. The summary of the map is shown in Table 3.3. As seen from the Table 3.3, 64.27% of the basin, which is the largest part, is covered by good forest. This also leads that evapotranspiration may be high in the basin. Also, the conversion of the precipitation to the surface runoff may be low and slow because the vegetation will slow down the surface flow, favor the infiltration. 7.31% of the basin is used as agricultural area and 13.68% of the basin is covered by bad forest. The meadow areas are about the 3.57% of the basin and the afforestation areas is about 0.5% of the basin. The lake of the dam covers 0.66% of the basin.
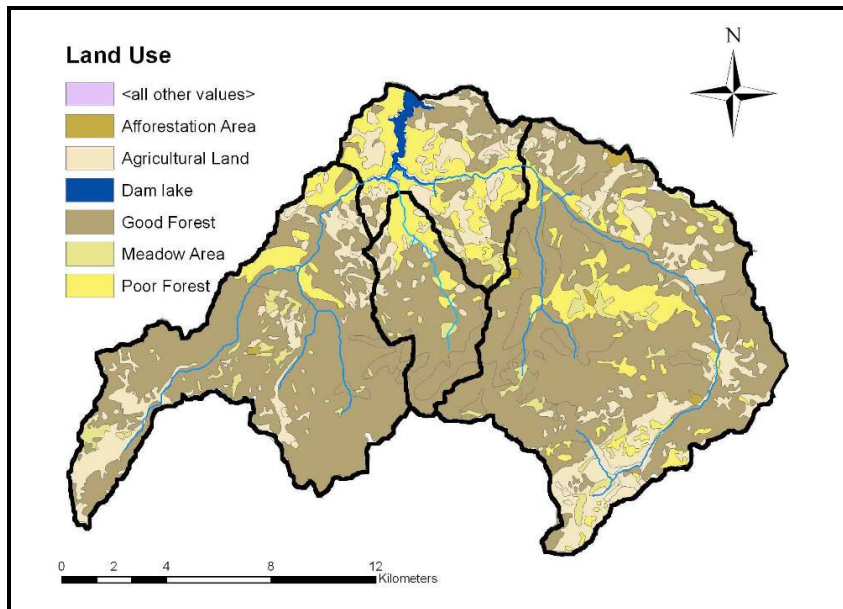
Figure 3.5. Land use map of Yuvacık basin

22

From this land use map, we can say that good forests are in the south part of the basin. Most of the agricultural areas are near the dam lake and in the places where the soil type is Alluvium. Bad forests are near the dam lake which is in the contributing catchment where there is too much settlement in nearby areas.

Table 3.3. Land use types and their areas within the basin

Land use classes	Area (km²)	Area (%)
Bad Forest	36.56	14.18
Good Forest	64.23	64.27
Agricultural Land	30.57	16.85
Meadow Areas	7.38	3.57
Afforestation Areas	1.21	0.47
Dam Lake	1.70	0.66
Total	**257.86**	**100.0**

3.2.4. Geology data

The geology map is obtained from the 1/25000 scaled geology map and by the help of land capability map, slope groups and soil map. The information about geological formations such as their areas with respect to the basin and their catchment is given in Table 3.4.
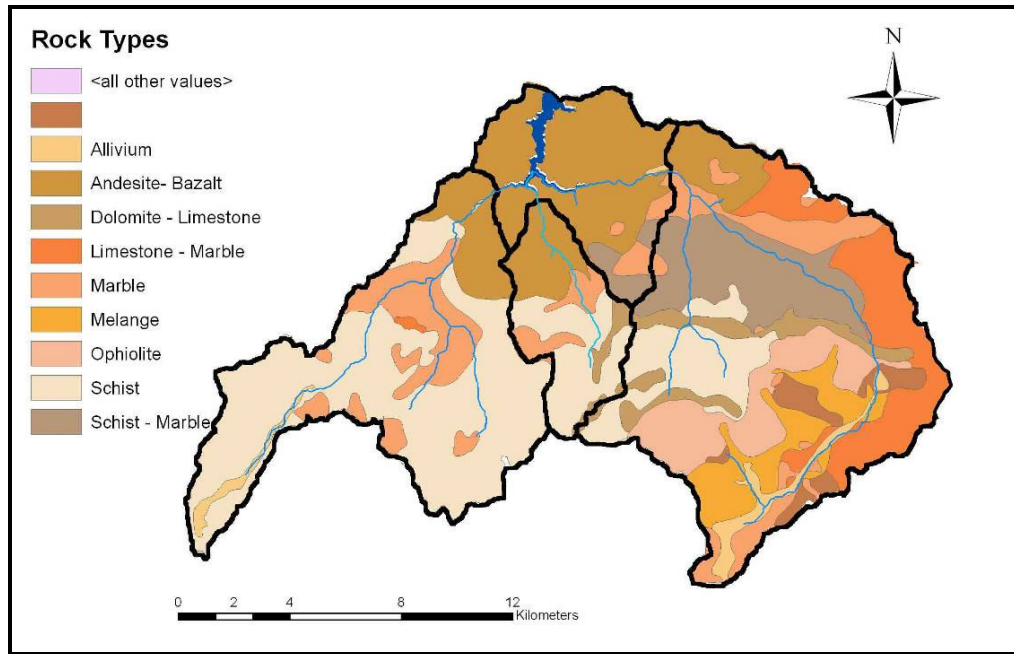
Figure 3.6. Main rock types map

Yuvacık Basin is mainly composed of shale (31% of the basin) and andesite and basalt rock types (20.38%). Also, there are a number of marble areas (14.2%) spread to different parts of the basin as shown in Figure 3.6.

Table 3.4. Yuvacık Basin main rock types and their areas

Geologic Formations	Area (km²)	Area (%)
Alluvium	5.89	2.28
Andesite-Basalt	52.56	20.38
Dolomite-Limestone	8.88	3.44
Limestone-Marl	23.19	8.99
Marble	36.63	14.20
Ophiolite	15.08	5.85
Melange	11.89	4.61
Shale	79.80	30.95
Schist-Marble	23.94	9.28
Total	**257.86**	**100.0**

3.2.5. DEM construction

The required digital contour map for DEM creation was obtained from DSI with scale of 1/25000. Estimation of elevations for each point of the defined grid is needed for the DEM construction. The gaps and unknown elevations which exist in the map sould be filled with estimated values for satisfying the needed desired solution. Here we can use the ability of spatial interpolation. There are several methods for interpolation used in GIS but Kriging is used in this study for the interpolation because it accounts for the spatial continuity inherent in the data set. Spatial continuity implies that two points located close together more likely have similar values than two separated points. Kriging differs from the more conventional methods, such as inverse distance to a power that uses a strictly mathematical expression to weight known points and estimate an unknown value. In other words, kriging utilizes the statistical, rather than geometrical, distance between points. Unlike ordinary interpolators, kriging also accounts for clustering of sample values by redistributing weights from neighboring clustered sample values to points farther a field but less redundant (Isaaks and Srivastava, 1989). The spatial resolution was selected as 10 m which is feasible for 1/25000 scale. The resulting DEM is visualized and shown in Figure 3.7.
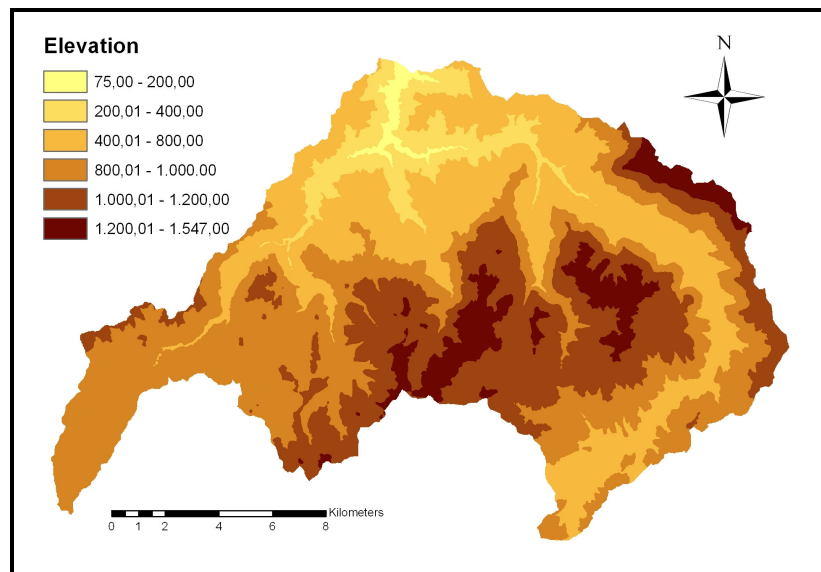
Figure 3.7. DEM of the Yuvacık basin

Yuvacık Basin is mainly composed of deep valleys originating in the south and with almost parallel flowing streams ending up in the north regions of the basin. There are three major valleys, and correspondingly, three major stream branches which can be named as Kirazdere, Kazandere, and Serindere, respectively from west to east of the basin. The northern parts of the basin (around the reservoir lake) have the smaller elevations than the southern parts as can be seen from the digital elevation model (DEM) of the basin (Figure 3.7). The minimum elevation of the basin is 75 meters, the maximum elevation is 1547 meters and the mean elevation is 848 meters. Elevation classes (per 400 meters) and corresponding percent areas of the basin are given in Table 3.5. The lower (75-400 meters) and the upper (1200-1547) elevation classes contain only small portion of the basin: 8.16% and 6.99%, respectively. The majority of the basin (84.86%) is within 400 to 1200 meters.

Table 3.5. Elevation classes and corresponding areas

Elevation (m)	Area (km²)	Area (%)
75 - 400	2.939	8.16
400 - 800	29.493	28.91
800 - 1200	81.692	55.95
1200 -1547	16.81	6.99
Total	**257.86**	**100**

3.2.6. Aspect and slope map

The slope and aspect maps of the basin which are the two important characteristics of the basin are determined from the DEM and shown in Figure 3.8 and Figure 3.9. When we look to the Table 3.6, it can be seen that 70% of Yuvacık Basin has a slope greater than 15 degrees, and more than 15% of the basin has slopes greater than 30 degrees. Nearly one third of the basin has slopes between 0 and 15 degrees. Steep regions (slopes more than 15 degrees) are generally accumulated around the stream branches (Figure 3.8).

26
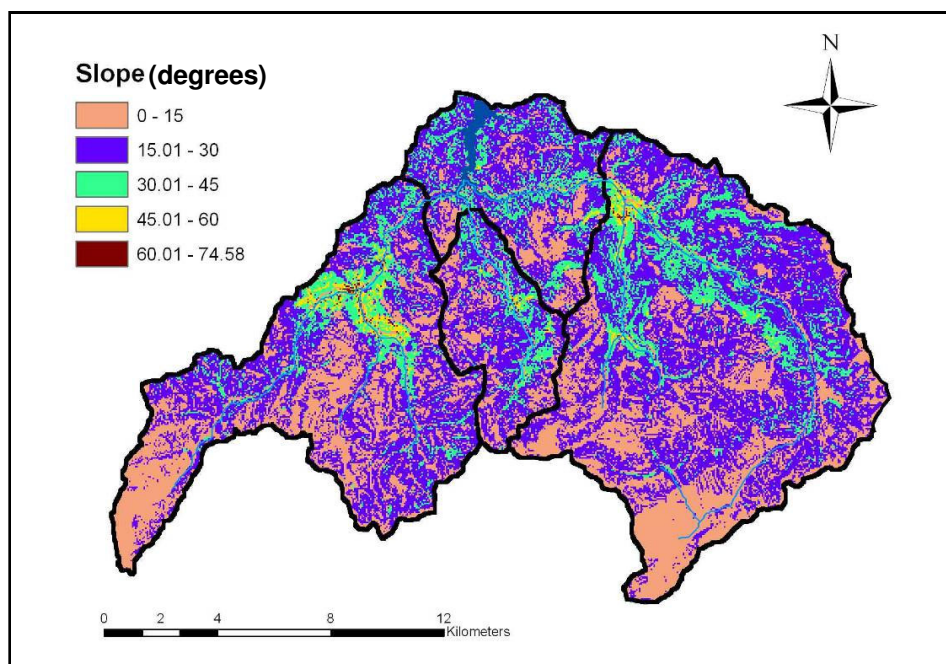
Figure 3.8. Slope map of Yuvacık basin

Table 3.6. Yuvacık Basin slope classes and their areas

Slope (degrees)	Area (km²)	Area (%)
0 - 15	82.098	31.84
15 - 30	133.600	51.81
30 - 45	39.153	15.18
45 - 60	2.984	1.16
60 – 74.58	0.025	0.01
Total	**257.86**	**100.0**

Aspect classes which is an important characteristic for the snowmelt in the basin is given in Table 3.7. As can be observed from the given Table 3.7, 10.38% of the basin faces north and 11% of the basin faces south. The portion of the basin facing west is 14.22% and facing east is 13.1%. The aspect map of the basin is given in Figure 3.9.
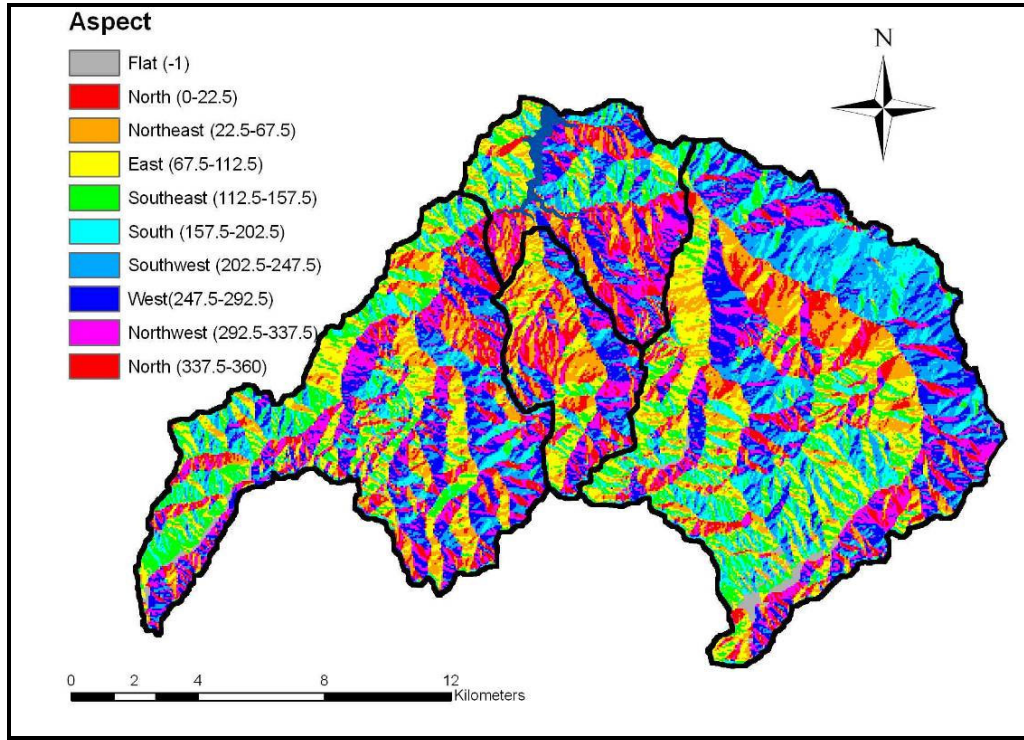
Figure 3.9. Aspect map of Yuvacık basin

Table 3.7. Yuvacık Basin aspect classes and their areas

Aspect	Area (km²)	Area (%)
North (0 - 22.5)	13.63	5.28
Northeast (22.5 - 67.5)	33.78	13.10
East (67.5 - 112.5)	33.62	13.04
Southeast (112.5 - 157.5)	30.56	11.85
South (157.5 - 202.5)	28.32	10.98
Southwest (202.5 - 247.5)	34.99	13.57
West (247.5 - 292.5)	36.66	14.22
Northwest (292.5 - 337.5)	33.17	12.86
North (337.5 - 360)	13.14	5.10
Total	**257.86**	**100.0**

3.2.7. Normalized difference vegetation index maps

All bands of Landsat ETM+ image acquired on 12 June 2001 were downloaded from GLCF (2003). These bands were converted into ERDAS imagine format and stacked into one file by using Layer Stack command of ERDAS Imagine. NDVI map is also created for further analysis by using built-in function of ERDAS Imagine. NDVI maps are shown in Figure 3.10 and the histogram of the map is shown in Figure 3.11.
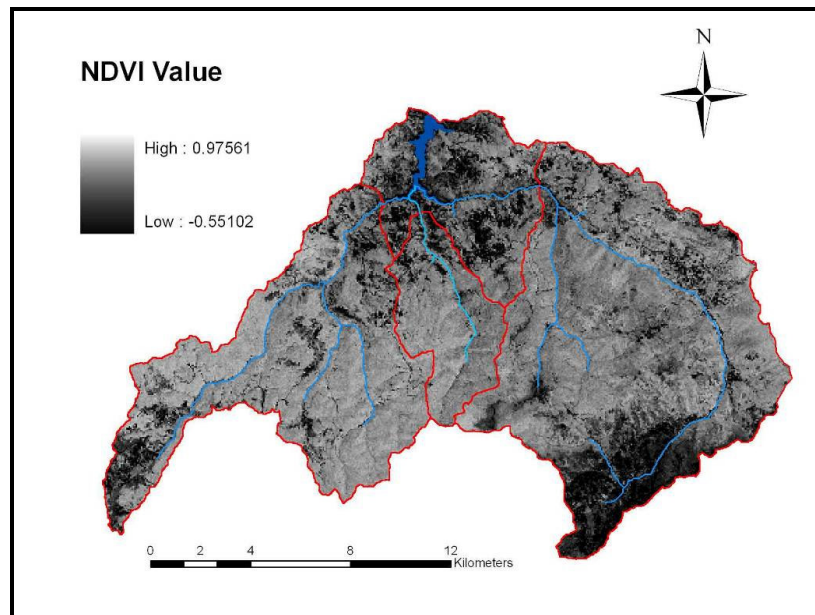
Figure 3.10. NDVI map of Yuvacık basin
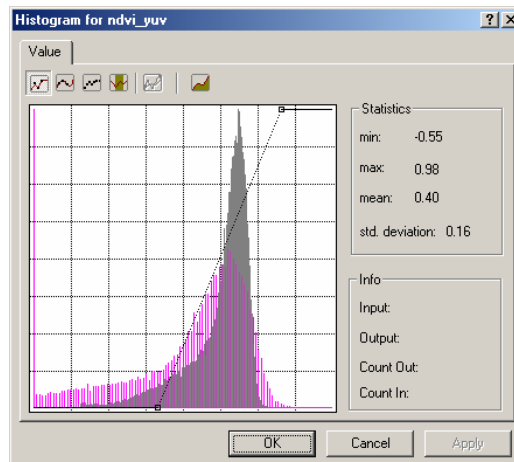
Figure 3.11. Histogram of NDVI for Yuvacık basin

NDVI value normally varies between -1 and 1, where low values can be found at water bodies, bare soil and built-up areas. NDVI is positively correlated with the amount of green biomass, so it can be used to give an indication for differences in green vegetation coverage. In Yuvacık basin, NDVI changes between -0.55 and 0.98.

Table 3.8. Distribution of NDVI for the sub-basins

Basin Name	Min	Max	Range	Mean	STD
Contributing	-0.55	0.98	1.53	0.29	0.21
Serindere	-0.37	0.71	1.08	0.39	0.15
Kirazdere	-0.34	0.75	1.09	0.45	0.13
Kazandere	-0.38	0.68	1.06	0.44	0.12

As seen from Table 3.8, the minimum mean in NDVI is in Contributing catchment where all types of land use exist and especially settlement and agricultural areas exists. The maximum mean is in Kirazdere catchment which means that green biomass is more in this catchment. The NDVI map was generated for comparing with the land use and was not used as a layer in future studies.

3.2.8. Basin boundary delineation

The Derived DEM is used with Arc-Hydro module of Arc-GIS for basin delineation. The possible sinks in the derived DEM is sinked for eliminating the unreasonable low elevation cells with respect to the surrounding cells. Then the flow direction of each cell is obtained. In order to determine the flow directions, the relations between the neighboring cells are searched. The elevation of each of the corresponding cell and its neighboring cells will determine the direction of water with the rule of water will flow to the neighboring cell which has the highest downward slope. The Deterministic 8-Direction (D8) algorithm used (Borwick 2002) for the flow direction map and shown in Figure 3.12. By the help of the flow direction of each cell, the flow accumulation map of each cell is determined. Flow accumulation value of a cell shows the number of the cells that will drain to this cell. The flow accumulation map of the basin is shown in Figure 3.13.
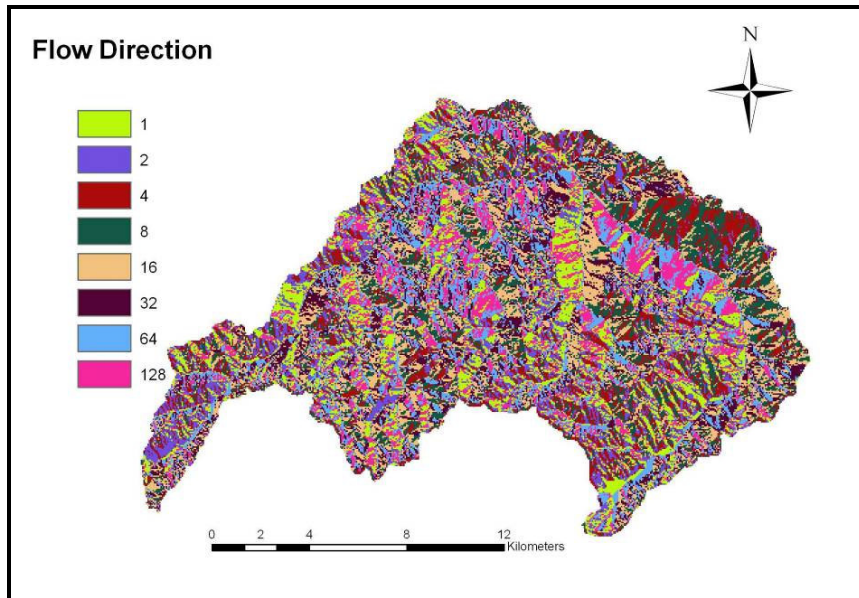
Figure 3.12. Flow direction map of Yuvacık basin
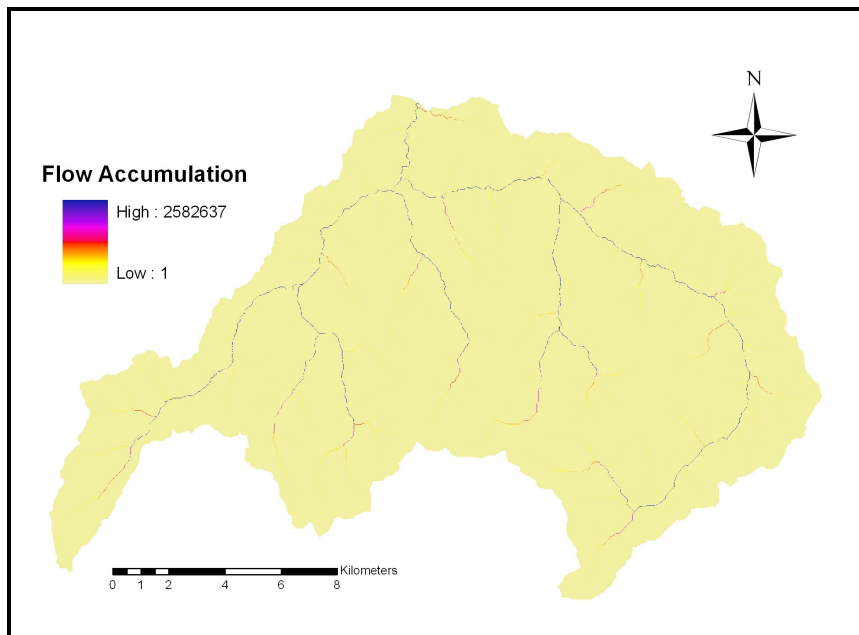
Figure 3.13. Flow accumulation map of Yuvacık basin

For obtaining the stream network in the basin, the program needs a threshold value which will represent the minimum number of drained cells to form a stream. When a small number of threshold values is used, the number of stream branches will

31

increase. So the threshold value must be selected such that the stream network which can represent the basin can be determined. The stream networks that are derived by using the values of 250, 500,1000,5000,10000 are compared and the best result is obtained from 5000 threshold value which corresponds to 0.5 km^2 in 10x10 cell size. The stream network map of the basin is shown in Figure 3.14.
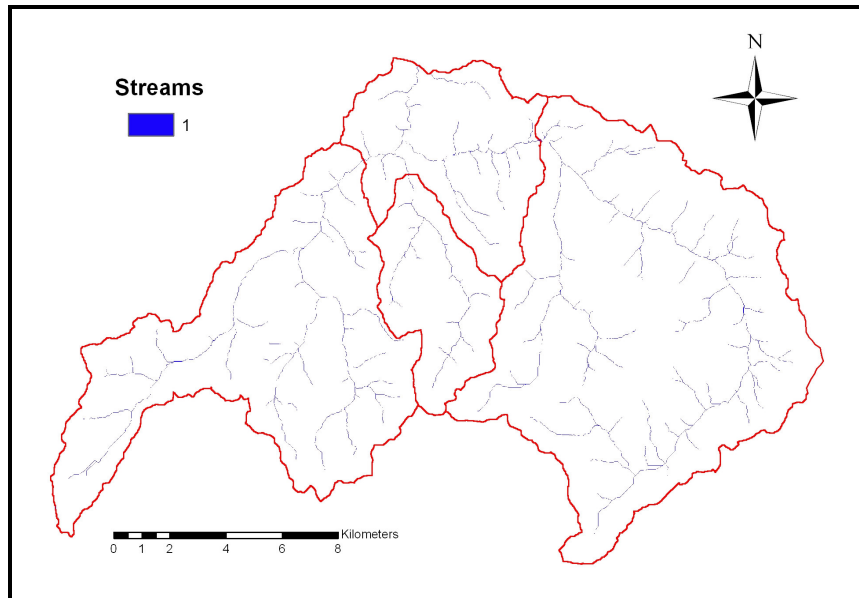
Figure 3.14. Obtained streams after threshold value definition

In order to obtain the catchments and basin polygons, a point must be defined as the outlet point of the basin. Here the dam body is selected as the outlet point of the basin. Then the program first creates the boundary of each catchment. The catchment is defined by the connection of the downstream of stream with another stream. The connection point becomes the outlet of the catchment. The boundary of the catchment is formed by the help of the flow accumulation data of the cells. This operation continued up to the outlet of the whole basin. Then the boundaries of the basin are converted to polygons by the help of the program. The resulting map is the catchments and the whole basin.

Normally with the help of the program 284 catchments are formed. But considering the ease of the use and the available flow data of each catchment, the basin is divided into 4 sub-catchments. The resulting map of the catchments can be seen in Figure 3.14. Also the areas of each catchment is calculated by the statistical analyst of Arc-View program and shown in Table 3.9.

Table 3.9. Catchments and their corresponding areas

Catchment	Area	%
Kirazdere	79.54	30,84
Kazandere	23.10	8,96
Serindere	120.53	46,74
Contributing	34.69	13,45
Total	257.86	100,00

3.2.9. Watershed geomorphometry

Hypsometric curve which is sometimes called curve to show the cumulative elevation frequency curve for the terrain is essentially a graph that shows the proportion of land area that exists at various elevations by plotting relative area against relative height (Britannica, 2005).

In GIS environment this method is based on a vectorization (polygons) of the DEM (elevation values as integers). In vector format it is easy to loop through the features and calculate the area. This curve can be drawn by using Spatial Analyst of ArcGIS. The floating values of cells were converted to integer values by using Raster Calculator of Spatial Analyst extension. The aim for performing this transformation was reducing the amount of cells that have various values; this operation is a simple classification of elevation. This integer valued DEM was converted to shape file through the Spatial Analyst. In order to summarize the area values of polygons with the same elevation values that are distributed over the terrain, shape file was converted to coverage. Summarized area values were exported to a dbf file. This file was manipulated with Microsoft Access and hypsometric curve of this watershed was created and shown in Figure 3.15. Hypsometric mean elevation (890 meter)

which is the elevation that corresponds to the 50% of this hypsometric curve is shown on Figure 3.15 with red color line.
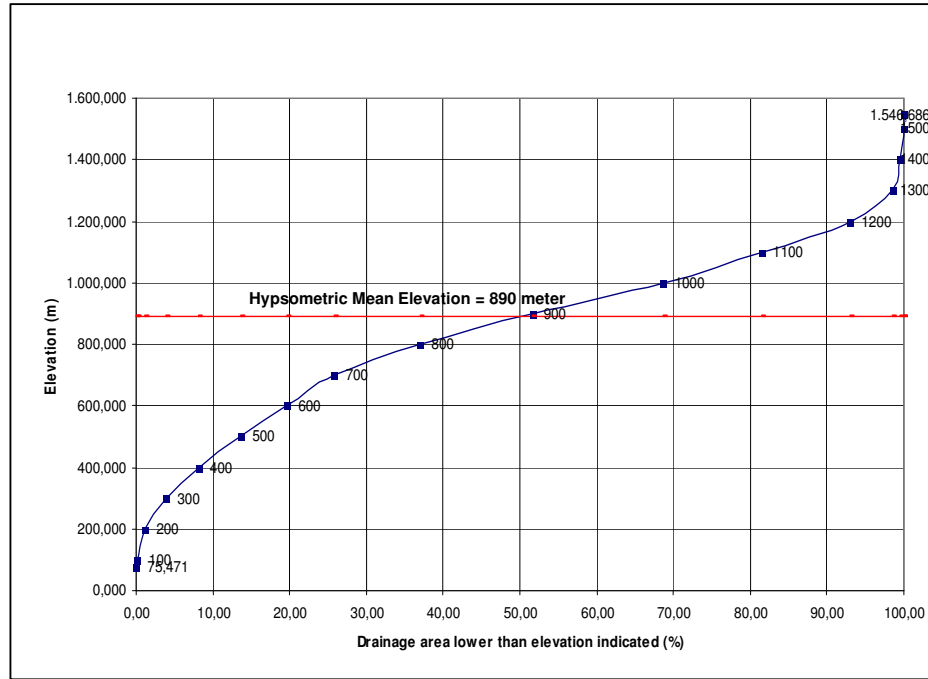
Figure 3.15. Hypsometric curve of Yuvacık basin

Time of concentration

Time of concentration values (T_c) which is defined as the time required for a drop of water to travel from the most hydrologically remote point in the subcatchment to the collection point are also computed using Kirpich's Equation that is given in Equation (3.1). This Equation (3.1) is suitable for rural areas where slope is greater than 10% and land cover is timber in more than 59% of the area. The equation can be applicable to study area with average slope being greater than 15% and land use being forest about 80%.

$$T_c = 0.0078\left(\frac{L^{0.77}}{S^{0.385}}\right)$$
(3.1)

Where, L is the main channel length, S is the average overland slope.

The L is calculated by the Longest Flow Path command of Arc Hydro module in ArcGIS and S is calculated from the slope map values. The calculated time of concentration for each sub-catchment is given in Table 3.10.

Table 3.10. Catchments and corresponding time of concentration values

Catchment Name	T_c (hr)
Kirazdere	2.52
Kazandere	1.46
Serindere	2.89

3.3. Methodology used in this study

The analysis of available rainfall and runoff data showed that the storm events can be classified as;

     1) Snowmelt and rain on snow events

     2) Rainfall events

Therefore, two different methodologies were used in this study. Two different modules of Mike11 is used, where the NAM module is used for the simulation of daily snowmelt and rain on snow events and Unit Hydrograph Method (UHM) module is used for the simulation of hourly rainfall events. Concerning the data of meteorological variables and model parameters, NAM module and UHM module was used in daily and hourly time steps for snowmelt and rainfall events respectively. The main objective to use two different modules is to experience two different modules with different parameter sets. Both of the modules can be utilized as a decision support tool to estimate the possible runoff with the recommended parameter set during the real time operation of the dam.   The flowcharts and methodologic summary of the two studies are given below and the detailed information and results are given in Chapter 5 and 6.

3.3.1. Simulation of daily snowmelt and rain on snow events

The largest peaks of inflow are observed when the storm events occur due to both snowmelt and rain on snow. The snow starts to accumulate at the mid of December and almost all of the snow reserve melts at the end of March except from the

locations at the higher elevations of the basin. Therefore, the simulation of the events is started from the beginning of December and extended to the end of April. The basin is preprocessed by the ArcHydro module of ArcGIS (ESRI, 2005) as shown in the flowchart, Figure 3.16. The basin is divided into three sub-basins where each sub-basin is represented by its own characteristics and the sub-basins are divided into elevation zones for snowmelt computations. Thus, the main inputs of model NAM module are prepared by the help of ArcHydro for the simulation of 2001-2006 events. Hydrometeorological data is generated as timeseries for the use of model. The parameters of the model were calibrated with the selected storm events, and the recommended parameters were obtained for different time periods of the year.
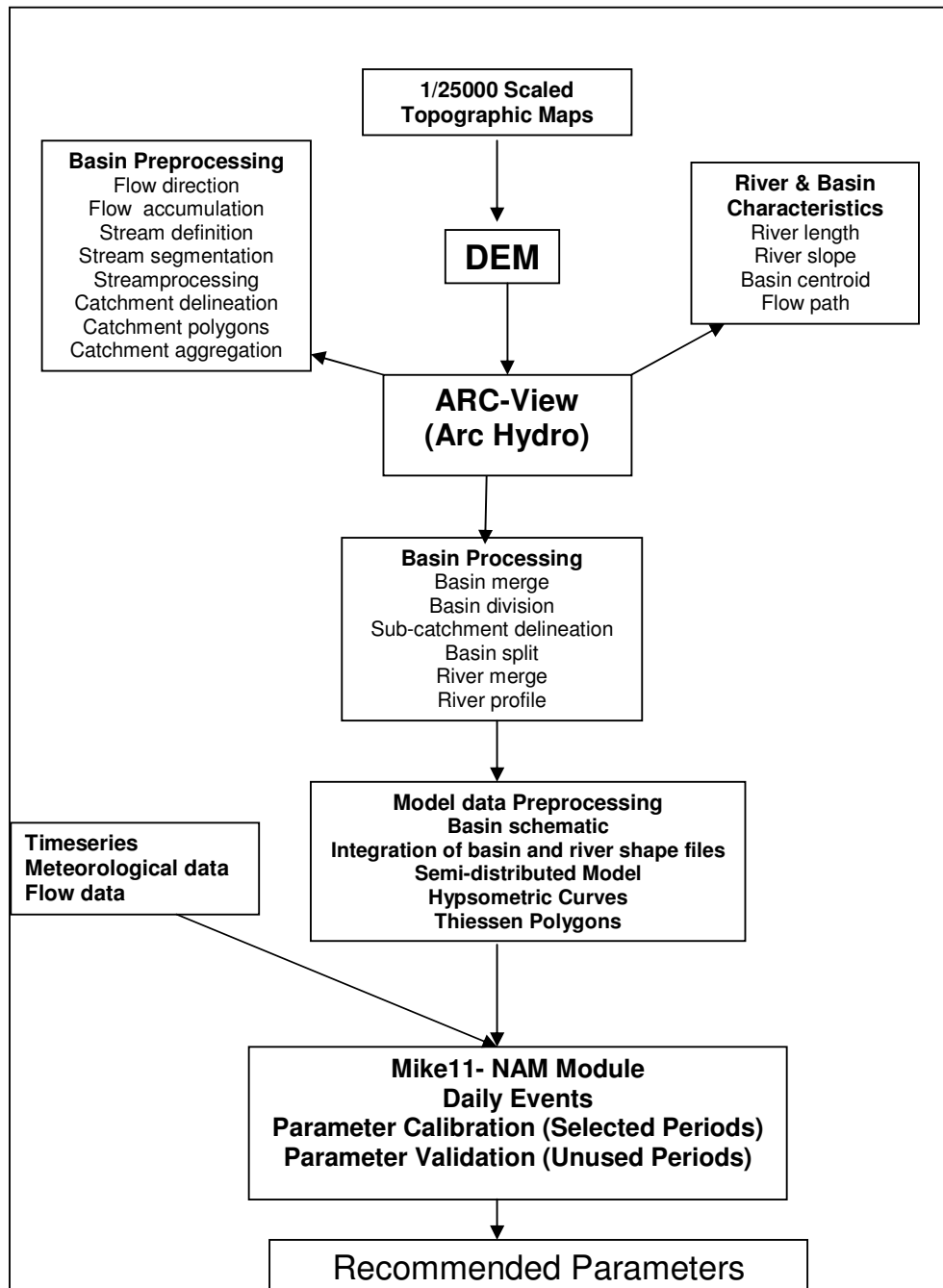
Figure 3.16. Flowchart diagram of simulation of daily snowmelt events

3.3.2. Simulation of hourly rainfall events

Mike11 UHM Module is used for the simulation of hourly rainfall events with hydrometeorological data. CN methodology is utilized in this part of the study, and

CN values obtained from the classical SCS-Curve Method and a new CN methodology are compared for the selected rainfall events during the period of 2001-2005. The general flowchart of the application is presented in Figure 3.17.

Topographic Index (TI), Fractional Area (A_f) and the CN values of each event are forming the key for this study. Topographic index is found from soil conductivity, slope and flow accumulation values of each raster data layer. The number of TI values is grouped according to the TI value in each cell by Microsoft Access. The fractional area of watershed that can be defined as the contributing area for a given storm event can be used to determine a critical TI value above which topographic areas are saturated and contributing to surface runoff. Finally, A_f versus TI graph which is used to determine TI value of each event is generated.

The initial abstraction method in UHM module is used to determine the initial abstraction, excess rainfall and runoff which forms the inputs for the calculation of frational area and CN for each event. The initial abstraction value at the beginning of each event and the excess rainfall is calculated by trial and error process. An average CN is calculated for each sub-catchment by using the calculated CN from event simulations. Then the common storm periods that are the same for at least two sub-catchments are selected for further analysis and a table is generated for the representation of the relation of TI, A_f and CN for the events. The Hydrological Sensitive Areas (HSA) are shown where the definition of HSA is the cells that are greater than the TI value for each event. The methodology showed that the CN can be found from the A_f and a relation exists between the TI and CN. The CN values found from this new methodology are compared with the CN values found by classical SCS-Curve Number method. The soil, geology and landuse data is used for SCS-Curve number method to assign a CN for each HSA for each selected event. The average CN value of the cells is calculated and taken as the CN value for each event. The CN values from two studies are compared and the results seem to be promising and explained in detail in Section 5.5.
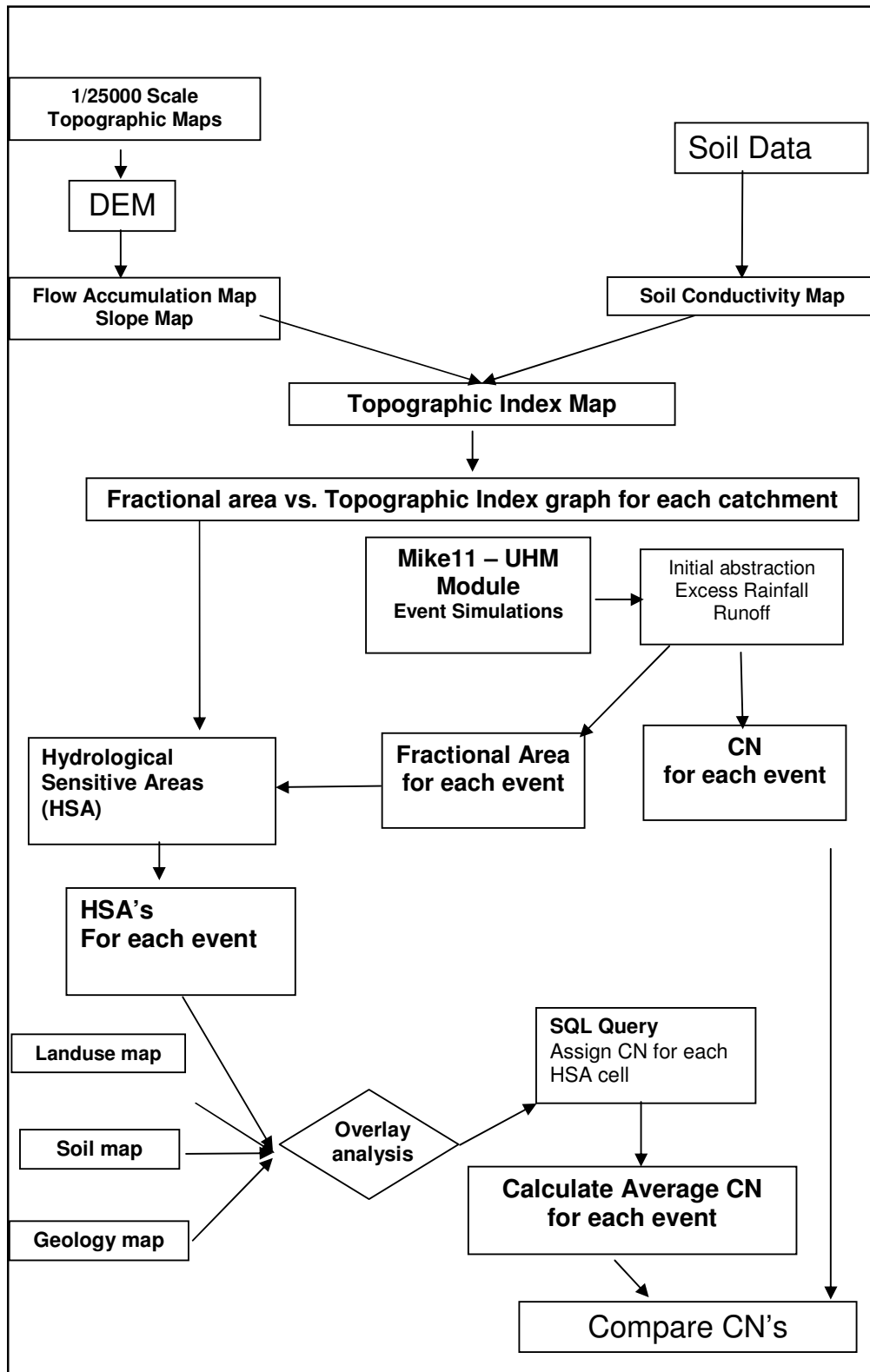
Figure 3.17. Flowchart diagram of CN study

CHAPTER 4

HYDROLOGICAL MODEL DESCRIPTION

4.1. Introduction

This chapter gives only introductory information about this software. The detailed information about the model can be found in the corresponding user's manuals.

Since some of the information given in this section are partially or sometimes fully-compiled from the user's manuals, the reference information is given at the beginning of the model description instead of attaching the reference information at the end of each paragraph. For this chapter, Mike11 Model Software refers to "Mike 11 User & Reference Manual", Danish Hydraulic Institute, Denmark.

Mike11 is one of the rainfall-runoff models in the world. It is developed by Danish Hydraulic Institute(DHI). DHI developed several models (Mike Basin, Mike Flood, Mike she, Mike11 etc.) for water management and modeling in the river basins and Mike 11 is the one of them which is used for Inflow forecasting for a specific point (such as dams). This study is done for the estimation and calibration of the inflow to Yuvacık Dam so, in this study Mike 11 NAM Module and UHM module are used in order to forecast the inflow to the Yuvacık Dam at a sub-catchment scale. The description of the two modules is given in the following sections below;

4.2. NAM module

NAM is the abbreviation of the Danish "Nedbør-Afstrømnings-Model", meaning precipitation-runoff-model. This model was originally developed by the Department of Hydrodynamics and Water Resources at the Technical University of Denmark.

The NAM hydrological model simulates the rainfall-runoff processes occurring at the catchment scale. NAM forms part of the rainfall-runoff (RR) module of the Mike 11 river modelling system. The rainfall-runoff module can either be applied independently or used to represent one or more contributing catchments that generate lateral inflows to a river network. In this manner it is possible to treat a single catchment or a large river basin containing numerous catchments and a complex network of rivers and channels within the same modelling framework.

4.2.1. Data requirements

The basic input requirements for the NAM model consist of:

- ➢ Model parameters (overland flow coefficient, interflow coefficient, etc.)
- ➢ Initial conditions(soil moisture, initial discharge etc.)
- ➢ Meteorological data(rainfall, evaporation, temperature, etc.)
- ➢ Streamflow data for model calibration and validation(observed discharge)

The basic meteorological data requirements are:
- ➢ Rainfall
- ➢ Potential evapotranspiration

In the case of snow modelling the additional meteorological data requirements are:
- ➢ Air Temperature
- ➢ Solar Radiation (optional)

In Yuvacık dam basin snow is very effective in rainfall-runoff process during ablation period of snow so it is included in the simulations, so the use of temperature data is a must in snow melt periods.

The NAM model also allows modelling of man-made interventions in the hydrological cycle in terms of irrigation and groundwater pumping. In this case time

series of irrigation and groundwater abstraction rates are required. But in this study irrigation and groundwater pumping components are neglected.

In the below sections the description of the meteorological and hydrological data are given. In the later sections the model parameters and initial conditions are described.

4.2.1.1. Meteorological data

Rainfall (mm)

The time resolution of the rainfall input depends on the objective of the study and on the time scale of the catchment response. In many cases daily rainfall values are sufficient, but in rapidly responding catchments where accurate representation of the peak flows is required, rainfall input on a finer resolution may be required. Rainfall data with any (variable) time increments can be specified in the rainfall input.

Potential evapotranspiration (mm)

When daily time steps which are the case of Yuvacık dam basin are used, monthly values of potential evapotranspiration are usually sufficient. In this case only minor improvements can be obtained by specifying daily values instead of monthly values.

Temperature (^{o}C)

Temperature data are required if snow accumulation and melt are included in the simulations. During the snow season, the time increments in the temperature data should reflect the length of the time step in the simulation, e.g. daily mean temperatures.

Mean area weighting of meteorological data

The NAM model simulates the rainfall-runoff process in a lumped fashion so provision is given for combining meteorological data from different stations within a single catchment or subcatchment into a single time series of weighted averages. The resulting time series will represent the mean area values of rainfall and potential evapotranspiration for a catchment.
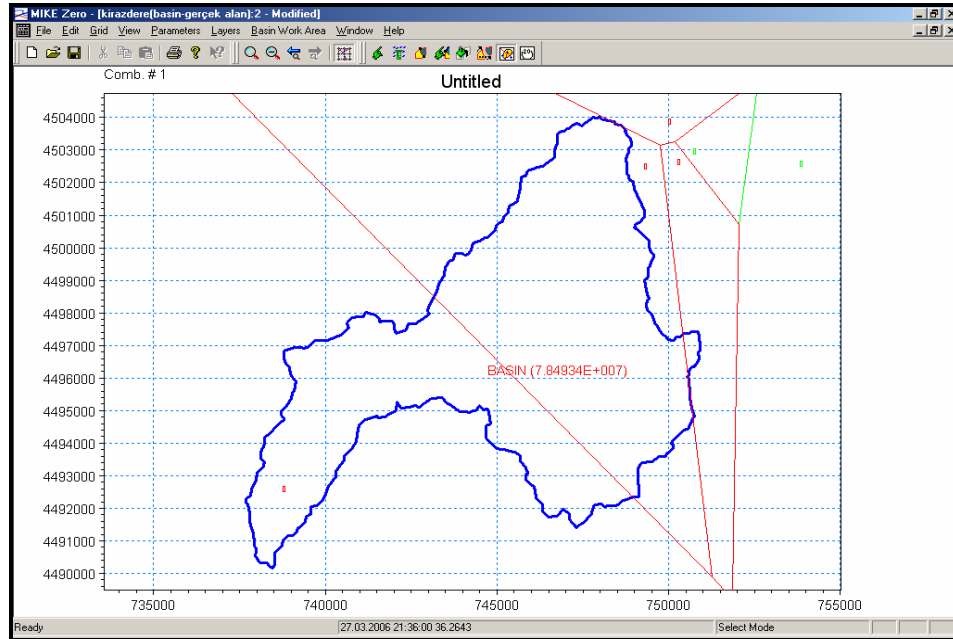
Figure 4.1. Thiessen polygons of Kirazdere basin

The weights are user-defined and can be determined based e.g. on the Thiessen method. An example for the thiessen method is given in Figure 4.1 for the Kirazdere cacthment. In the case of missing values the weighting procedure will redistribute the weights appropriately. Therefore, it is not necessary to specify weight combinations for all possible combinations of missing stations.

4.2.1.2. Hydrological data

Discharge (m³/s)

Observed discharge data at the catchment outlet are required for comparison with the simulated runoff for model calibration and validation. The discharge data at any particular time is the average discharge since the last entered data.

Irrigation (mm)

If the irrigation module is included in the NAM simulation, an additional irrigation time series is required to provide information on the amount of irrigation water.

Groundwater abstraction (mm)

When the effect of groundwater abstraction is expected to have a significant effect on the overall groundwater levels or catchment baseflow, pumping rates can be specified to account for these withdrawals.

4.2.2. Model structure

A conceptual model like NAM is based on physical structures and equations used together with semi-empirical ones. Being a lumped model, NAM treats each catchment as a single unit. It means that the shape of the basin is not important. The catchment must be divided into smaller catchments if the shape of the basin is important. The parameters and variables represent, therefore, average values for the entire catchment. As a result some of the model parameters can be evaluated from physical catchment data, but the final parameter estimation must be performed by calibration against time series of hydrological observations.
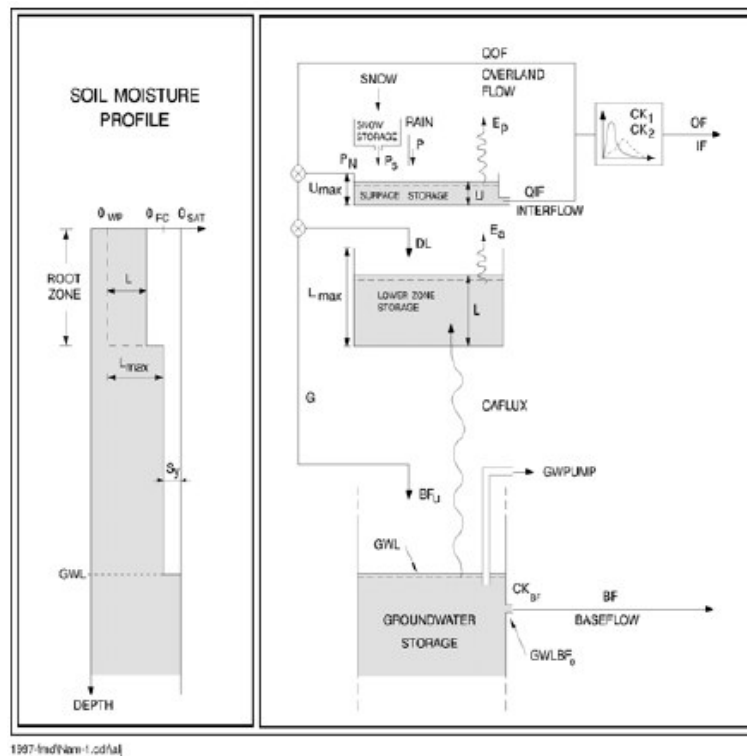
Figure 4.2. Model structure of NAM

The model structure is shown in the above Figure 4.2. It is an imitation of the land phase of the hydrological cycle. NAM simulates the rainfall-runoff process by continuously accounting for the water content in four different and mutually interrelated storages that represent different physical elements of the catchment. These storages are:

- ➢ Snow storage
- ➢ Surface storage
- ➢ Lower or root zone storage
- ➢ Groundwater storage

In addition NAM allows treatment of man-made interventions in the hydrological cycle such as irrigation and groundwater pumping. Based on the meteorological input data NAM produces catchment runoff as well as information about other elements of the land phase of the hydrological cycle, such as the temporal variation of the evapotranspiration, soil moisture content, groundwater recharge, and groundwater levels. The resulting catchment runoff is split conceptually into overland flow, interflow and baseflow components.

4.2.3. Basic modelling components

Surface storage

Moisture intercepted on the vegetation as well as water trapped in depressions and in the uppermost, cultivated part of the ground is represented as surface storage. Umax denotes the upper limit of the amount of water in the surface storage.

The amount of water, U, in the surface storage is continuously diminished by evaporative consumption as well as by horizontal leakage (interflow). When there is maximum surface storage, some of the excess water, PN, will enter the streams as overland flow, whereas the remainder is diverted as infiltration into the lower zone and groundwater storage.

Lower zone or root zone storage

The soil moisture in the root zone, a soil layer below the surface from which the vegetation can draw water for transpiration, is represented as lower zone storage. Lmax denotes the upper limit of the amount of water in this storage.

Moisture in the lower zone storage is subject to consumptive loss from transpiration. The moisture content controls the amount of water that enters the groundwater storage as recharge and the interflow and overland flow components.

Evapotranspiration

Evapotranspiration demands are first met at the potential rate from the surface storage. If the moisture content U in the surface storage is less than these requirements ($U < E_p$), the remaining fraction is assumed to be withdrawn by root activity from the lower zone storage at an actual rate Ea. Ea is proportional to the potential evapotranspiration and varies linearly with the relative soil moisture content, L/Lmax, of the lower zone storage.

Overland flow

When the surface storage spills, i.e. when U > Umax, the excess water PN gives rise to overland flow as well as to infiltration. QOF denotes the part of PN that contributes to overland flow. It is assumed to be proportional to PN and to vary linearly with the relative soil moisture content, L/Lmax, of the lower zone storage where

$$QOF = \begin{cases} CQOF\dfrac{L/L\max - TOF}{1 - TOF}P_N & forL/L\max > TOF \\ 0 & forL/L\max \leq TOF \end{cases} \qquad (4.1)$$

CQOF is the overland flow runoff coefficient ($0 \leq CQOF \leq 1$)
TOF is the threshold value for overland flow ($0 \leq TOF \leq 1$).

The proportion of the excess water P_N that does not run off as overland flow infiltrates into the lower zone storage. A portion, ΔL, of the water available for infiltration, (PN -QOF), is assumed to increase the moisture content L in the lower

46

zone storage. The remaining amount of infiltrating moisture, G, is assumed to percolate deeper and recharge the groundwater storage.

Interflow

The interflow contribution, QIF, is assumed to be proportional to U and to vary linearly with the relative moisture content of the lower zone storage.

$$QIF = \begin{cases} CKIF\dfrac{L/L\max - TIF}{1-TIF}P_N & forL/L\max > TIF \\ 0 & forL/L\max \leq TIF \end{cases} \tag{4.2}$$

where CKIF is the time constant for interflow, and TIF is the root zone threshold value for interflow ($0 \leq TIF \leq 1$).

Interflow and overland flow routing

The interflow is routed through two linear reservoirs in series with the same time constant CK_{12}. The overland flow routing is also based on the linear reservoir concept but with a variable time constant

$$CK = \begin{cases} CK_{12} & for\ OF < OF_{min} \\ CK_{12}\left(\dfrac{OF}{OF_{min}}\right)^{-\beta} & for\ OF \geq OF_{min} \end{cases} \tag{4.3}$$

Where; OF is the overland flow (mm/hour), OF_{min} is the upper limit for linear routing (= 0.4 mm/hour), and $\beta = 0.4$. The constant $\beta = 0.4$ corresponds to using the Manning formula for modelling the overland flow. Above equation ensures in practice that the routing of real surface flow is kinematic, while subsurface flow being interpreted by NAM as overland flow (in catchments with no real surface flow component) is routed as a linear reservoir.

Groundwater recharge

The amount of infiltrating water G recharging the groundwater storage depends on the soil moisture content in the root zone

47

$$
G = \begin{cases} P_N - QOF \dfrac{L/L\max - TG}{1-TG} PN & forL \ / \ L\max \ > TG \\ 0 & forL \ / \ L\max \ \leq TG \end{cases}
\tag{4.4}
$$

Where;

TG is the root zone threshold value for groundwater recharge ($0 \leq TG \leq 1$).

Soil moisture content

The lower zone storage represents the water content within the root zone. After apportioning the net rainfall between overland flow and infiltration to groundwater, the remainder of the net rainfall increases the moisture content L within the lower zone storage by the amount ΔL

$$
\Delta L = P_N - QOF - G
\tag{4.5}
$$

Baseflow

The baseflow BF from the groundwater storage is calculated as the outflow from a linear reservoir with time constant CKBF.

4.2.4. Snow module

Snow accumulation and melt are important hydrological processes in river basins where the snow pack acts as a storage in which precipitation is retained during the cold season and subsequently released as melt water during the warmer parts of the year.

The snow melt component of the runoff is incorporated as an integrated module within NAM. This component is optional and temperature data is only required if the snow routine is selected. Normally the precipitation enters directly into the surface storage. However, during cold periods precipitation is retained in the snow storage from which it is melted in warmer periods. Two different models can be applied; a

simple lumped calculation or a more general approach that divides the catchment into a number of altitude zones with separate snow melt parameters, temperature and precipitation input for each zone.

Accumulation and melting of snow

Several investigations have shown that the shift between precipitation in the form of rain and snow usually takes place when the air temperature is within a narrow interval close to 0°C. In the snow module it is assumed that the precipitation falls as rain when the air temperature is above a certain base temperature level, T0, which can be specified by the user.

The snowmelt QS is calculated using a degree-day approach

$$QS = \begin{cases} C_{snow}(T-T_0) & for\ T>T_0 \\ 0 & for\ T \leq T_0 \end{cases}$$

(4.6)

where Csnow is the degree-day coefficient. The generated melt water is retained in the snow storage as liquid water until the total amount of liquid water exceeds the water retention capacity of the snow storage. The excess melt water PS is routed to the NAM model where it contributes to the surface storage. The excess melt water contribution PS to NAM is

$$PS = \begin{cases} Q_{melt} & for\ WR \geq C_{wr}S_{snow} \\ 0 & for\ WR < C_{wr}S_{snow} \end{cases}$$

(4.7)

where WR is the water retention in the snow storage, C_{wr} is the water retention coefficient, and Ssnow is the snow storage. The new snow storage is calculated by subtracting the excess melt water P_S from the snow storage. The rain fraction is added as liquid water and is retained in the snow storage if the total liquid water content of the snow pack is below its water retaining capacity. When the air temperature is below T_0, the liquid water content in the snow storage freezes with rate C_{snow}. Evaporation from the snow pack is neglected.

49

Altitude-distributed snowmelt model

In mountainous areas temperature, precipitation and snow cover often vary significantly within a single catchment. The runoff simulations for such areas can be improved by dividing the catchment into smaller zones and maintain individual snow storage calculations in each zone. The altitude-distributed snow model calculates melt water in a number of altitude zones using the degree-day approach. Since in many cases the hydro-meteorological information from mountain basins is quite sparse, the module also includes facilities for distribution of the meteorological information with altitude.

Structure of the altitude-distributed snowmelt module

The snow melt module allows the user to define a number of altitude zones within a NAM catchment and adjust the snow melt parameters and the temperature and precipitation input to the model for each zone. The snow melt module maintains individual snow storages and calculates accumulation and melting of snow for each altitude zone. The simulated melt water from all zones is subsequently superposed and routed through the NAM model as illustrated in the below Figure 4.3. This implies that the same model parameters for infiltration, runoff and groundwater routing are applied for all altitude zones. Such an approach will be appropriate for the large majority of mountain catchments.
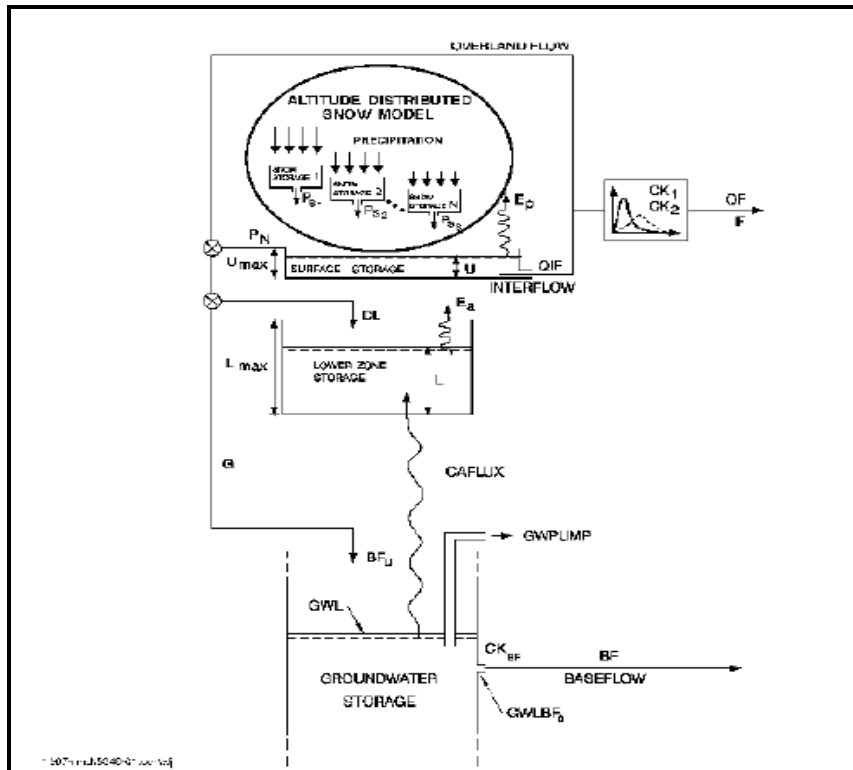
Figure 4.3. Model structure of the altitude-distributed snowmelt module

In special cases where differentiation is needed also in the other parameters the catchment in question can be divided into two or more sub-catchments. The total simulated discharge is then found by accumulating the simulated discharge from the different sub-catchments using the combined catchment approach in the Mike 11 RR editor.

In the altitude-distributed snow model, snow melting only takes place from the snow-covered part of each zone. When the water equivalent of the snow pack falls under a user-specified value (minimum storage for full coverage), the area coverage will be reduced linearly with the snow storage in the zone.

Snow will not necessarily melt on the location where it falls. Due to wind transport the snow accumulation at wind exposed sites may often be significantly smaller than at locations well sheltered against wind. Wind exposed conditions are often present

at higher altitudes where vegetation is sparse and wind velocities generally high. Furthermore, for the higher parts of mountain ranges, steep slopes having a limited snow storage capacity will often dominate. Snow storage in excess of this capacity will at such locations generate avalanches which transport the snow to lower altitudes. Hence, some of the snow falling on wind exposed and/or steep highlands may not melt on the location but be deposited and melting at lower altitudes. To account for such re-distribution of snow and avoid unrealistic accumulation of snow in the cold upper zones a user specified upper limit of the snow storage in the individual zones has been introduced in the model. Snow storage exceeding this value will be transferred to the neighboring lower zone.

Adjustment of temperature and precipitation to altitude zones

The altitude-distributed snow model operates with three meteorological reference time series; precipitation, temperature and potential evapotranspiration. In order to account for the large variations in precipitation and temperature with altitude the reference series can be adjusted for each altitude zone in two different ways:

Lapse rate corrections

The lapse rate correction approach is a very simple but powerful way of adjustment in which the temperature and the precipitation are assumed to vary linearly with the altitude. The only input data required are the average altitude of the various zones, a reference altitude of the time series, and the lapse rates. The temperature lapse rates, however, are known to be quite variable, ranging from high values under dry conditions to lower values under wet conditions. Hence, in the model it is possible to specify two different temperature lapse rates to be used during dry and wet weather conditions, respectively. The model applies the "wet" lapse rate during days with precipitation and the "dry" lapse rate during the rest of the time. The temperature in each zone is adjusted by the following formula:

$$T_{zone} = \begin{cases} T_{ref} + (H_{zone} - H_{ref})\beta_{dry} & for\ P=0 \\ T_{ref} + (H_{zone} - H_{ref})\beta_{wet} & for\ P>0 \end{cases} \quad (4.8)$$

Where T_{zone} temperature in the considered zone

T_{ref} temperature at the reference temperature station

H_{zone} average height in the zone

H_{ref} height at the reference temperature station

β_{dry} temperature lapse rate for dry conditions

β_{wet} temperature lapse rate for wet conditions

The precipitation in each altitude zone is calculated from the precipitation at the reference station:

$$P_{zone} = P_{ref}\,(1+(H_{zone}-H_{ref})\alpha) \tag{4.9}$$

Where

P_{ref} precipitation at the reference precipitation station

H_{ref} height at the reference precipitation series

α precipitation lapse rate

Extended components

Seasonal variation of degree-day coefficient

The simple degree-day approach for calculating snow melt can be extended by using a seasonal variation of the degree-day coefficient C_{snow}. This variation reflects in a conceptual way the seasonal variation of the incoming short wave radiation and the variation in the albedo of the snow surface during the snow season.

Radiation

The melting effects caused by the absorbed short wave radiation can be explicitly modelled. In this case an additional snow melting is calculated as

$$\Delta QS \;=\; C_{rad}\; R \tag{4.12}$$

where C_{rad} is the radiation coefficient, and R is the incoming short wave radiation.

Condensation of humid air and heat contribution from rainfall

The melting effects from condensation of humid air on the snow surface and the advective heat transferred to the snow pack by precipitation can be explicitly modelled. The effects are calculated as an additional snowmelt

$$\Delta QS = C_{rain} \ P(T - T_0) \tag{4.13}$$

where C_{rain} is a degree-day coefficient, and P is the rainfall.

Irrigation module

Minor irrigation schemes within a catchment will normally have negligible influence on the catchment hydrology, unless transfer of water over catchment boundaries is involved. Large schemes, however, may significantly affect the runoff and the groundwater recharge through local increases in evapotranspiration and infiltration as well as through operational and field losses.

4.2.5. Model parameters

The description of the model parameters are given in Table 4.1, 4.2 and 4.3. The description of surface and root zone parameters is given in Table 4.1 and the groundwater parameters are given in Table 4.2.

Table 4.1. Surface and root zone parameters

Parameter	Description
Umax	Maximum water content in surface storage
	This storage is interpreted as including the water content in the interception storage (on vegetation), in surface depression storages, and in the uppermost few cm's of the ground. One important characteristic of the model is that the surface storage must be at its maximum capacity before any excess water occurs.
Lmax	Maximum water content in the root zone storage
	Lmax can be interpreted as the maximum soil moisture content in the root zone available for the vegetative transpiration. Ideally, Lmax can then be estimated by multiplying the difference between field capacity and wilting point of the actual soil with the effective root depth. The difference between field capacity and wilting point is referred to as the available water holding capacity.
CQOF	Overland flow runoff coefficient
	CQOF is a very important parameter, determining the extent to which excess rainfall runs off as overland flow and the magnitude of infiltration. CQOF is dimensionless with values between 0 and 1. Physically, in a lumped manner, it reflects the infiltration and also to some extent the recharge conditions. Small values of CQOF are expected for a flat catchment having coarse, sandy soils and a large unsaturated zone, whereas large CQOF-values are expected for catchments having low, permeable soils such as clay or bare rocks
CKIF	Time constant for interflow
	CKIF determines together with Umax the amount of interflow ((CKIF)-1 is the quantity of the surface water content that is drained to interflow every hour). It is the dominant routing parameter of the interflow because CKIF $\gg$ CK$_{12}$.
TOF	Root zone threshold value for overland flow
	TOF is a threshold value for overland flow in the sense that no overland flow is generated if the relative moisture content of the lower zone storage, L/Lmax, is less than TOF.
TIF	Root zone threshold value for inter flow
	The root zone threshold value for interflow has the same function for interflow as TOF has for the overland flow. It is usually not a very important parameter, and it can in most cases be given a value equal to zero.
CK$_{12}$	Time constant for routing overland flow
	The time constant for routing interflow and overland flow CK$_{12}$ [hours] determines the shape of hydrograph peaks. The value of CK$_{12}$ depends on the size of the catchment and how fast it responds to rainfall

Table 4.2. Groundwater parameters

TG	Root zone threshold value for recharge
	The root zone threshold value for recharge has the same effect on recharge as TOF has on the overland flow. It is an important parameter for simulating the rise of the groundwater Table in the beginning of a wet season.
CKBF	Time constant for routing base flow
	The time constant for baseflow determines the shape of the simulated hydrograph in dry periods. CKBF can be estimated from hydrograph recession analysis. If the recession analysis indicates that the shape of the hydrograph changes to a slower recession after a certain time, additional (lower) groundwater storage can be added to improve the description of the baseflow.

Table 4.3. Snow module parameters

T_0	Base temperature (snow/rain)
	The precipitation is assumed to fall as snow if the temperature is below the base temperature T_0 [°C]. For temperatures above T_0 the snow in the snow storage is melting.
Crad	Radiation coefficient
	The radiation coefficient Crad [m^2/W/mm/day] determines the rate of snow melting caused by the absorbed short wave radiation.
C_{rain}	Rainfall degree-day coefficient
	The rainfall degree-day coefficient C_{rain} [mm/mm/°C/day] determines the rate of snow melting caused by condensation of humid air on the snow surface and the advective heat transferred to the snow pack by precipitation.
C_{snow}	Degree-day coefficient
	The snow melts at a rate defined by the degree-day coefficient Csnow [mm/°C/day]. A seasonal variation of C_{snow} can be defined in order to account for the seasonal variations of the incoming short wave radiation and the albedo of the snow surface.

4.2.6. Initial conditions

The initial conditions required by the NAM model consist of the initial water contents in the surface and root zone storages, together with initial values of overland flow, interflow, and baseflow.

If a lower groundwater reservoir is specified, the initial baseflow from both the upper and the lower reservoir should be specified. If the snow module is included, the initial value of the snow storage should be specified.

If a simulation commences at the end of a dry period, it is often sufficient to set all initial values to zero, except the water content in the root zone and the baseflow. The water content in the root zone should be about 10- 30% of the capacity and the baseflow should be given a value close to the observed discharge.

Improved estimates of the initial conditions may be obtained from a previous simulation, covering several years, by noting the appropriate moisture contents of the root zone and baseflow at the same time of the year as the new simulation will start.

In general it is recommended to disregard the first 3-6 months of the NAM simulation in order to eliminate the influence of erroneous initial conditions.

4.2.7. Model calibration

In the NAM model the parameters and variables represent average values for the entire catchment. While in some cases a range of likely parameter values can be estimated, it is not possible, in general, to determine the values of the NAM parameters on the basis of the physiographic, climatic and soil physical characteristics of the catchment, since most of the parameters are of an empirical and conceptual nature. Thus, the final parameter estimation must be performed by calibration against time series of hydrological observations.

4.2.7.1. Calibration objectives

The following objectives are usually considered in the model calibration

- A good agreement between the average simulated and observed catchment runoff (i.e. a good water balance)
- A good overall agreement of the shape of the hydrograph

- A good agreement of the peak flows with respect to timing, rate and volume
- A good agreement for low flows

In this respect it is important to note that, in general, trade-offs exist between the different objectives. For instance, one may find a set of parameters that provide a very good simulation of peak flows but a poor simulation of low flows, and vice versa.

In the calibration process, the different calibration objectives should be taken into account. If the objectives are of equal importance, one should seek to balance all the objectives, whereas in the case of priority to a certain objective this objective should be favored.

In model calibration only error source should be minimized. In this respect it is important to distinguish between the different error sources since calibration of model parameters may compensate for errors in data and model structure. For catchments with a low quantity or quality of data, less accurate calibration results may have to be accepted.

Satisfactory calibrations over a full range of flows usually require continuous observations of runoff for a period of 3-5 years. Runoff series of a shorter duration, however, will also be useful for calibration, although they do not ensure an efficient calibration of the model. For a proper evaluation of the reliability and hydrological soundness of the calibrated model it is recommended to validate the model on data not used for model calibration (split-sample test).

4.2.7.2. Manual calibration

The process of model calibration is normally done either manually or by using computer-based automatic procedures. In this section a manual calibration strategy for the NAM model is outlined. Application of an automatic optimization routine for calibration of the basic NAM model is described in the subsequent section.

In manual calibration, a trial-and-error parameter adjustment is made until satisfactory results are obtained. It is recommended, especially for the less experienced users, to change only one parameter between each trial, so that the effect of the change can be easily discerned. The manual calibration strategy outlined below is based on the different rainfall-runoff process descriptions for calibration of the relevant model parameters, i.e. the parameters that mostly affect the considered process description

A calibration usually commences by adjusting the water balance in the system. The total evapotranspiration over a certain period should correspond to the accumulated net precipitation minus runoff. The evapotranspiration will increase when increasing the maximum water contents in the surface storage Umax and the root zone storage Lmax, and vice versa. The peak runoff events are caused by large quantities of overland flow. The peak volume can be adjusted by changing the overland flow runoff coefficient (CQOF), whereas the shape of the peak depends on the time constant used in the runoff routing (CK_{12}).

The amount of base flow is affected by the other runoff components; a decrease in overland flow or interflow will result in a higher baseflow, and vice versa. The shape of the baseflow recession is a function of the baseflow time constant (CKBF).

Initially, the root zone threshold values TOF, TIF and TG can be set to zero. After a first round of calibration of the parameters Umax, Lmax, CQOF, CK_{12} and CKBF, the threshold parameters can be adjusted for further refinement of the simulation results. The snow module parameters are calibrated against periods with snowmelt runoff.

4.2.7.3. Automatic calibration routine

For calibration of the basic NAM model, including the 9 model parameters listed in the below Table an automatic optimization routine is available. The automatic

calibration routine is based on a multi-objective optimization strategy in which the four different calibration objectives given above can be optimized simultaneously.

Multi-objective calibration measures

In automatic calibration, the calibration objectives have to be formulated as numerical goodness-of fit measures that are optimized automatically. For the four calibration objectives defined above the following numerical performance measures are used:

- Agreement between the average simulated and observed catchment runoff: overall volume error.
- Overall agreement of the shape of the hydrograph: overall root mean square error (RMSE).
- Agreement of peak flows: average RMSE of peak flow events.
- Agreement of low flows: average RMSE of low flow events.

User specifications

The use can specify four criteria for the NAM auto-calibration module, these are :
- ➢ Calibration parameters
- ➢ Range of calibration parameters
- ➢ Objective functions
- ➢ Stopping criterion

Calibration parameters

The automatic calibration routine includes the 9 model parameters shown in the Table 4.1. The user specifies the subset of these parameters that should be calibrated automatically.

Range of calibration parameters

For the subset of NAM parameters to be calibrated automatically the user specifies the hypercube search space, i.e. lower and upper bounds on each parameter. The

range of the different parameters should reflect the prior knowledge of experienced values for the type of catchment being considered.

Default limits based on physical and mathematical model constraints and experienced values for a range of different catchments are provided in Table 4.4.

Table 4.4. Default limits for NAM parameters

Parameter	Unit	Lower Bound	Upper Bound
U_{max}	mm	5	35
L_{max}	mm	50	400
C_{KQF}	-	0	1
C_{KIF}	hours	200	2000
$CK_{1,2}$	hours	3	72
T_{OF}	-	0	0.99
T_{IF}	-	0	0.99
T_G	-	0	0.99
C_{KBF}	hours	500	5000

Stopping criterion

The stopping criterion for the optimization algorithm is the maximum number of model evaluations. For a model calibration that includes all 9 parameters, a maximum number of model evaluations in the range 1000-2000 normally ensures an efficient calibration.

Besides the user-defined stopping criterion, the optimization algorithm includes a parameter convergence criterion. In this case the optimization algorithm stops if the entire population of parameter sets in an optimization loop has converged into the same parameter values.

Calibration process

Most of the NAM parameters have empirical nature so parameters must be determined by calibration procedure.Generally it is recommended in the manual to

change only one parameter between each run and try to fit the observed and the simulated runoff. The NAM module have autocalibration mode for calibration procedure. But this mode is not enough for an accurate calibration. Generally model try to catch the parameters but sometimes the resulted parameters have no physical meaning for hydrological purposes.

Automatic optimization routine using multi-objective optimization strategy tries to fit by complex shuffled algorithm. All of the objectives can be selected or can be used one by one. It is easy to use but, evaluation of variable values required to judge hydrological sensibility. The best method to fit the simulated flow to the observed flow is the trial and error process by judging the hydrological sensitivity.

4.3. UHM module

UHM module simulates the runoff from single storm events by the use of the well known unit hydrograph techniques and constitutes an alternative to the NAM model for flood simulation in areas where no streamflow records are available or where unit hydrograph techniques have already been well established. The module calculates simultaneously the runoff from several catchments and includes facilities for presentation and extraction of the results. The output from the module can further be used as lateral inflow to the advanced hydrodynamic module in NAM Module. In the unit hydrograph module the excess rain is calculated assuming that the losses to infiltration can be described as:

- fixed initial and constant loss,
- proportional loss (the rational method)
- SCS curve number method.

The excess rainfall is routed to the river by unit hydrograph methods. The module includes the SCS-dimensionless hydrographs as well as facilities for establishing and management of databases with user defined unit hydrographs and time series of recorded rainfall and streamflow.

The loss model

During a storm a part of the total rainfall infiltrates the soil. A large part of the infiltration evaporates or reaches the river a long time after the end of storm as baseflow. Hence in event models as the present one, it is reasonable to describe the major part of the infiltration as loss. The amount of rain actually reaching the river, i.e. the total amount of rainfall less the loss is termed the excess rainfall.

The unit hydrograph module includes three optional methods for calculation of the excess rainfall. They are all lumped models considering each catchment as one unit and hence the parameters represent average values for the catchment.

4.3.1. Proportional loss

In this method the losses are assumed to be proportional to the rainfall rate and thus the excess rainfall is given by:

$$P_{excess} = a * A_f * P \tag{4.19}$$

where:

P_{excess} : Excess rainfall (mm/hr)

a : User defined run-off coefficient between 0 and 1

A_f : Areal adjustment factor

P : Rainfall (mm/hr)

4.3.2. Fixed initial loss and constant loss

Following this method no excess rainfall will be generated before a user specified initial loss demand has been met. Subsequently excess rainfall will be generated whenever rainfall rate exceeds a specified constant loss rate i.e. where:

$$P_{excess} = \begin{cases} 0 & ; for \ P_{sum} < I_a + I_c \bullet dt \\ A_f * P \bullet I_c & ; for \ P_{sum} > I_a \end{cases} \tag{4.20}$$

P_{excess} : Excess rainfall (mm/hr).

P_{sum} : Accumulated precipitation since start of storm event (mm).

I_a : User defined Initial loss (mm)

I_c : User defined constant loss rate (mm/h)

A_f : Areal adjustment factor

P   : Rainfall (mm/hr)

dt   : Calculation time step (hr)

To some extent this method accounts for the losses being highest at the start of the storm.

4.3.3. The SCS loss method

The U.S. Soil Conservation Service (SCS) developed this method for computing losses from storm rainfall in 1972. For the storm as a whole, the depth of excess precipitation or direct runoff (P_e) is always less than or equal to the depth of precipitation P; likewise, after runoff begins, the additional depth of water retained in the watershed, F_a, is less than or equal to some potential maximum retention S. There is some amount of rainfall I_a, (initial loss before ponding) for which no runoff will occur, so the potential runoff is $P-I_a$.

The hypothesis of the SCS method is that the ratios of the two actual to the two potential quantities are equal, that is

$$\frac{F_a}{S} = \frac{P_e}{P - I_a}$$
(4.21)

From the discontinuity principle;

$$P = P_e + I_a + F_a$$
(4.22)

which is the basic equation for computing the depth of excess rainfall or direct runoff from a storm by the SCS method.

By study of results from many small experimental watersheds, an empirical relation was developed. Combining equations (4.21) and (4.22) the basic equation used in this model is derived.

$$P_e = \frac{(P - I_a)^2}{P - I_a + S}$$
(4.23)

$$I_a = 0.2S \tag{4.24}$$

$$P_e = \frac{(P - 0.2S)^2}{P + 0.8S} \tag{4.25}$$

The potential maximum retention S is calculated from a dimensionless curve number (CN) using the empirical formula derived by SCS on the basis of rainfall runoff analyses of a large number of catchments.

$$S = ((1000 / CN) - 10) \bullet 25.4 (mm) \tag{4.26}$$

The curve number depends on the soil type, the land use and the antecedent moisture condition (AMC) at the beginning of the storm. CN varies between 0, resulting in no runoff, and 100 which generates an excess rain equal to the rainfall. For natural catchments normally $50 < CN < 100$.

The model operates with three different antecedent moisture conditions namely:

AMC(I) : Dry conditions close to wilting point.

AMC(II) : Average wet conditions close to field capacity.

AMC(III): Wet conditions close to saturation.

For each calculation time step the excess rainfall is calculated as the difference between the accumulated excess rainfall P_e at the start and the end of the time step.

CHAPTER 5

DETERMINATION OF EVENT BASED RUNOFF SOURCE AREAS USING CLASSICAL SCS METHOD COMBINED WITH TOPOGRAPHIC INDEX

5.1. Introduction

In hydrology curve number approach (CN) is used to determine how much rainfall infiltrates into a soil or an aquifer and how much rainfall becomes surface runoff. A high curve number means high runoff and low infiltration (such as in urban areas), whereas a low curve number means low runoff and high infiltration (such as dry soil). Recent studies were also showed that the curve number is mostly affected by land use and hydrologic soil group. Several studies have been done for the calculation of CN for a long time, however the discussions about CN and methodologies have not been completed yet. There are ongoing studies for the methodology and the affecting basin characteristics. In this chapter, a new methodological approach is proposed for the determination of CN for the same pilot basin. This chapter consists of four parts, in the first part (see Section 5.2), the study related with CN computation for event based simulations with UHM module of the model is described. The fractional area, initial abstraction and excess rainfall is calculated for the selected hourly events. The determination of the topographic index (TI) and the assumptions about the soil groups are explained in the second part (see Section 5.3). The TI value for each event is determined and the hydrological sensitive areas (HSA) are shown. In the third part (see Section 5.4), the classical SCS-CN method is used for the determination of CN of the events. Finally, in the fourth part, the results of two CN computation methodologies are compared and the results are discussed.

5.2. Determination of CN by event based simulations

The distributed CN–Variable Source Areas (VSA) method is a rainfall–runoff model that predicts the fraction of watershed that is saturated and the location of these areas. Predicting rainfall amount and size of the saturated area have been discussed previously by Steenhuis et al. (1995). A watershed can be divided into two parts, a saturated, runoff generating part and an unsaturated, infiltrating part. The traditional SCS-CN equation, in the typical form (Rallison, 1980) is given as

$$Q = \frac{(P - I_a)^2}{(P + S - I_a)} \qquad for P > I_a$$
$$Q = 0 \qquad for P \leq I_a \qquad (5.1)$$

where Q is the runoff depth (or excess rainfall) (cm), P is the precipitation (cm), S is the amount of water storage available in the soil profile or the maximum storage (cm), and I_a is initial abstraction (cm). Steenhuis et al. (1995) showed that Equation (5.1) can be differentiated to express the saturated fraction contributing runoff, A_f,

$$A_f = 1 - \frac{S^2}{(P_e + S)^2} \qquad (5.2)$$

where P_e is the effective precipitation (mm) and defined as (P- I_a) or the amount of water required to initiate runoff. It should be noted that, for this method, P_e is actually 'effective rainfall' but has been termed as effective precipitation for consistent terminology with Steenhuis et al. (1995). Traditionally, I_a is almost always set equal to 0.2S in the SCS-CN equation. Hawkins (1993) showed that using 0.2S for I_a did not result in good runoff prediction unless S was dependent on rainfall amounts. Steenhuis et al. (1995) calculated I_a as the amount of water needed to bring the shallowest soil to saturation and calculated moisture content for periods between runoff events using the Thornthwaite–Mather (TM) procedure (Thornthwaite and Mather, 1955, 1957; Steenhuis and van der Molen, 1986). The TM procedure assumes that above field capacity the evapotranspiration is at the potential rate and below field capacity the evapotranspiration decreases linearly with moisture content to zero when the soil is at the wilting point. Steenhuis et al. (1995) showed that S can be expressed as the ratio of the total volume of water that can be stored in the watershed between conditions where overland flow first occurs and the maximum

watershed saturation to the watershed total area. The traditional SCS-CN equation, modified to take into account these new, theoretically defensible, definitions of I_a and S, gave good results for watersheds in the north-eastern USA, especially considering that the method required little extra information relative to the more common application of the method (Steenhuis et al., 1995). The contributing areas are calculated by the Equation 5.2 and it predicts the fractional area of the watershed contributing to runoff without indicating important information about where that area is located in a watershed. Also, TI can be used to determine relative propensities for saturation within a watershed and are, in fact, the basis of the popular TOPMODEL (Beven and Kirkby, 1979). As discussed by Western et al. (2002), there are many instances where topographic index fail to capture spatial variation in patterns of soil moisture. However, this index was developed to predict zones of surface saturation and perform well in moderately wet periods when water distributions are strongly driven by topography (Western et al., 2002).

So for any event, if the I_a, Q, P_e and A_f is known, CN can be calculated by the Equation (4.25). The fixed initial loss and constant loss method of UHM module is used for the calculation of I_a, Q, P_e and A_f .Hourly rainfall events for the period of 2001-2005 were used for this study. The criterion for the selection of events is described below;

5.2.1. Selection of hourly events

After the analysis of observed hydrographs and rainfall hyetographs, 44 hourly events are selected to be used in the simulation studies for the whole period. These events consist of rainfall and snowmelt events. The thresholds that are used in the rainfall event selection process were 1,250,000 m³ for a total daily reservoir inflow and 30 mm for a total daily precipitation. After applying the selection thresholds 18 events were selected where 10 events for Kirazdere catchment, 4 separate events for Kazandere and Serindere catchments. The rainfall events are shown in Table 5.1.

Table 5.1. Selected hourly rainfall events for each catchment

Event Period	Event Recorded(X)		
	Kirazdere	**Kazandere**	**Serindere**
29-31 March 2002	**X**		
5-8 April 2002	**X**		
12-19 April 2002	**X**		
11-15 July 2002	**X**		
13-17 April 2003	**X**		
4-6 January 2004	**X**		**X**
9-10 June 2004	**X**	**X**	**X**
19-21June 2004	**X**	**X**	
23-25 June 2004	**X**	**X**	
05-10 Mar 2005		**X**	**X**
31May - 5June 2005	**X**		**X**

5.2.2. Hourly rainfall event simulations

Several simulations were done to find the initial abstraction and the uniform abstraction. The runoff values are simulated to match the observed runoff by trial and error method. As seen from the example graph of the simulation given in Figure 5.1, the peak values are nearly same but there is a difference between the simulated and the observed volume. Equation (5.2) was used in the calculation of A_f and the CN and S for each event is calculated by the Equation (5.3) and (5.4). After determination of CN for each event, an average CN was calculated by taking the average of all CN value of the events for each catchment separately. The results are shown in Tables 5.2 to 5.4 for each catchment.

$$Q = \frac{P_e^{\;2}}{P_e + S} \tag{5.3}$$

$$CN = \frac{2540}{S + 25.4} \tag{5.4}$$
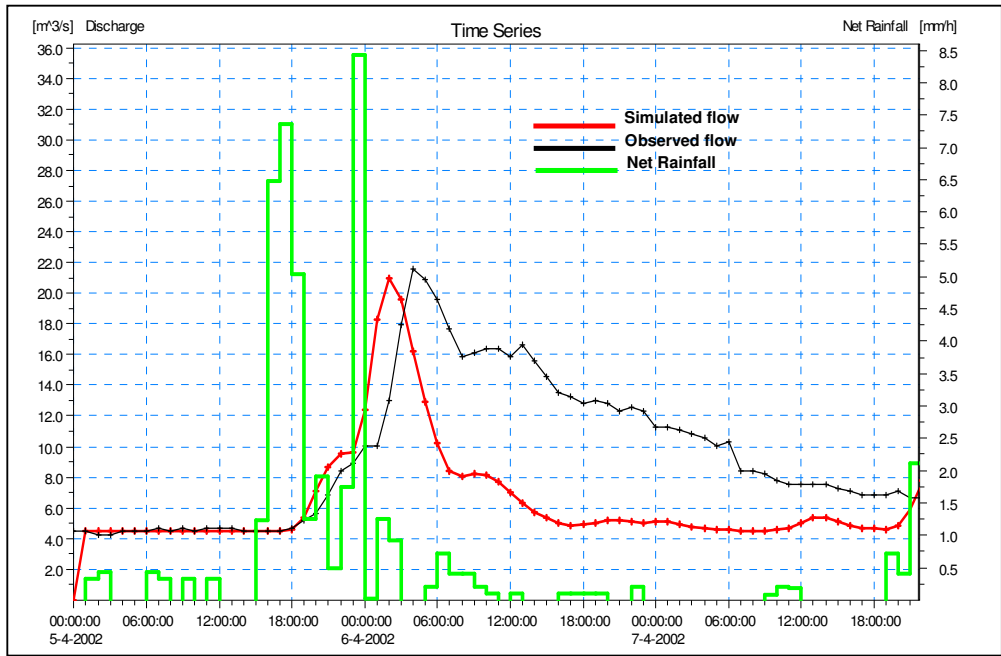
Figure 5.1. Example of a resulting graph with hourly event simulations by UHM module (05.04.2002-08.04.2002)

Table 5.2. Hourly event based simulation results for Kirazdere catchment

Event	P (cm)	Ia (cm)	Pe (cm)	Q (cm)	S	CN	Af (%)
9-10 June 2004	2,387	2,000	0,387	0,016	8,801	74,266	8,246
19-21June 2004	2,214	1,750	0,464	0,021	9,788	72,183	8,847
23-25 June 2004	2,123	1,600	0,523	0,030	8,595	74,718	11,143
29-31 March 2002	1,146	0,140	1,006	0,084	11,008	69,765	16,046
4-6 January 2004	2,502	1,500	1,002	0,088	10,407	70,936	16,794
12-19 April 2002	2,613	1,400	1,213	0,150	8,596	74,714	23,203
11-15 July 2002	1,925	0,500	1,425	0,220	7,805	76,494	28,494
31May - 5June 2005	5,691	3,800	1,891	0,352	8,268	75,443	33,764
13-17 April 2003	2,585	0,260	2,325	0,515	8,171	75,660	39,395
5-8 April 2002	4,886	1,460	3,426	0,855	10,302	71,144	43,684
				Average CN		**73,532 ~ 74**	

70

Table 5.3. Hourly event based simulation results for Kazandere catchment

Event	P Total Prec. (cm)	Ia Initial Abs. (cm)	Pe Excess Prec. (cm)	Q Direct Runoff (cm)	S	CN	Af (%)
19-21June 2004	1,742	1,350	0,392	0,015	9,852	72,05	7,51
9-10 June 2004	2,316	1,800	0,516	0,029	8,665	74,56	10,92
23-25 June 2004	0,667	0,013	0,654	0,057	6,850	78,76	16,67
05-10 Mar 2005	3,804	0,220	3,584	1,092	8,179	75,64	51,65

Average CN   75,25 ~ 75

Table 5.4. Hourly event based simulation results for Serindere catchment

Event	P Total Prec. (cm)	Ia Initial Abs. (cm)	Pe Excess Prec. (cm)	Q Direct Runoff (cm)	S	CN	Af (%)
19-21June 2004	0,455	0,100	0,355	0,010	12,248	67,47	5,55
4-6 January 2004	3,566	1,900	1,666	0,186	13,256	65,71	21,08
31May-05 June 2005	5,534	3,750	1,784	0,214	13,088	65,99	22,55
05-10 March 2005	3,728	0,020	3,708	0,997	10,083	71,58	46,55

Average CN   67,688 ~ 68

As seen from Tables 5.2 to 5.4, the average CN for Kirazdere catchment is about 73.5, for Kazandere 75.2 and for Serindere 67.7. These events are all rainfall events so the areal contribution of the events changes between 5.55% and 51.65%. When the CN values are examined, it can be seen that CN values of Kirazdere and Kazandere catchments are similar to each other but Serindere catchment CN is very different.

The resulting graphs of the hourly simulations are given in Appendix A. The model efficiency is tested with visual and statistical methods such as coefficient of

determination or Nash-Sutcliffe coefficient. The graphical evaluation includes comparison of the simulated and observed hydrograph, and comparison of the simulated and observed accumulated runoff. The numerical performance measures include the overall water balance error (i.e. the difference between the average simulated and observed runoff). The statistical results of all events for each sub-catchment are given in Table 5.5 to 5.7.

Table 5.5. Summary of simulations for Kirazdere catchment.

Simulation Period	NSE (Nash&Sutcliffe Eff.)	R²	Volume Difference (%)	Peak Difference (%)
29-31 March 2002	0.640	0.558	-5.27	2.81
5-8 April 2002	0.315	0.268	-33.67	-2.70
12-19 April 2002	0.593	0.632	-8.73	9.52
11-15 July 2002	0.714	0.731	-8.39	3.41
13-17 April 2003	0.801	0.817	-12.05	-3.06
4-6 January 2004	0.654	0.669	-8.92	-0.12
9-10 June 2004	0.889	0.921	-2.60	2.83
19-21June 2004	0.737	0.779	1.56	0.60
23-25 June 2004	0.581	0.599	-0.88	-3.87
31May - 5June 2005	0.670	0.691	-20.37	-2.23

Table 5.6. Summary of simulations for Kazandere catchment.

Simulation Period	NSE (Nash&Sutcliffe Eff.)	R²	Volume Difference (%)	Peak Difference (%)
9-10 June 2004	0.815	0.825	-19.90	5.48
19-21June 2004	0.475	0.482	-22.79	-3.57
23-25 June 2004	0.617	0.621	17.63	-3.45
05-10 Mar 2005	0.621	0.647	-47.23	4.49

Table 5.7. Summary of simulations for Serindere catchment.

Simulation Period	NSE (Nash&Sutcliffe Eff.)	R²	Volume Difference (%)	Peak Difference (%)
4-6 January 2004	0.475	0.489	-12.27	9.07
19-21June 2004	0.699	0.720	-6.46	5.10
05-10 Mar 2005	0.776	0.787	-13.79	-0.78
31May - 5June 2005	0.201	0.209	-62.68	6.05

Statistical analysis generally yields high goodness of fit for all sub-catchments. The model efficiencies are higher than 0.6 at least for half of the events for all of the sub-catchments. Either the percent peak and volume percent difference or model efficiency is in the acceptable ranges for almost all simulations.

5.3. Determination of TI for each event

TI is a characteristic of the basin where areal contribution and slope of basin is used to define saturated areas. TI has been used successfully to predict the location of surface saturated areas, water table elevations and subsurface flow conditions. TI can be used to represent the relative likelihood of saturation of the overburden at a given location by subsurface flow from further upslope.

In its most basic form, the TI, for any point in a watershed, is defined as the natural log of the area of the upslope watershed per unit contour length "a" divided by the local surface topographic slope (m), tan (β), from an elevation map. Soil depth and saturated hydraulic conductivity can be included in the index using the following relationship in the case of shallow soils.

$$TI = \ln\left(\frac{\sum a}{\tan(\beta)D\hat{K}_s}\right) \tag{5.5}$$

where D is the depth of the soil (m) and K_s is the mean saturated hydraulic conductivity (m/hour). Locations with a large TI are more prone to saturation than locations with a small TI. At a minimum, a digital elevation model (DEM) is needed to determine a and tan (β). The fractional area of watershed that is saturated for a given storm event can be used to determine a critical TI value below which areas are infiltrating and above which areas are saturated and runoff is generated. This is done by assuming that areas saturate in order from highest to lowest TI value. The fractional area of each event was calculated in the previous section (Section 5.2).

For the calculation of modified TI, the flow accumulation map, slope map and map of mean saturated hydraulic conductivity values with respect to soil groups are

required. Therefore, as a first step, slope map of the basin is formed using the DEM as described in chapter 3. The slope is an important parameter in the calculation of TI. The range of slope is between 0 - 74.58 degrees and they are transformed to radians in order to be used in the calculations.

The steps how to form flow accumulation map were explained in the third chapter. The flow accumulation values are used to determine the number of drained cells to the corresponding cell.

After forming the flow accumulation map and slope map, the next step is the formation of mean saturated hydraulic conductivity with respect to soil groups map. The details of the study and analysis of the soil groups is described in Section 5.3.1;

5.3.1. Soil type groups

As mentioned in the third chapter, soil investigations were done in the basin by taking 32 soil in situ data. The depth of the soil sample point is 80 cm. Soil samples were taken for four layers as 0-20cm, 20-40 cm, 40-60 cm, 60-80 cm. The number of the soil samples in Serindere catchment is more than the ones in Kirazdere and Kazandere. The location of the soil samples in each catchment is shown in Figure 3.4 and the number of soil samples in each catchment is given in Table 3.1.

The soil types are grouped according to their conductivity values. First of all, the Conductivity (K_s) values of the soils are tabulated, in this categorization, the K_s value for the 0-20 cm, and Geometric Average of K_s values for four layers (0-80 cm) and Geometric Average of K_s values for 2 layers (40-80 cm) are used. The relation between the soil types and K_s values is more significant for the Geometric Average of the third and forth layers, 40-80 cm. compared to whole soil layer. On the other hand, for some of the soil sample locations 'no data' is obtained as can be seen in Table 5.5. The soil samples can not be taken from the hard rock under the soil. This restriction of measurement for 40-80 cm layer led to the usage of K_s values for the whole layer of 0-80 cm during the study.

Table 5.8. K_s value, main rock type of the points of soil sample locations

HOLE ID	K_s Value (0-20 cm)	Geometric Average of K_s (0-80 cm)	Geometric Average of K_s (40-80 cm)	Main Rock Type
1	133.7	9.42	1.53	Andesite-Basalt
2	145.8	9.88	6.28	Andesite-Basalt
3	249.5	10.81	1.19	Andesite-Basalt
4	134.6	134.6	No data	Andesite-Basalt
5	14.3	12.2	8.09	Andesite-Basalt
6	228.6	0.81	0.05	Andesite-Basalt
7	151.9	23.65	10.91	Andesite-Basalt
8	28.2	5.21	0.95	Andesite-Basalt
9	2.9	28.31	31.12	Andesite-Basalt
10	101.8	101.8	No data	Andesite-Basalt
11	25.6	25.6	No data	Andesite-Basalt
12	149.5	81.07	142.15	Alluvium
13	363.8	97.62	30.99	Andesite-Basalt
14	137.1	137.1	No data	Schist-Marble
15	174.2	14.32	4.26	Marble
16	456.7	63.43	21.45	Ophiolite
17	280.7	72.21	26.3	Shale
18	132.4	35.84	No data	Marble
19	91	51.19	No data	Ophiolite
20	72.5	5.4	2.26	Schist-Marble
21	249.5	35.08	14.02	Meta-Basalt
22	228.6	62.73	25.23	Shale
23	233.9	125.51	No data	Ophiolite
24	772.7	68.95	11.66	Shale
25	213.8	63.58	19.42	Shale
26	15.4	2.62	1.27	Alluvium
27	109.4	20.89	10.49	Melange
28	3.7	2	2.18	Alluvium
29	29.7	2.3	1.53	Alluvium
30	112.33	140.26	No data	Schist-Marble
31	28.17	28.17	No data	Schist-Marble
32	143.17	3.3	0.4	Dolomite-Limestone

As seen in Table 5.8, the soil with the same main rock type has different conductivity values. The conductivity values for "sm" are changing in between 140.26 and 5.4 which indicate a significant change in the values. To make a new grouping, the K_s values are plotted on a graph according to their soil types. The soil grouping is done by looking at the minimum value of K_s for each soil type, the soil types that have

same or near minimum K_s value are taken as one soil group. The mean value of all the soil types K_s value is taken as the K_s value of that soil group. The grouping process results with 6 soil groups as shown in Table 5.9.

Table 5.9. New soil group which forms after grouping

Soil group	K_s(m/Hr)
Andesite-Basalt, Alluvium, Dolomite-Limestone	0.324
Marble	0.251
Ophiolite, Shale	0.725
Schist-Marble, Limestone-Marl	0.777
Melange	0.209
Meta-Basalt	0.351

5.3.2. Calculation of TI and redistribution for each sub-catchment

The TI is formed by its formula as shown in Equation 5.5 with the help of the maps that was previously prepared. The resulting map for the TI is shown in Figure 5.2.
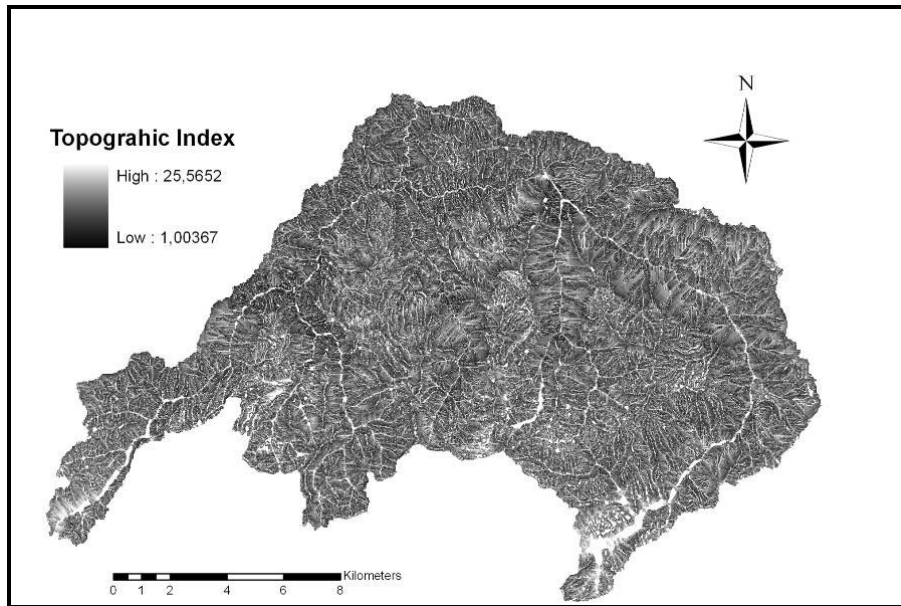
Figure 5.2. TI map of Yuvacık basin

The fractional area A_f for each event of the relevant sub-catchment was calculated in section 5.2. The HSAs of each event can be shown by the help of the fractional area. The needed thing is the graph of the relation between TI and fractional area. The TI

76

map is in raster format, so floating values of cells were converted to integer values by using Raster Calculator of Spatial Analyst extension. The reason for performing this transformation was to decrease the amount of cells that have different values. This transformed TI map was converted to shape file through the Spatial Analyst. In order to summarize the area values of polygons with the same TI values, shape file was converted to coverage. Summarized area values were exported to a dbf file. This file was manipulated with Microsoft Access and TI vs. A_f of the catchment was created and shown in Figure 5.3. The TI values for each event are presented in Tables 5.10 to 5.12.
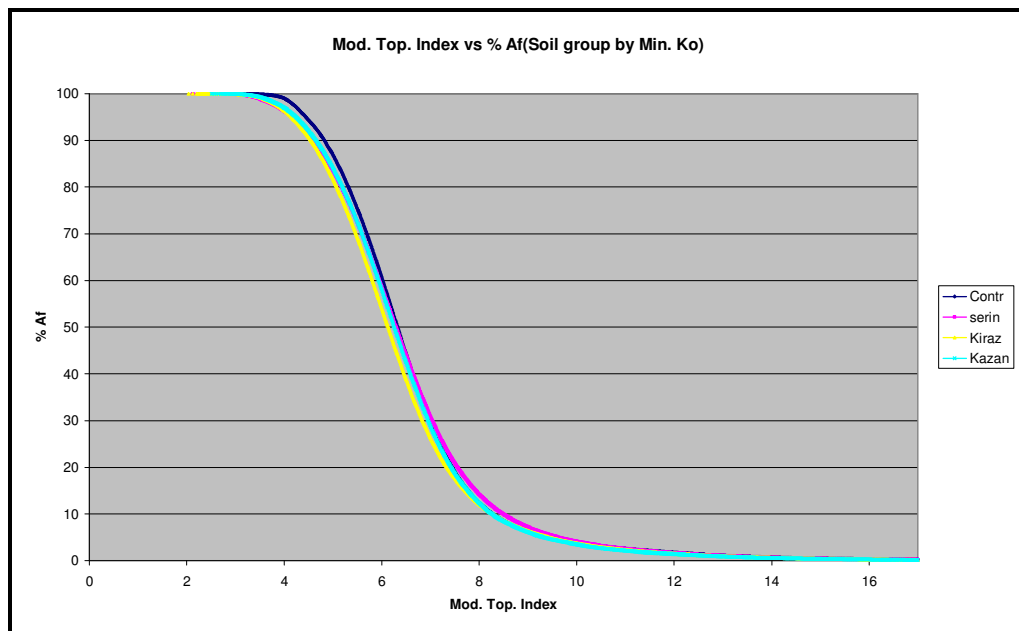
Figure 5.3. Resulting graph of fractional area vs. TI

Table 5.10. TI and A_f Values for each event in Kirazdere catchment

Event	Q (cm)	S	CN	Af (%)	TI
9-10 June 2004	0,016	8,801	74,26	8,25	7,650
19-21June 2004	0,021	9,788	72,18	8,85	7,530
23-25 June 2004	0,03	8,595	74,71	11,14	7,210
29-31 March 2002	0,084	11,008	69,76	16,05	6,740
4-6 January 2004	0,088	10,407	70,93	16,79	6,690
12-19 April 2002	0,15	8,596	74,71	23,20	6,310
11-15 July 2002	0,22	7,805	76,49	28,49	6,070
31May - 5June 2005	0,352	8,268	75,44	33,76	5,870
13-17 April 2003	0,515	8,171	75,66	39,39	5,670
5-8 April 2002	0,855	10,302	71,14	43,68	5,530

Table 5.11. TI and A_f values for each event in Kazandere catchment

Event	Q (cm)	S	CN	Af (%)	TI
19-21June 2004	0,010	9,852	72,05	7,51	7,620
9-10 June 2004	0,186	8,665	74,56	10,92	7,110
23-25 June 2004	0,214	6,850	78,76	16,67	6,600
05-10 Mar 2005	0,997	8,179	75,64	51,65	5,200

Table 5.12. TI and A_f Values for each event in Serindere catchment

Event	Q (cm)	S	CN	Af (%)	TI
19-21June 2004	0,010	12,248	67,46	5,55	8,400
4-6 January 2004	0,186	13,256	65,70	21,08	6,530
31May-05 June 2005	0,214	13,088	65,99	22,55	6,450
05-10 March 2005	0,997	10,083	71,54	46,54	5,540

The HSAs of the basin for each specific event is formed and an example is shown in Figure 5.4 where the figure corresponds to the event occurred at 19-21 June 2004 in all three subcatchments. The threshold TI value for this event is 7.62, 7.53, 8.40 for Kazandere, Kirazdere and Serindere catchments respectively. The blue colored areas are the HSAs of which the TI value of the corresponding cell is greater than the TI value of the specific event. These areas can also be used in the water pollution studies in the basin where the runoff generating areas have great importance.
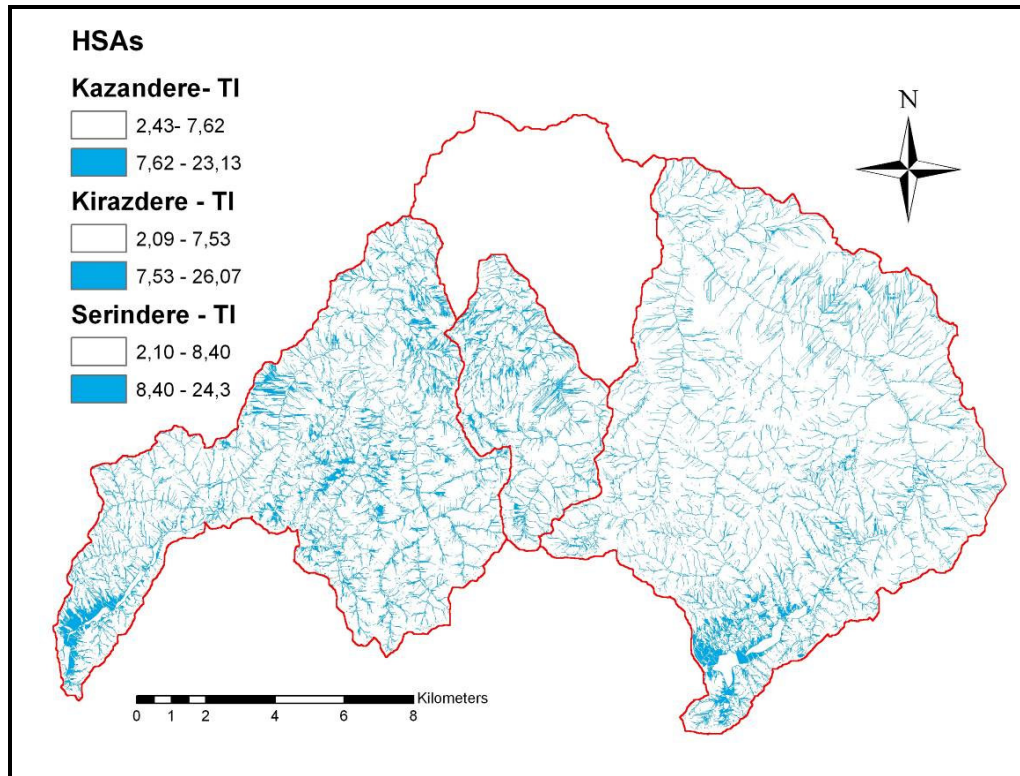
Figure 5.4. Representation of HSAs for 19-21 June 2004 event

5.4. Determination of CN by classical SCS-CN method

The determination of CN values for all of the selected rainfall events have been done in the previous section. The difference and reaction of each sub-catchment to the same event is important to see the difference between two sub-catchments. So in this part of the study just the events that the have same periods at least in two sub-catchments are selected. Due to the fact that most of the probable water would come from the HSAs, HSAs are generated by the help of the TI. So the rest of the study focus to the HSAs and the study has been done just for the HSAs. The selected events are presented in Table 5.13.

Table 5.13. Selected events for each sub-catchment

Catchment	Kirazdere	Kazandere	Serindere
Similar Events	(19-21June2004)	19-21 June 2004	19-21 June 2004
	(9-10June2004)	09-10 June 2004	-
	(23-25June2004)	23-24 June 2004	-
	-	05-10 March 2005	05-10 March 2005
	(31May-5June 2005)	-	31May-05 June 2005

The soil, geology and land use values under each HSA is used in the calculation of CN by classical SCS-CN method. The soil, geology and land use map is converted to raster format and the "intersect" method of Arc MAP (ESRI, 2005) is used to assign a value to the map.

As seen from the Table 3.3 for land use, there are 4 main land use types which are agricultural, meadow, bad forest and good forest areas. The afforestation areas are taken as thin cover areas. The highest area belongs to the good forest type where it means that the area is highly vegetated. This is also verified by the NDVI map of the basin.

The soil type is another important parameter which affects the resulting CN value for each catchment. The soil sample results are analyzed and depending on the silt, clay and sand amount in the soil, new soil groups are formed. There exists 3 soil groups as shown below. The characteristics of tk and al are different than others, so there are in identical groups.

1. *Soil group*
Andesite-Basalt, Meta-Basalt, Ophiolite, Marble, Shale, Dolomite-Limestone
2. *Soil group*
Melange
3. *Soil group*
Alluvium

The next step is to find the CN value of each cell for the defined Antecedent Moisture Condition (AMC) of the soil. To simplify the method the AMC II is used for the initial moisture conditions of the soil. The Table of AMC II which is shown in Table 5.14 is used for the determination of CN value.

Table 5.14. CN values for AMC II

Main Usage	Soil Group			
	A	**B**	**C**	**D**
Agricultural	67	77	83	87
Meadow	30	58	71	78
Woods(Thick cover)	30	55	70	77
Woods(Thin cover)	43	65	76	82

The 1st soil group is assigned to group B, 2nd soil group is assigned to group B and 3rd soil group is assigned to group A. For the determination of a CN value for each cell, first soil and land use map is converted to raster format. The maps are then intersected within each other. Then SQL query method is used to assign a value for each cell. After assigning a value, the average CN value is found by taking the average CN value which is defined for each cell in each specific catchment. The resulting CN for each catchment is presented in Tables 5.15 to 5.17.

Table 5.15. CN values found by SCS-CN Method for Kirazdere catchment

Event	CN value
9-10 June 2004	72.11
19-21 June 2004	73.41
23-25 June 2004	73.93
31May – 5 June 2005	73.44
Average	**73.22 ~ 73**

Table 5.16. CN values found by SCS-CN Method for Kazandere catchment

Event	CN value
19-21 June 2004	73.18
09-10 June 2004	73.1
23-24 June 2004	72.15
05-10 March 2005	72.33
Average	**72.69 ~ 73**

Table 5.17. CN values found by SCS-CN Method for Kazandere catchment

Event	CN value
19-21 June 2004	70.47
31May-05 June 2005	70.33
05-10 March 2005	73.65
Average	**71.48 ~ 71**

5.5 Comparison of CN values and discussion

This study suggests one way of determination of CN values by combining TI and fractional area. Also it was seen that combining the traditional SCS-CN method with spatial distribution of a modified TI will help to form a simple method to predict the location of runoff areas. Calculation of the TI and calculation of Areal fraction of the basin can lead us to find the CN of the basin for a specific event. This can be developed as a new methodology where CN values are calculated from TI and areal fraction values.

The two CN values which were found by UHM module of model and Classical SCS-CN method are presented in Tables 5.18 to 5.20. The values that are found by two methods are consistent. The CN values found by initial abstraction method for Kirazdere and Serindere catchments are different from each other, which means that the basin characteristics are different. The difference can not be realized in the CN

values which are determined by GIS analysis because the soil and land use data are not different within two catchments.

Table 5.18. Comparison of CN values for Kirazdere catchment

Event	CN found by UHM Method	CN found by Analysis	Af (%)	TI
(9-10Jun2004)	74.27	72.11	8.25	7.65
(19-21Jun2004)	72.18	73.41	8.85	7.53
(23-25Jun2004)	74.72	73.93	11.14	7.21
(31May-5Jun2005)	75.44	73.44	33.76	5.87
Average	**73.53 ~ 74**	**73.22 ~ 73**		

Table 5.19. Comparison of CN values for Kazandere catchment

Event	CN found by UHM Method	CN found by Analysis	Af (%)	TI
19-21 Jun 2004	72.05	73.18	7.51	7.62
09-10 Jun 2004	74.56	73.1	10.92	7.11
23-24 Jun 2004	78.76	72.15	16.67	6.6
05-10 Mar 2005	75.64	72.33	51.65	5.2
Average	**75.25 ~ 75**	**72.69 ~73**		

Table 5.20 : Comparison of CN values for Serindere catchment

Event	CN found by UHM Method	CN found by Analysis	Af (%)	TI
19-21 June 2004	67.47	70.47	5.55	8.4
31May-05 June 2005	65.99	70.33	22.55	6.45
05-10 Mar 2005	71.58	73.65	46.55	5.54
Average	**67.69 ~ 68**	**71.48 ~71**		

The simulations are performed again for examining the effect of the CN value difference with average CN values which are found from different CN studies. The resulting simulation graph is given in Figure 5.5. The difference between the two CN values corresponds to 6% volume difference and 4% peak difference.
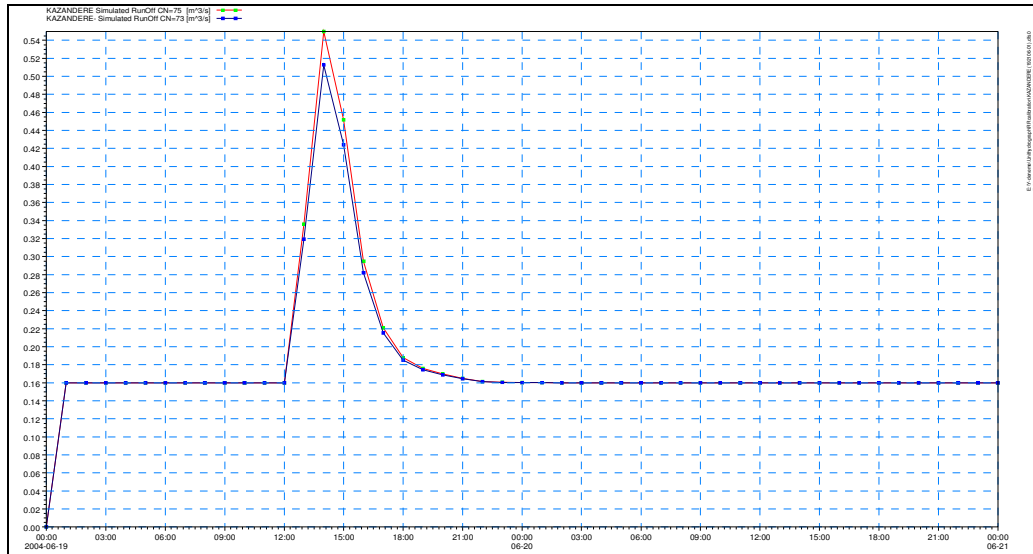
Figure 5.5. Comparison of the simulation graphs

CHAPTER 6

DAILY SNOWMELT EVENTS WITH MIKE11 NAM MODULE

6.1. General

In this study Mike11 NAM module is used as the hydrological model. The detailed description of the model is given in the fourth chapter (see Section 4.2).

As mentioned in the third chapter, all of the available hydrological and meteorological data of the Yuvacık basin are collected and processed. Daily mean values of data and monthly evaporation data are used as input in the model.

Model run (simulation) periods

Most of the high runoff peaks were recorded in winter and spring season in 2001-2006 due to snow melt, so this study focuses on the period starting from December up to May, where snowmelt is very effective in rainfall-runoff process. The simulated periods for each catchment are shown in Table 6.1. Some of the periods are used for the calibration of the model and some of them are used as shown in bold for the validation of the results. As it can be seen from Table 6.1 that, Kazandere and Serindere basins do not have runoff data continuously from 2001-2005. This is because of the missing records due to the discontinuities in the measurement devices.

Table 6.1. Simulation periods used for modeling

Period	Kirazdere	Kazandere	Serindere
2001-2002	20/11/01-10/12/01 09/12/01-15/01/02 15/01/02-15/03/02 15/03/02-15/04/02		
2002-2003	**15/12/02-16/01/03** **15/01/03-16/03/03** **15/03/03-22/04/03**	20/03/03-18/04/03	20/12/02-15/01/03 **03/02/03-20/02/03** 20/03/03-22/04/03
2003-2004	21/12/03-09/01/04 19/02/04-15/03/04	21/12/03-09/01/04 19/02/04-15/03/04	17/12/03-06/01/04
2004-2005	16/01/05-13/02/05 13/02/05-15/03/05	**16/01/05-13/02/05** 15/02/05-15/03/05	16/01/05-13/02/05 13/02/05-15/03/05
2005-2006	01/02/06-10/03/06 10/03/06-10/04/06	01/02/06-10/03/06 10/03/06-10/04/06	01/02/06-10/03/06 10/03/06-10/04/06

Rainfall distribution

Available rainfall data of all the recording stations are used to find daily areal mean rainfall of the catchments. For the period of 2001-2005 water year Inverse Distance Weighted method is used for distributing the rainfall and for 2006 water year, thiessen polygon method is used. The thiessen polygons method is selected within the hydrological model internally and checked by ARC-GIS program. The station weights that is used for each catchment is shown in Table 6.2 for the period of 2001-2005 and in Table 6.3 for the period of 2005-2006. As mentioned in the third chapter, the available rainfall data is recorded by TWT from the stations RG1-RG6. The stations are close to each other, so there is a high correlation between them. HO station is in a high elevation (900 m) and KE is in a low elevation (76 m). Those two stations (KE, HO) is included in this study for representing the higher and lower elevations for the sub-catchments.

Table 6.2. Station thiessen weights for the period of 2001-2005

Kirazdere		Kazandere		Serindere	
Gage	Weight	Gage	Weight	Gage	Weight
RG3	0.5163	RG2	0.4423	RG4	0.8356
HO	0.4243	RG5	0.4925	HO	0.0922
KE	0.0595	HO	0.0428	KE	0.0722
		KE	0.0224		

Table 6.3. Station thiessen weights for the period of 2005-2006

Kirazdere		Kazandere		Serindere	
Gage	Weight	Gage	Weight	Gage	Weight
HO	0.211	M1	0.30	RG4	0.34
M1	0.020	RG5	0.11	RG7	0.07
M2	0.476	RG7	0.21	RG10	0.59
M3	0.148	RG8	0.38		
RG3	0.043				
RG8	0.102				

Since the TWT rainfall stations (RG1-RG6) are recording stations in scada system and recording the data at 5 minutes time intervals, these data are converted to daily cumulative values to use in the model.

Elevation zones

Also as mentioned in the fourth chapter, the catchments are divided into three elevation zones as shown in Table 6.4.

Table 6.4. Elevation bands for each catchment

Catchment	Zone ID	Elevation Range	Average Elev. (m)	Area (km²)	Area (%)
Kirazdere	1	179 - 550	350 (428)	7.57	9.52
	2	550 - 900	725 (820)	27.839	35.00
	3	900 - 1312	1106 (978)	44.126	55.48
			Total Basin Area	**79.535**	**100**
Kazandere	1	186.4 - 600	393 (441)	4.589	19.87
	2	600 - 1000	800 (800)	8.103	35.08
	3	1000 – 1347.1	1173 (1157)	10.407	45.05
			Total Basin Area	**23.099**	**100**
Serindere	1	272.2 - 700	486 (580)	16.762	13.91
	2	700 - 1100	900 (884)	69.275	57.48
	3	1100 – 1546.7	1323 (1182)	34.474	28.61
			Total Basin Area	**120.51**	**100**

As seen from Table 6.4, the elevation ranges are selected as 300-350 meter intervals. These elevation ranges are found after several tries. The average elevation of an elevation zone can be considered as the average altitude of that elevation zone; but the hypsometric mean altitude, by considering the area factor in it, is more representative for an average elevation. Therefore, the hypsometric curve of each elevation zone is derived from the hypsometric curve of each catchment and the elevation which corresponds to 50% area is selected as hypsometric mean elevation. The hypsometric curve for the whole basin is presented in chapter 3. These values are provided in the same Table within the parenthesis. The representation of each elevation band with in each catchment is carried to the GIS environment and shown in Figure 6.1.
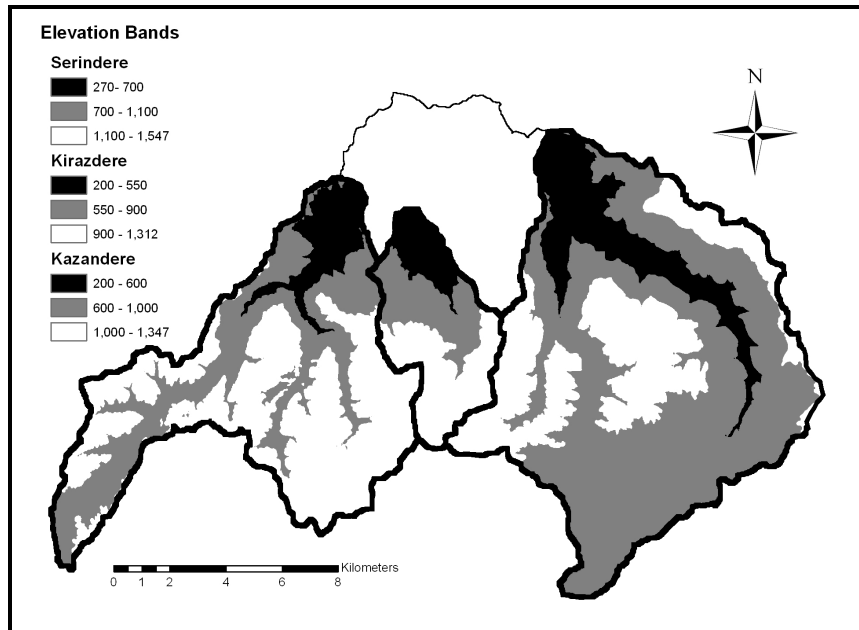
Figure 6.1. Elevation bands for each catchment

Snow water equivalent (SWE)

As mentioned before snow melt is very effective in rainfall-runoff process. The snow water equivalent for each elevation band must be specified so that the effect and amount of snowmelt on runoff can be shown correctly. As mentioned before in third chapter, the snow depth measurement was not done by the earlier raingauge stations. Just the rainfall and flow are recorded. No measurement was done to analyze the relation between the rainfall and snow depth, nor for the relation between the temperature and snow depth. So defining the snow depth and related snow water equivalent value for each elevation band is very complicated issue in the basin which is attempted in this study.

The only snow depth measurement was done in HO station which is operated by DSI for the period of 2001-2005. But in this station no measurement was done for the snow water equivalent. Although the snow water equivalent value is not known, because of being the only station, the measured snow depth data is very valuable for the study.

89

After the installation of new rainfall stations, snow depth measurements are being carried by TWT for the 2006 water year. Although the records are just for one year, they are very valuable. Also we have the snow depth measurements at HO station. So we have the chance to compare the snow depths in the basin for 2006 water year. Also three field study was done for the snow depth and snow water equivalent relation in the basin in 2006. The results of the field work are shown in Table 6.5, As seen from the Table 6.5, no snow measurement was done in Kartepe (RG9) station. This is because of the non accessible roads by winter conditions. The snow density is between 14% at RG10 (elevation 805 m) lowest at 02.02.2006 and 45% at RG7 (Elevation 700 m) highest at 23.02.2006.

Table 6.5. Measured snow depth and density in Yuvacık basin

Measurement Date	Measurement Place	Elevation (m)	Snow Depth (mm)	Snow Density (%)	Min. Snow Cover Altitude
26.12.2005	Tepecik(RG7)	700	221	18	172
27.12.2005	Çilekli(RG10)	805	102	25	172
26.12.2005	Aytepe(RG8)	953	441	16	172
02.02.2006	Tepecik(RG7)	700	648	24	-
02.02.2006	Çilekli(RG10)	805	178	**14**	
02.02.2006	Aytepe(RG8)	953	1372	30	-
23.02.2006	Tepecik(RG7)	700	954	**45**	690
23.02.2006	Çilekli(RG10)	805	114	22	690
23.02.2006	Aytepe(RG8)	953	1158	42	690

The snow measurements were being done at four permanent stations (RG7, RG8, RG9,and RG10) automatically in 5 minutes time intervals and daily in HO station by manual measurement. The elevation of the stations RG7, RG8, RG9, RG10, HO are 700, 953, 1487, 805, 900 meters respectively. When we look at the hypsometric mean elevations of each catchments, we can see that the mean elevations differ from catchment to catchment and does not coincide with the elevations of snow measurement stations. So this forces us to make several assumptions for the snow

depths and snow water equivalent for each elevation band. The study is described for Kirazdere catchment and a similar methodology is followed for the other two catchments.

As seen from the Figure 6.2, although the elevation difference is about 50 meters between the RG8 and HO stations, the snow depth between the two stations is about twice. This is an interesting thing to be studied. Several tries were done to estimate the snow depth for each band for 2001-2005 periods. The only measurement is in HO station. At the end it was seen that taking snow depth of HO station for the first elevation band provides a good trial. Then comes the problem of the snow water equivalent. On the basis of the measurements which were done in 2006 showed that 30-35% can be accepted as the snow water equivalent value for the catchment. When the simulation start time is in snow depositing period, the SWE is taken as %30, and when it is in melting period the SWE is taken as 35%. The studies on snow showed that the snow water equivalent change is about 60-67%, for each 300-350 meter elevation difference. So the SWE for the second and the third band is found by increasing the first band SWE value by 60-67% for each 300-350 meter elevation difference.
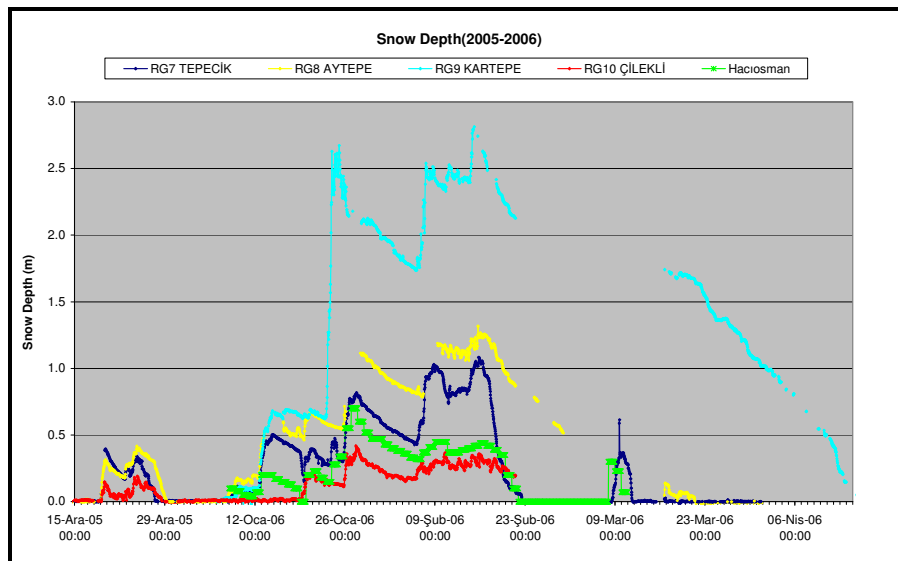

Figure 6.2. Measured snow depths in snow stations

For the simulations of 2006 water year the SWE value is also taken as 30-35%. After several tries, the snow depth of each elevation band is as follows;

1. Band   Snow depth of RG10 Çilekli station
2. Band   Average of snow depth of RG7 Tepecik and RG8 Aytepe stations
3. Band   Snow depth of RG8 Aytepe station.

Change in temperature with altitude

The altitude dependent snow model in hydrological models operates with three meteorological reference time series; precipitation, temperature and potential evapotranspiration. We do not have the opportunity to measure the temperature in the whole basin for each altitude variations. So in order to account for the large variations temperature with altitude the reference series can be adjusted for each altitude zone in two different ways

> lapse rate corrections
> individual correction factors applied for each zone

Lapse rate corrections

The lapse rate correction approach is a very simple but powerful way of adjustment in which the temperature and the precipitation are assumed to vary linearly with the altitude. The only input data required are the average altitude of the various zones, a reference altitude of the time series, and the lapse rates. The temperature lapse rates, however, are known to be quite variable, ranging from high values under dry conditions to lower values under wet conditions. Hence, in some models (in case of Mike 11) it is possible to specify two different temperature lapse rates to be used during dry and wet weather conditions, respectively. The model applies the "wet" lapse rate during days with precipitation larger than 10 mm and the "dry" lapse rate during the rest of the time (DHI, 2004). The temperature in each zone is adjusted by Equation 4.8.

Determination of the Temperature Lapse Rate of Yuvacık Dam Basin

Yuvacık dam drainage area is a mountainous basin. Because of the high elevation difference, the catchments are divided into three elevation zones to help the hydrological model. The temperature measurements in the basin are not available before the start of the project. In the nearby stations the only available temperature data is in the Kocaeli (76 m altitude) which is being operated by DMI. After the initiation of the project, 7 new stations were installed in the basin. The temperature is very important for the snow melt and snow melt runoff in the basin. So the temperature difference with altitude that is to say temperature lapse rate must be derived from the measurements of new installed stations data. In literature the lapse rate ranges in between (-)0.5-0.7 $^{\circ}$C per 100 m elevation increase. The average of all of these stations temperature data is calculated for the period of January 06,2006 to April 24,2006. The results of the study are presented on the following pages.

Table 6.6. Temperature lapse rate per 100 m elevation increase

Station (Altitude)	Kartepe (1487 m)	Aytepe (953 m)	M2 (915 m)	Çilekli (805 m)	M1 (732 m)	Tepecik (700 m)	M3 (546 m)	Avg. Lapse Rate of all stations to Kocaeli
Kocaeli	-0.63	-0.61	-0.69	-0.68	-0.58	-0.49	-0.5	
M3	-0.69	-0.74	-0.95	-1	-0.8	-0.47	**0**	
Tepecik	-0.74	-0.9	-1.29	-1.79	-2.35	**0**	-0.47	
M1	-0.67	-0.69	-1.11	-1.54	**0**	-2.35	-0.8	**-0.60**
Çilekli	-0.57	-0.27	**0.35**	**0**	-1.54	-1.79	-1	
M2	-0.53	**1.29**	**0**	0.35	-1.11	-1.29	-0.95	
Aytepe	-0.57	**0**	1.29	-0.27	-0.69	-0.9	-0.74	
Kartepe	**0**	-0.57	-0.53	-0.57	-0.67	-0.74	-0.69	
Avg. Lapse Rate of all stations to Kartepe	**-0.63**							

As seen from the Table 6.6, most of the lapse rate between the stations is negative with the elevation increase as expected. But for two stations the value is positive. This can be due to measurements of different sensors. The consistency between the values of Kocaeli station with respect to all stations and the Kartepe station with respect to all stations is very good. The range is between -0.53 to -0.74 for Kartepe

station. The range is – 0.49 to -0.68 for Kocaeli station. And when the average of all these values for each station is calculated, the value of -0.60 is found for Kocaeli station and -0.63 is found for Kartepe station. The Kocaeli station is operated by DMİ so the data transfer from this station will not be easy, so it is not selected as the base station. The M1,M2 and M3 stations are mobile stations, so they will be removed (at least two of them) from the basin. The Kartepe station is not selected especially for the bad road conditions in winter. So the only station which is near to the average of the Kocaeli station is the Aytepe (953 m) station with a value of -0.61 per 100 meter. This station is selected as the base temperature station for the basin. The Dry Lapse rate is taken as $-0.6\,^{o}C/100$ meter. The wet lapse rate is taken as $-0.4\,^{o}C/100$ meter for the basin because of the best fit of several simulations done for the basin.

The real values of all stations and the values that is calculated by the $-0.6\,^{o}C/100m$ dry lapse rate from Aytepe Temperature values is plotted graphically and is shown in shown in Figure 6.3. The best fit is observed in the graph of Kocaeli station as expected. Because as seen from the Table 6.6, the average value of Aytepe with respect to Kocaeli station ($-0.61\,^{o}C$) is very near to the average value of Kocaeli with respect to all stations. Also the M3 station graph fits well with the values of Aytepe station after the application of lapse rate. The resulting graphs for the -0.6 temperature lapse rate are presented in Figure 6.3.

Also the hydrological model needs a value for the wet temperature lapse rate which is the lapse rate used where there is more than 10 mm precipitation. In literature the values of wet temperature lapse rate is between $(-)0.3-0.5\,^{o}C$, so $-0.4\,^{o}C$ value is used as the wet temperature lapse rate.
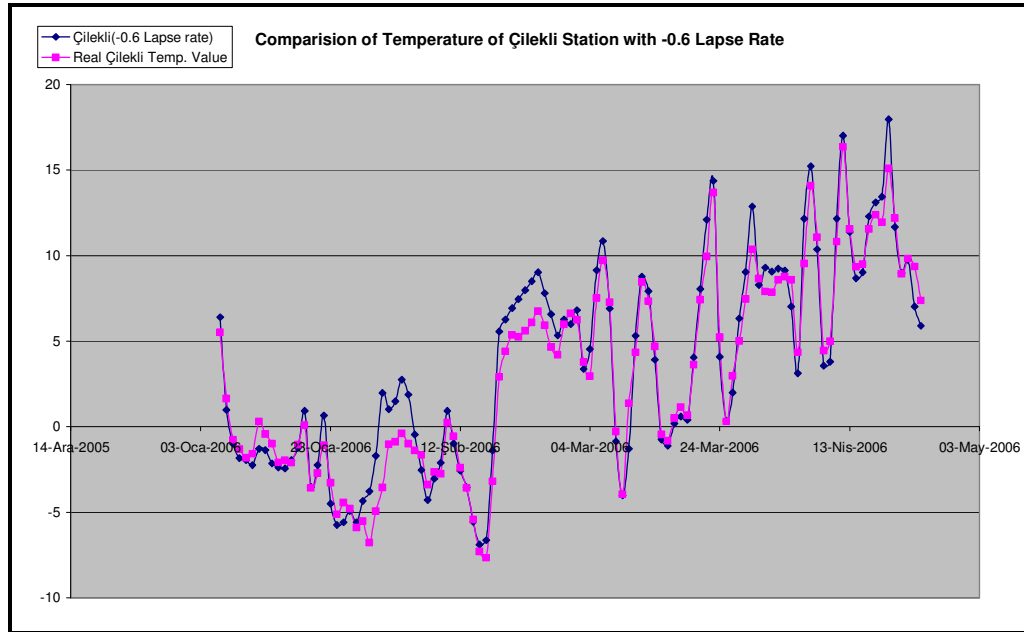
Figure 6.3. Comparison of the real air and lapse rate modified temperature for RG8

As seen from the Figure 6.3, the largest difference occurs between January 30 and March 1. The other graphs that compare the lapse rate temperature and the real measured temperature is given in Appendix D.

Selection of base temperature station

The hydrological model needs a base temperature station and its elevation for the simulation. For the 2001-2005 periods, the only temperature measurement is in Kocaeli station, so Kocaeli station daily values are used as base temperature station value and corrected with the temperature lapse rate given above. As mentioned before, the RG8 station temperature data can be used for the simulations. But in the simulation trials it was seen that the RG8 station values fit well for Kirazdere catchment, but not for the other two. So new trials were done for finding the base temperature station. After several trials, it was seen that the RG7 station values fit well for Kazandere and RG10 station values for Serindere. These stations values are stored in real time, so they were used in the model simulations. The detailed explanation for preparation of timeseries and simulation files is given in Appendix C.

Simulation results and selected parameter values of the model

As described in Appendix C and also in the fourth chapter, the RR module in NAM is used for the parameter adjustment. The RR module parameter set and simulation periods were changed during the calibration process. The rainfall, flow and temperature data is used as daily time base and the evaporation data as monthly values. The simulation periods are mentioned earlier in Table 6.1.

As mentioned in the previous chapters, snow melt has very much influence on rainfall-runoff process in the basin. It was seen that the used methods to distribute rainfall over the catchment is not very good. The proposed methods can not show the real deposition of snow in the basin, so the winter periods are divided into smaller periods so that new snow depths can be given to the model.

The calibrated parameters and their units are listed in Table 6.7. The suggested values for these parameters are listed in Table 6.8. Extended groundwater and irrigation component of the module is not used because no irrigation and groundwater measurement data exist in the basin. The tested parameters are Lmax, Umax, CQOF, CKIF, TOF, TIF, $CK_{1,2}$, CKBF, TG. Parameters values are found by trial and error as suggested in the user manual of the model. After several tries it is seen that Lmax, Umax, CKOF, CKIF are more sensitive on simulation results than the others. These parameters are also used to adjust the baseflow in the simulation. The effect of the parameters on the simulation results is described below;

Maximum water content in surface storage (Umax) and in root zone storage (Lmax)

The maximum water content in surface storage, Umax, and maximum water content in root zone storage, Lmax, are important parameters which have high influence on the baseflow. They must be found by trial and error as suggested in the manual of hydrological model. The recommended values for Umax are between 10-20 mm but it can be taken any value. In this study the value of Umax is taken as 22 which is found by trial and error. The recommended value for Lmax is about Umax*10. It

96

must be a starting point for the trial and error process but it can be any value. In this study values changing between 130-300 mm are used. When the values of Umax and Lmax are increased together, baseflow is decreased. An example of the effect of these parameters on baseflow is shown in Figure 6.4.
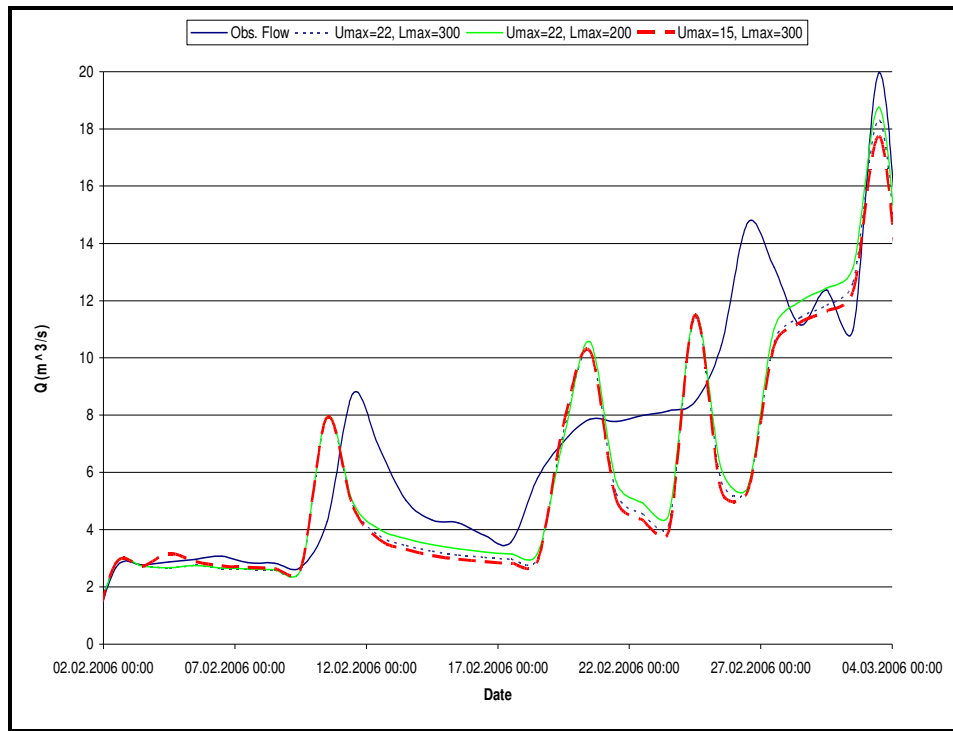

Figure 6.4. Effect of Lmax and Umax on the simulation

Overland flow runoff coefficient (CQOF)

Overland flow runoff coefficient (CQOF) is also one of the important parameters that affect baseflow. Several simulations with different values of CQOF were tried. The values of CQOF are changing between 0-1. If the CQOF is decreased, peak also decreases. So CQOF is an effective parameter to define the peaks also. The tested values change between 0.45-0.6 and selected value is 0.6. An example of the effect of this parameter on base flow and peaks is shown in Figure 6.5.
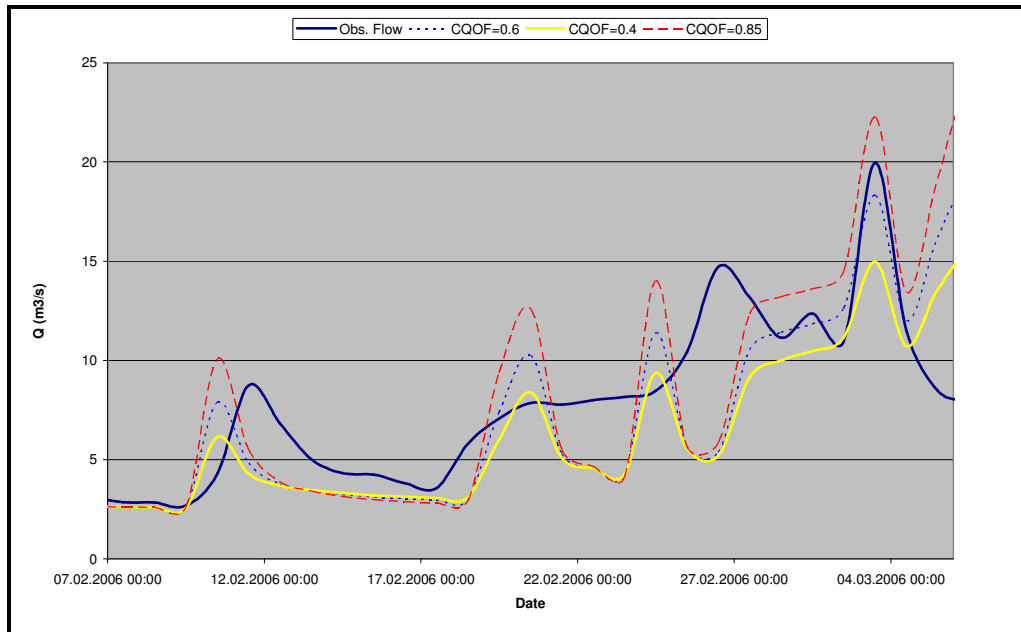
Figure 6.5. Effect of CQOF on the simulation

Time Constant for routing interflow and overland flow (CK_{12})

Time Constant for Routing Interflow and Overland Flow, CK_{12}, is the parameter that affects the shape of the hydrograph peaks. That is to say if the shape of the hydrograph is not good although several tries are done, then CK_{12} values must be changed so that the needed shape is reached. When the CK_{12} increases peak value decreases. The recommended values of CK_{12} are between 3-48 hours. The tested values in this study are between 13 and 38 which are found by several tries. An example of the effect of this parameter on the peak is shown in Figure 6.6.
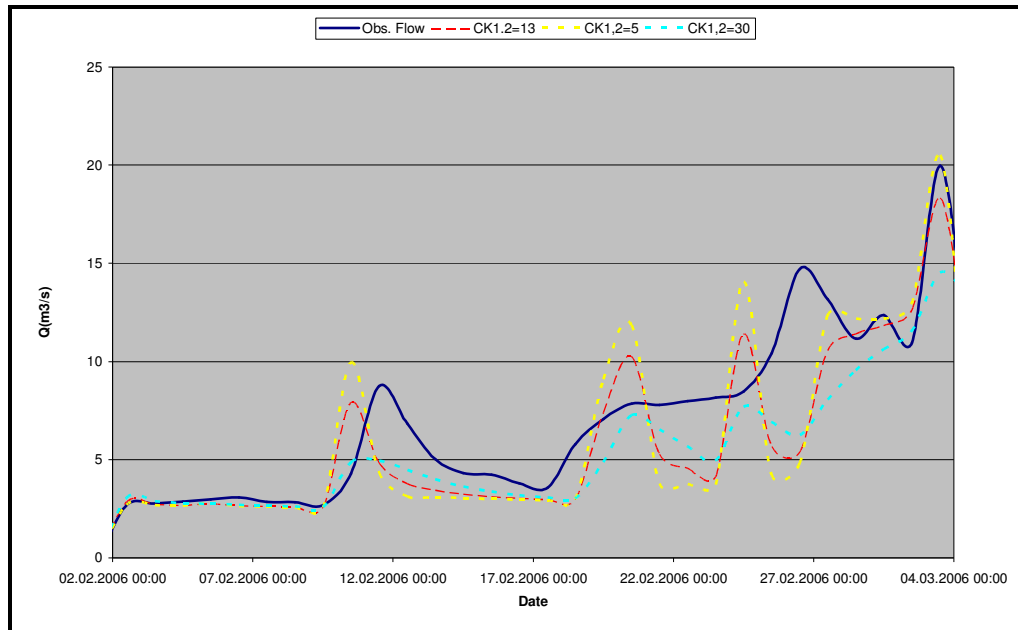
Figure 6.6. Effect of CK_{12} on the simulation

Time constant for interflow (CKIF)

Time constant for interflow parameter, CKIF, is an important parameter to define the effect of the interflow in the simulations. CKIF decreases the peak but also increases the baseflow. But the effect of this parameter on baseflow is not so high.   The recommended values for this parameter is changing between 500-1000 hours. This parameter represents a characteristic of the basin. Several tries are done for fixing this parameter value between 500-1000, but the resulting shapes of the simulations is not good. So the values 100-300 is used in this study. An example of the effect of this parameter on the peak and base flow is shown in Figure 6.7.
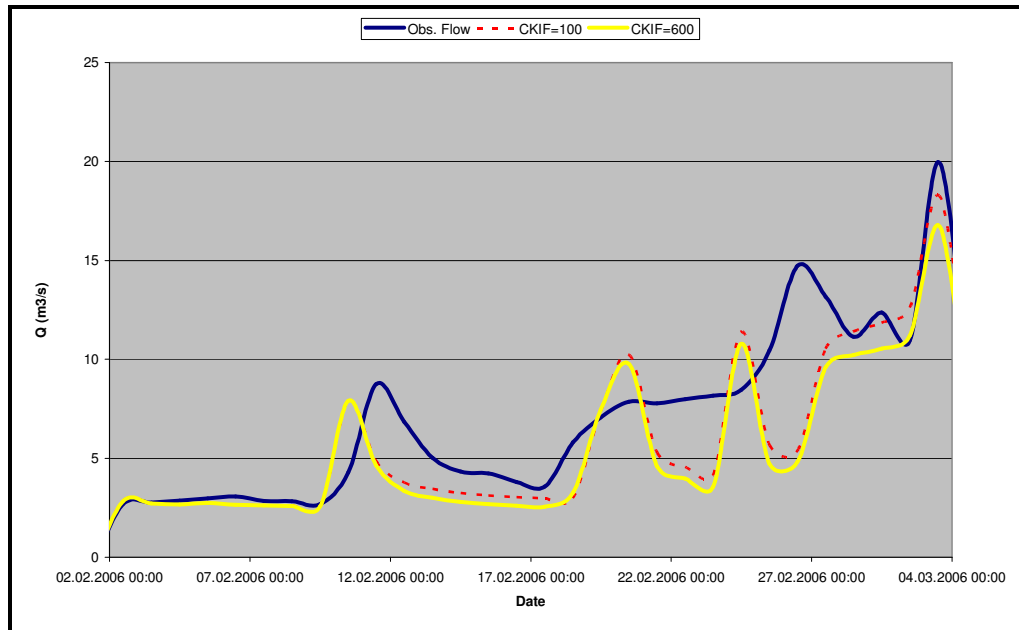
Figure 6.7. Effect of CKIF on the simulation

Root zone threshold value for overland flow (TOF)

Root zone threshold value for overland flow parameter, TOF, is not a sensitive parameter that affects the peak and baseflow. But TOF is effective to define when to start the overland flow. This parameter affects together with moisture content of the lower zone storage. No overland flow is generated if the relative moisture content of the lower zone storage, L/Lmax, is less than TOF. The parameter has an impact only during the first few weeks of the wet season. The values of TOF are between 0-1. High values result the overland flow start later. In this study values between 0.1-0.95 is used for the simulations. An example of the effect of this parameter on the flow is shown in Figure 6.8.
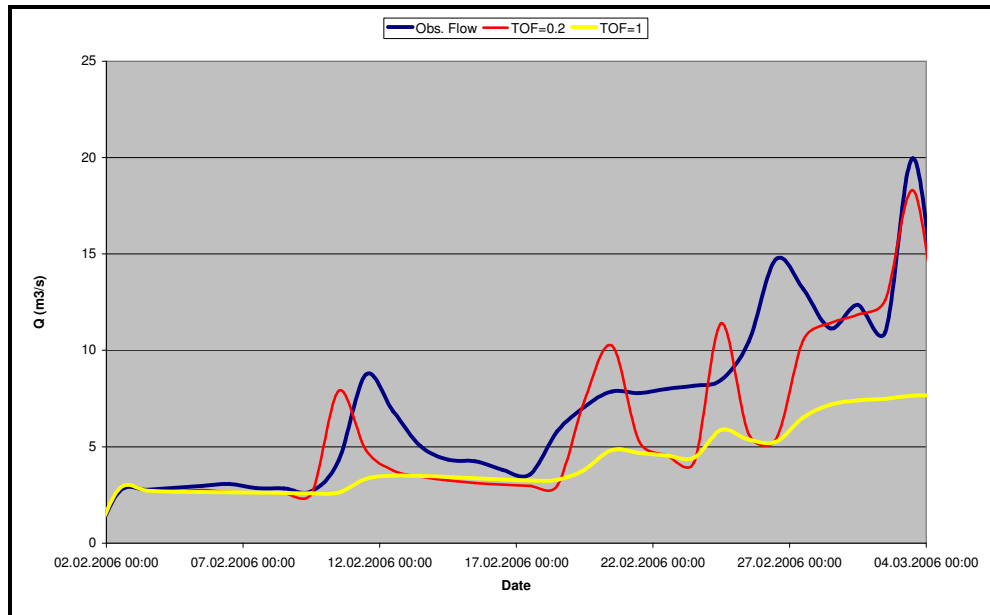
Figure 6.8. Effect of TOF on the simulation

Root zone threshold value for interflow (TIF)

The root zone threshold value for interflow has the same function for interflow as TOF has for the overland flow. This parameter must be used when the interflow has high effect on the flow. Otherwise it will have no effect on the flow. The values of TIF is between 0-1. High values result the interflow start later. In this study values between 0.1-0.9 is used for the simulations. An example of the effect of this parameter on the flow is shown in Figure 6.9.
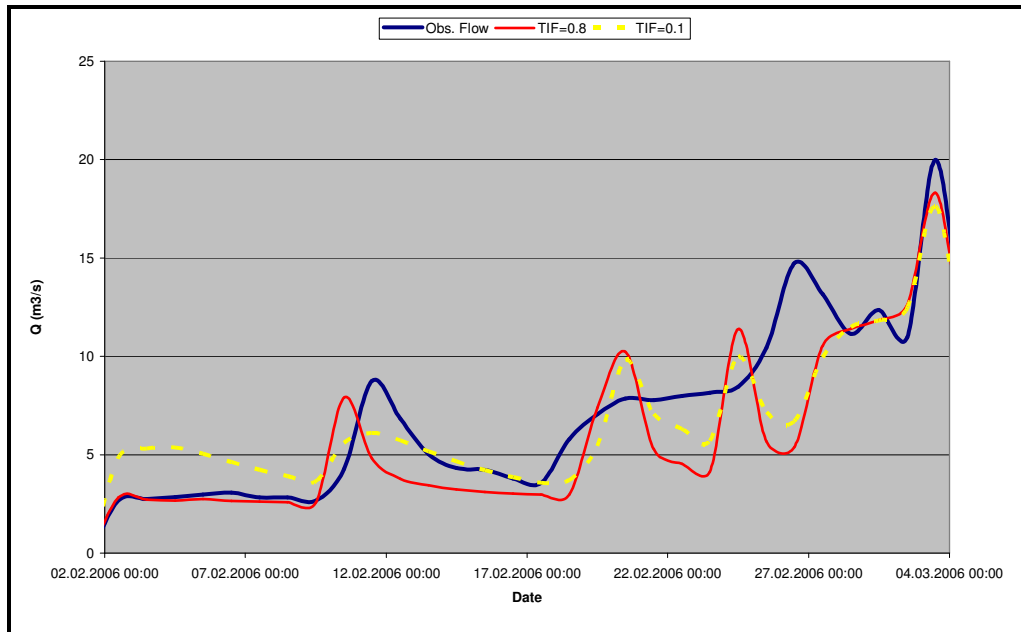
Figure 6.9. Effect of TIF on the simulation

Baseflow time constant (CKBF)

The time constant for baseflow, CKBF, effects the shape of the hydrograph in dry period's simulation. So it can be changed when the simulations are done in dry periods. The recommended values for CKBF, is between 500-5000 hours. After the calibration processes a value of 3000 is used for the simulations.

Root zone threshold value for groundwater recharge (TG)

The root zone threshold value for groundwater recharge, TG, has the same effect on groundwater recharge as TOF has on the overland flow. It is an important parameter for simulating the rise of the groundwater Table in the beginning of a wet season. High values of TG mean that the recharge will start later. Recommended values for TOF is between 0-1. In this study values between 0.3-0.7 is used for the simulations.

After carrying several trials it was seen that the most effective parameters are Lmax, Umax, CKOF, and CKIF which also defines the base flow in the basin. The effect of the parameters on the simulation results are explained in previous sections. Finally it was found that the parameters which are Lmax, Umax, CKOF, CKIF, TG, CKBF can

be taken as the same value through out the calibration process. But these values differ from catchment to catchment as expected. Fortunately for these 6 parameters, the Kazandere catchment parameters and the Kirazdere parameters are same. But in Serindere catchment it they differ. The other three parameters which are CK_{12}, TOF, TIF vary from period to period. But they do not have too much influence on the total volume in the simulations. The recommended and tested values for 9 parameters are presented in Table 6.7 for each catchment. The recommended parameters which are found from the calibration processes is given in Table 6.8. The resulting graphs of these simulations are given in Appendix B. The parameters that are used and their statistical results for each simulation period are presented in Tables 6.10 to 6.12 for three sub-catchments.

Table 6.7. Recommended and tested values for the parameters

Parameter	Unit	Recommended Values in the manual	Tested Values
U_{max}	mm	5-35	5-35
L_{max}	mm	50-400	50-400
C_{KQF}	-	0-1	0-1
C_{KIF}	hours	200-2000	200-2000
$CK_{1,2}$	hours	3-72	3-72
T_{OF}	-	0-0.99	0-0.99
T_{IF}	-	0-0.99	0-0.99
T_G	-	0-0.99	0-0.99
C_{KBF}	hours	500-5000	500-5000

Table 6.8. Recommended values for the parameters for the basin

Parameter	Unit	Recommended Values for Kirazdere	Recommended Values for Kazandere	Recommended Values for Serindere
U_{max}	mm	22	22	22
L_{max}	mm	300	300	300
C_{KQF}	-	0.6	0.6	0.6
C_{KIF}	hours	100-200	100-300	300
$CK_{1,2}$	hours	13	13-27	17-38
T_{OF}	-	0-0.95	0-0.2	0-0.85
T_{IF}	-	0.05-0.8	0-0.8	0.1-0.9
T_G	-	0.7	0.7	0.3
C_{KBF}	hours	3000	3000	3000

One other important parameter is the degree-day parameter which is defined as seasonal variation for each month in a year. Several tries were done for these also. The recommended values for each month are given in Table 6.9. As it can be seen from Table 6.9, the degree-day coefficient starts to increase at the end of the year and then decrease after April. The detailed monthly melt rates used for each catchment are presented in Tables 6.13 to 6.15.

Table 6.9. Recommended degree day coefficients for the basin

Months	Degree day coefficient(mm/day/^{o}C)		
	Kirazdere	Kazandere	Serindere
December	1	1	1
January	1.5-2.5	2.5	1.5-2.5
February	3	3	2.5-3
March	1.5-3	3	2.25-3
April	2-4	2-4	2.75-4

Table 6.10. Kirazdere model inputs and statistical results

		KIRAZDERE	KIRAZDERE	KIRAZDERE	KIRAZDERE	KIRAZDERE	KIRAZDERE	KIRAZDERE	KIRAZDERE	KIRAZDERE	KIRAZDERE	KIRAZDERE	KIRAZDERE	KIRAZDERE
	BASIN:													
	START:	20-Nov-2001	9-Dec-2001	15-Jan-2002	15-Mar-2002	15-Dec-2002	15-Jan-2003	15-Mar-2003	21-Dec-2003	19-Feb-2004	16-Jan-2005	13-Feb-2005	1-Feb-2006	10-Mar-2006
	END:	10-Dec-2001	15-Jan-2002	15-Mar-2002	15-Apr-2002	15-Jan-2003	16-Mar-2003	22-Apr-2003	9-Jan-2004	15-Mar-2004	13-Feb-2005	15-Mar-2005	10-Mar-2006	10-Apr-2006
Initial Conditons	U/Umax	1	1	1	0.3	1	0.7	0.6	1	0.7	1	0.8	0.75	1
	L/Lmax	0.05	0.65	0.1	0.6	0.3	0.5	0.1	0.2	0.1	0.1	0.9	0.8	0.8
	QOF(m^3/s)	2	3	0.1	0.5	0.1	0.01	5	0.1	3	1	0.1	0.1	3
	QIF(m3/s)	0.5	2	0.1	0.5	0.05	0.01	0.1	0.1	1	0.7	0.1	0.4	1
	QBF(m3/s)	0.5	2	2	2	0.05	0.5	0.5	2	1	0.7	2	2.4	5
Model Parameters	Umax(mm)	22	22	22	22	22	22	22	22	22	22	22	22	22
	Lmax(mm)	300	300	300	130	300	300	300	300	300	300	300	300	300
	CKQF	0.6	0.6	0.6	0.6	0.6	0.6	0.6	0.6	0.6	0.6	0.6	0.6	0.6
	CKIF(Hour)	100	100	200	100	100	150	100	100	100	100	100	100	100
	CK1,2(Hour)	13	13	13	13	13	13	13	13	13	13	13	13	13
	TOF	0.2	0.2	0.95	0.2	0.2	0.4	0	0.2	0.2	0.2	0.2	0.2	0.2
	TIF	0.8	0.8	0.05	0.8	0.8	0.55	0.8	0.8	0.8	0.8	0.8	0.8	0.8
	TG	0.7	0.7	0.7	0.7	0.7	0.7	0.7	0.7	0.7	0.7	0.7	0.7	0.7
	CKBF(Hour)	3000	3000	3000	3000	3000	3000	3000	3000	3000	3000	3000	3000	3000
SNOW	Base Temp(^{o}C)	-1	-1	-1	-1	-1	-1	-1	-1	-1	-1	-1	-1	-1
	Water Content(Zone1,2,3)	5,3,3%	5,3,3%	5,3,3%	5,3,3%	5,3,3%	5,3,3%	5,3,3%	5,3,3%	5,3,3%	5,3,3%	5,3,3%	5,3,3%	5,3,3%
	Dry Lapse Rate (^{o}C/100m)	-0.6	-0.6	-0.5	-0.6	-0.5	-0.5	-0.5	-0.5	-0.5	-0.5	-0.5	-0.6	-0.6
	Wet Lapse Rate (^{o}C/100m)	-0.4	-0.4	-0.4	-0.4	-0.4	-0.4	-0.4	-0.4	-0.4	-0.4	-0.4	-0.4	-0.4
	Snow Depth at H0 (mm)	0	150	620	0	50	0	420	620	700	200	180	430	7
	SWE at each zone (mm)	0,0,0	45, 75, 125	200, 320, 560	0, 0, 0	20, 35, 60	0, 0, 0	150, 240, 410	185,310,520	210, 350, 525	60,100,160	63,110,180	150,260,440	40,75,110
	Rainfall Deg. Day Coef.(mm/^{o}C/day)	1	1	1	1	1	1	1	1	1	1	1	1	1
MODEL RELIABILITY	NSE (Nash&Sutcliffe Eff.)	0.770	0.828	0.520	0.652	0.860	0.585	0.677	-4.407	-2.659	0.630	-0.812	0.276	
	Correlation coeficient R2	0.773	0.773	0.864	0.568	0.695	0.888	0.608	0.580	0.110	0.126	0.718	0.091	0.524
	Max. positive difference(m^3/s)	4.910	4.910	2.874	2.006	3.753	1.262	0.634	-0.281	3.423	3.611	4.725	9.831	9.617
	Max. negative difference(m^3/s)	-7.428	-7.428	-5.570	-3.047	-1.707	-1.942	-2.973	-7.869	-1.678	-1.973	-4.894	-6.138	-9.562
	Volume observed(m^3)	8422026.164	8422026.164	17227925.201	16202048.324	10653248.742	3349900.829	5373236.749	17407094.407	4834457.961	6637032.020	9386668.817	15147043.269	23178959.977
	Volume modelled(m^3)	7950948.905	7950948.905	18177896.060	16542502.216	12055958.490	2930822.026	5374215.906	8691312.671	5111577.843	6727786.685	8102939.612	17499668.304	21422353.999
	Volume error (%)	-5.593	-5.593	5.514	2.101	13.167	-12.510	0.018	-50.070	5.732	1.367	-13.676	15.532	-7.578
	Peak observed value (m^3/s)	20.083	20.083	23.406	7.258	15.119	7.170	4.050	11.946	3.541	5.349	12.372	13.710	19.980
	Peak modelled value (m^3/s)	14.730	14.730	19.081	6.105	13.412	5.886	3.700	7.337	5.654	6.513	13.638	19.843	17.958
	Peak error (%)	-26.657	-18.479	-15.884	-11.288	-17.912	-8.648	-38.58	59.671	21.766	10.234	44.735	-10.118	0.812

Table 6.11. Kazandere model inputs and statistical results

	BASIN:	KAZANDERE	KAZANDERE	KAZANDERE	KAZANDERE	KAZANDERE	KAZANDERE	KAZANDERE
	START:	20-Mar-2003	21-Dec-2003	19-Feb-2004	16-Jan-2005	15-Feb-2005	1-Feb-2006	10-Mar-2006
	END:	18-Apr-2003	9-Jan-2004	15-Mar-2004	13-Feb-2005	15-Mar-2005	10-Mar-2006	10-Apr-2006
Initial Conditons	U/Umax	1	1	1	1	0.8	0.8	0.8
	L/Lmax	0.3	0.3	0.2	0.2	0.35	0.35	0.35
	QOF(m^3/s)	0.1	0.1	0.05	0.05	0.1	0.1	0.1
	QIF(m3/s)	0.1	0.1	0.05	0.05	0.1	0.1	0.1
	QBF(m3/s)	0.4	0.4	0.8	0.8	0.7	0.7	0.7
Model Parameters	Umax(mm)	22	22	22	22	22	22	22
	Lmax(mm)	300	300	300	300	300	300	300
	CKQF	0.6	0.6	0.6	0.6	0.6	0.6	0.6
	CKIF(Hour)	100	100	100	100	100	100	100
	CK1,2(Hour)	13	26	13	13	13	13	27
	TOF	0.2	0.1	0.2	0.2	0.2	0.2	0
	TIF	0.8	0.8	0.8	0.8	0.8	0.8	0
	TG	0.7	0.7	0.7	0.7	0.7	0.7	0.7
	CKBF(Hour)	3000	3000	3000	3000	3000	3000	3000
SNOW	Base Temp(^{o}C)	-1	-1	-1	-1	-1	-1	-1
	Water Content(Zone1,2,3)	5,3,3%	5,3,3%	5,3,3%	5,3,3%	5,3,3%	5,3,3%	5,3,3%
	Dry Lapse Rate (^{o}C/100m)	-0.5	-0.5	-0.5	-0.5	-0.5	-0.6	-0.6
	Wet Lapse Rate (^{o}C/100m)	-0.4	-0.4	-0.4	-0.4	-0.4	-0.4	-0.4
	Snow Depth at HO (mm)	480	620	700	200	180	430	7
	SWE at each zone (mm)	170, 285, 470	185, 310, 520	210, 350, 525	60, 100, 160	60,100,160	150, 260, 440	70,110, 190
	Rainfall Deg. Day Coef.(mm/^{o}C/day)	1	1	1	1	1	1	1
MODEL RELIABILITY	NSE (Nash&Sutcliffe Eff.)	0.705	0.412	0.594	0.500	0.528	0.625	0.733
	Correlation coeficient R2	0.853	0.309	0.803	0.511	0.593	0.597	0.672
	Max. positive difference(m^3/s)	1.536	1.243	1.433	1.892	0.682	1.786	1.413
	Max. negative difference(m^3/s)	-0.717	-1.065	-0.629	-1.852	-0.778	-2.260	-2.051
	Volume observed(m^3)	3915820.825	2707689.599	3973017.579	2680732.797	3457036.792	6321887.998	5161967.972
	Volume modelled(m^3)	4411284.437	2975806.353	4860484.420	2807627.262	3727591.780	6328893.198	5046194.207
	Volume error (%)	12.653	9.902	22.337	4.734	7.826	0.111	-2.243
	Peak observed value (m^3/s)	3.155	3.204	3.748	4.084	3.231	5.530	5.810
	Peak modelled value (m^3/s)	4.684	2.841	4.305	3.471	2.536	3.783	3.970
	Peak error (%)	48.451	-11.336	14.853	-15.013	-21.506	-31.589	-31.671

Table 6.12. Serindere model inputs and statistical results

		SERİNDERE	SERİNDERE	SERİNDERE	SERİNDERE	SERİNDERE	SERİNDERE	SERİNDERE	SERİNDERE
	BASIN:								
	START:	20-Dec-2002	3-Feb-2003	20-Mar-2003	17-Dec-2003	16-Jan-2005	13-Feb-2005	1-Feb-2006	10-Mar-2006
	END:	15-Jan-2003	20-Feb-2003	22-Apr-2003	6-Jan-2004	13-Feb-2005	15-Mar-2005	10-Mar-2006	5-Apr-2006
Initial Conditons	U/Umax	1	0.85	0.4	0.1	1	1	1	0.8
	L/Lmax	0.05	0.03	0.3	0.7	0.2	0.1	0.4	0.65
	QOF(m^3/s)	0.1	1	0.1	2.7	4	2	0.4	2
	QIF(m3/s)	0.1	0.5	0.1	1	0.1	0.1	0.1	1
	QBF(m3/s)	1	0.8	2.2	0.7	1	0.5	2	1
Model Parameters	Umax(mm)	22	22	22	22	22	22	22	22
	Lmax(mm)	130	130	130	130	130	130	130	130
	CKQF	0.4	0.4	0.4	0.4	0.4	0.4	0.4	0.4
	CKIF(Hour)	300	300	300	300	300	300	300	300
	CK1,2(Hour)	17	17	20	38	25	30	17	33
	TOF	0.1	0.1	0.85	0.7	0.8	0	0	0.3
	TIF	0.3	0.3	0.1	0.95	0.95	0.6	0.9	0.3
	TG	0.3	0.3	0.3	0.3	0.3	0.3	0.3	0.3
	CKBF(Hour)	3000	3000	3000	3000	3000	3000	3000	3000
SNOW	Base Temp(^{o}C)	-1	-1	-1	-1	-1	-1	-1	-1
	Water Content(Zone1,2,3)	5,3,3%	5,3,3%	5,3,3%	5,3,3%	5,3,3%	5,3,3%	5,3,3%	5,3,3%
	Dry Lapse Rate (ºC/100m)	-0.5	-0.5	-0.5	-0.5	-0.5	-0.5	-0.6	-0.6
	Wet Lapse Rate (ºC/100m)	-0.4	-0.4	-0.4	-0.4	-0.4	-0.4	-0.4	-0.4
	Snow Depth at HO (mm)	550	120	480	80	200	180	430	7
	SWE at each zone (mm)	165, 275, 460	40,65,110	170,275,470	24,40,65	60,100,160	60,100,160	150,260,440	70, 110, 180
	Rainfall Deg. Day Coef.(mm/^{o}C/day)	1	1	1	1	1	1	1	1
MODEL RELIABILITY	NSE (Nash&Sutcliffe Eff.)	0.685	0.765	0.344	0.725	0.346	0.335	0.495	0.754
	Correlation coeficient R^2	0.860	0.853	0.481	0.748	0.484	0.245	0.637	0.760
	Max. positive difference(m^3/s)	10.050	3.319	4.122	1.395	3.184	3.884	6.951	2.790
	Max. negative difference(m^3/s)	0.923	-4.240	-5.349	-1.011	-2.324	-4.885	-3.812	-3.074
	Volume observed(m^3)	3339532.829	3954830.474	16115587.180	6243955.201	6036767.933	10461052.719	15437087.934	8827920.063
	Volume modelled(m^3)	12481767.851	3812864.310	16115528.224	6243953.388	7097501.548	11059956.573	16652955.091	9901429.682
	Volume error (%)	273.758	-3.590	0.000	0.000	17.571	5.725	7.876	12.160
	Peak observed value (m^3/s)	7.170	12.871	11.946	6.660	7.950	12.679	14.120	10.270
	Peak modelled value (m^3/s)	15.357	8.631	10.841	5.98	5.626	7.794	11.701	8.454
	Peak error (%)	114.188	-32.94	-9.251	-10.21	-29.234	-38.53	-17.134	-17.678

Table 6.13. Monthly melt rates used for Kirazdere catchment

	January(mm/^{o}C/day)	2.5	2.5	2.5	2.5	2.5	2.5	2.5	1.5	2.5	2.5	2.5	2.5	2.5
	February(mm/^{o}C/day)	3	3	3	3	3	3	3	3	2	3	2.5	3	3
	March(mm/^{o}C/day)	3	3	3	3	3	3	1.5	3	2	3	2.5	3	3
	April(mm/^{o}C/day)	4	4	4	4	4	4	2	4	4	4	4	4	4
	May(mm/^{o}C/day)	1	1	1	1	1	1	1	1	1	1	1	1	1
Seasonal Melt Rate	June(mm/^{o}C/day)	0	0	0	0	0	0	0	0	0	0	0	0	0
	July(mm/^{o}C/day)	0	0	0	0	0	0	0	0	0	0	0	0	0
	August(mm/^{o}C/day)	0	0	0	0	0	0	0	0	0	0	0	0	0
	September(mm/^{o}C/day)	0	0	0	0	0	0	0	0	0	0	0	0	0
	October(mm/^{o}C/day)	0	0	0	0	0	0	0	0	0	0	0	0	0
	November(mm/^{o}C/day)	1	1	1	1	1	1	1	1	1	1	1	1	1
	December(mm/^{o}C/day)	1	1	1	1	1	1	1	1	1	1	1	1	1

Table 6.14. Monthly melt rates used for Kazandere catchment

	January(mm/^{o}C/day)	2.5	2.5	2.5	2.5	2.5	2.5	2.5
	February(mm/^{o}C/day)	3	3	3	3	3	3	3
	March(mm/^{o}C/day)	3	3	3	3	3	3	3
	April(mm/^{o}C/day)	4	4	4	4	4	4	4
	May(mm/^{o}C/day)	1	1	1	1	1	1	1
Seasonal Melt Rate	June(mm/^{o}C/day)	0	0	0	0	0	0	0
	July(mm/^{o}C/day)	0	0	0	0	0	0	0
	August(mm/^{o}C/day)	0	0	0	0	0	0	0
	September(mm/^{o}C/day)	0	0	0	0	0	0	0
	October(mm/^{o}C/day)	0	0	0	0	0	0	0
	November(mm/^{o}C/day)	1	1	1	1	1	1	1
	December(mm/^{o}C/day)	1	1	1	1	1	1	1

Table 6.15. Monthly melt rates used for Serindere catchment

	January(mm/^{o}C/day)	2.5	2.5	2.5	2	1.5	1.5	2.5	2.5
	February(mm/^{o}C/day)	3	2.5	3	3	2.5	2.5	2.5	3
	March(mm/^{o}C/day)	3.1	3.1	2.25	3.1	3.1	3	3.1	3.1
	April(mm/^{o}C/day)	4	4	2.7	4	4	4	4	4
	May(mm/^{o}C/day)	1	1	1	1	1	1	1	1
Seasonal Melt Rate	June(mm/^{o}C/day)	0	0	0	0	0	0	0	0
	July(mm/^{o}C/day)	0	0	0	0	0	0	0	0
	August(mm/^{o}C/day)	0	0	0	0	0	0	0	0
	September(mm/^{o}C/day)	0	0	0	0	0	0	0	0
	October(mm/^{o}C/day)	0	0	0	0	0	0	0	0
	November(mm/^{o}C/day)	1	1	1	1	1	1	1	1
	December(mm/^{o}C/day)	1	1	1	1	1	1	1	1

6.2. Performance criteria used in Mike 11

6.2.1. Percent peak and volume differences

Mike 11 normally does not show the percent peak and volume differences in the results but with the help of Mike view program, it can get the output data for further analysis. So the percent peak and volume differences can be calculated by Mike view. The computation principle is very simple when determining these percent differences as given in Equations 6.1 and 6.2.

% Peak Error $\quad = [\ (Sim_{peak} - Obs_{peak})/\ Obs_{peak}\ ]\ x\ 100$ $\qquad\qquad$ (6.1)

% Volume Error $\quad = [(Sim_{vol} - Obs_{vol})/\ Obs_{vol}\ ]\ x\ 100$ $\qquad\qquad$ (6.2)

where, Sim_{peak} and Obs_{peak} are simulated and observed flow peaks, respectively; and Sim_{vol} and Obs_{vol} are simulated and observed flow volumes, respectively.

Percent error in peak does not give any information about hydrograph shape, volume and peak timing, so it must be used only when peak flow is taken into consideration such as flood events. Similarly, percent error in volume is a value that shows the volume difference between simulated and observed flows, so it must be used in a performance evaluation only when flow volume is important such as reservoir operation.

6.3. Statistical evaluation criteria

6.3.1. Coefficient of determination (R^2)

The coefficient of determination is the square of the Pearson's Product Moment Correlation Coefficient (Pearson, 1932) and describes the proportion of the total variance in the observed data that can be explained by the model. It is defined with the ratio of explained variation to the total variation (EV/TV) (McCuen, 1993). It ranges from 0.0 (poor model) to 1.0 (perfect model) and is given by:

$$R^2 = \left[\frac{\sum_{i=1}^{N}(O_i - \overline{O})(P_i - \overline{P})}{\left[\sum_{i=1}^{N}(O_i - \overline{O})^2\right]^{0.5}\left[\sum_{i=1}^{N}(P_i - \overline{P})^2\right]^{0.5}} \right] \tag{6.3}$$

where, P: simulated data and O: observed data, and the overbar denotes the mean for the entire period of the evaluation.

The correlation based coefficient of determination have been widely used to evaluate the goodness-of-fit of hydrologic and hydroclimatic models. It is oversensitive to extreme values (outliers) and is insensitive to additive and proportional differences between model predictions and observations (Legates, 1999). These limitations are well documented in the literature (Willmott, 1981; Moore, 1991; Kessler and Neas, 1994). However, coefficient of determination is still widely used in hydrological model performance evaluation.

6.3.2. Nash and Sutcliffe model efficiency (NSE)

NSE is widely used to evaluate the performance of hydrologic models (e.g. Şorman, 2005; Wilcox et al., 1990). NSE is defined by Nash and Sutcliffe (1970) which ranges from minus infinity (poor model) to 1.0 (perfect model) as:

$$NSE = 1 - \frac{\sum_{i=1}^{N}(O_i - P_i)^2}{\sum_{i=1}^{N}(O_i - \overline{O})^2} \tag{6.4}$$

where, P: predicted data and O: observed data, and the overbar denotes the mean for the entire period of the evaluation. If the value of NSE is less than "0", then the observed mean flow is better than the model prediction. If the value of NSE is equal to "0", then the observed mean is as good as the model prediction. Values of NSE from "0" approaching to "1" show the increasing improvement obtained by the model prediction over the observed mean flow. NSE is an improved evaluation index

compared to R^2 because it is sensitive to differences in the observed and simulated means and variances (Legates, 1999). But NSE is oversensitive to outliers, too.

6.4. Overall evaluation of the results

Both graphical and numerical performance measures is applied in testing the model efficiency. The graphical evaluation includes comparison of the simulated and observed hydrograph, and comparison of the simulated and observed accumulated runoff. The numerical performance measures include the overall water balance error (i.e. the difference between the average simulated and observed runoff), and a measure of the overall shape of the hydrograph based on the coefficient of determination or Nash-Sutcliffe coefficient. Moreover, the results were also analyzed in terms of the percent volume and peak error. The statistical summary of the daily simulations are given in Tables 6.16 to 6.18.

Statistical analysis yields high goodness of fit for Kirazdere sub-basin, the possible reason is the availability of appropriate modeling data. The model efficiencies are higher than 0.7 at least for half of the events for Kazandere and Serindere. The model efficiency reduces with low flows which is the main issue for Kazandere sub-basin. Either the percent peak and volume percent difference or model efficiency is in the acceptable ranges for almost all simulations. Parameters that are found in the calibration process are applicable in the validation process. So these values can be used in any hydrological simulation within the basin.

Table 6.16. Summary of simulations for Kirazdere catchment.

Simulation Period		NSE (Nash&Sutcliffe Eff.)	R²	Volume Difference (%)	Peak Difference (%)
START	END				
20-Nov-2001	10-Dec-2001	0.770	0.773	-5.6	-26.7
9-Dec-2001	15-Jan-2002	0.828	0.864	5.5	-18.5
15-Jan-2002	15-Mar-2002	0.520	0.568	2.1	-15.9
15-Mar-2002	15-Apr-2002	0.652	0.695	13.2	-11.3
15-Dec-2002	15-Jan-2003	0.860	0.888	-12.5	-17.9
15-Jan-2003	16-Mar-2003	0.585	0.608	0.0	-8.6
15-Mar-2003	22-Apr-2003	0.677	0.580	-50.0	-38.5
21-Dec-2003	9-Jan-2004	NA	0.126	1.4	21.8
19-Feb-2004	15-Mar-2004	NA	0.718	-13.7	10.2
16-Jan-2005	13-Feb-2005	0.630	0.718	-13.7	10.2
13-Feb-2005	15-Mar-2005	-0.812	0.091	15.5	44.7
1-Feb-2006	10-Mar-2006	0.276	0.524	-7.6	-10.1
10-Mar-2006	10-Apr-2006	0.762	0.756	-2.7	0.8

Table 6.17. Summary of simulations for Serindere catchment.

Simulation Period		NSE (Nash&Sutcliffe Eff.)	R²	Volume Difference (%)	Peak Difference (%)
START	END				
20-Dec-2002	15-Jan-2003	0.685	0.685	273.8	-3.6
3-Feb-2003	20-Feb-2003	0.765	0.765	114.1	-32.9
20-Mar-2003	22-Apr-2003	0.344	0.481	0.0	-9.2
17-Dec-2003	6-Jan-2004	0.725	0.748	0.0	-10.2
16-Jan-2005	13-Feb-2005	0.346	0.484	17.6	-29.2
13-Feb-2005	15-Mar-2005	0.335	0.245	5.7	-38.5
1-Feb-2006	10-Mar-2006	0.495	0.637	7.9	-17.1
10-Mar-2006	5-Apr-2006	0.754	0.760	12.1	-17.7

Table 6.18. Summary of simulations for Kazandere catchment.

Simulation Period		NSE (Nash& Sutcliffe Eff.)	R²	Volume Difference (%)	Peak Difference (%)
START	END				
20-Mar-2003	18-Apr-2003	0.705	0.853	12.6	48.4
21-Dec-2003	9-Jan-2004	0.412	0.309	9.9	-11.3
19-Feb-2004	15-Mar-2004	0.594	0.803	22.3	14.8
16-Jan-2005	13-Feb-2005	0.500	0.511	4.7	-15.0
13-Feb-2005	15-Mar-2005	0.528	0.593	7.8	-21.5
1-Feb-2006	10-Mar-2006	0.625	0.597	0.1	-31.6
10-Mar-2006	5-Apr-2006	0.733	0.672	-2.2	-31.7

6.5. Validation of the results

After determining the parameters, the determined parameters should be validated with another set of data which was not used in the calibration. For Kirazdere catchment, for the calibration 2001-02, 2003-04, 2004-05 and 2005-06 water year periods are used. For the validation 2002-2003 water year period is used. Because of the limited calibration periods for Kazandere and Serindere catchments only one period from the year 2005 and the year 2003 are selected for model validation. The parameters that are used in the validation are the same with the ones that are used in previous section.

Some selected graphs for the simulations which are used for the calibration and validation process is shown in Figures 6.10 to 6.15. The red colored line is the observed flow (m^3/s) and the black line is the simulated flow (m^3/s).
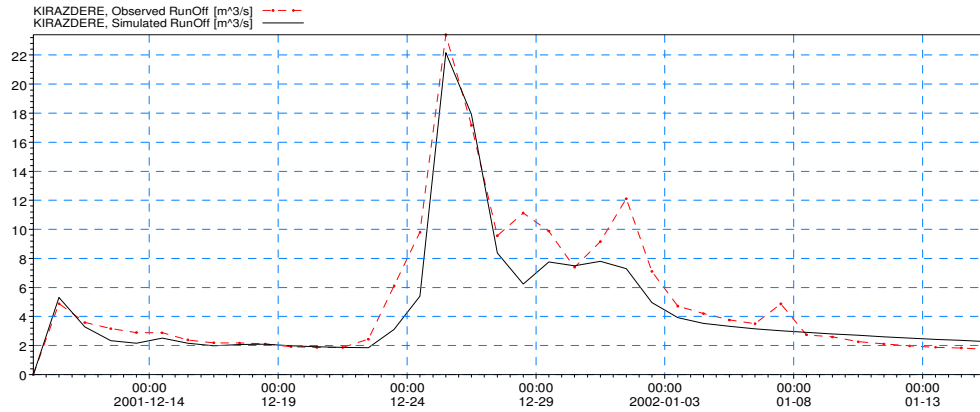
Figure 6.10. Kirazdere calibration result graph (09.12.2001 - 15.01.2002)
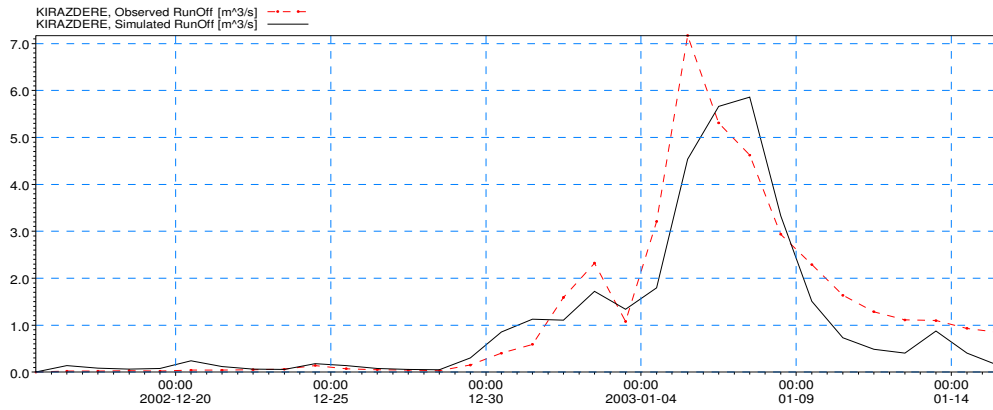
Figure 6.11. Kirazdere validation result graph (15.12.2002 – 16.01.2003)
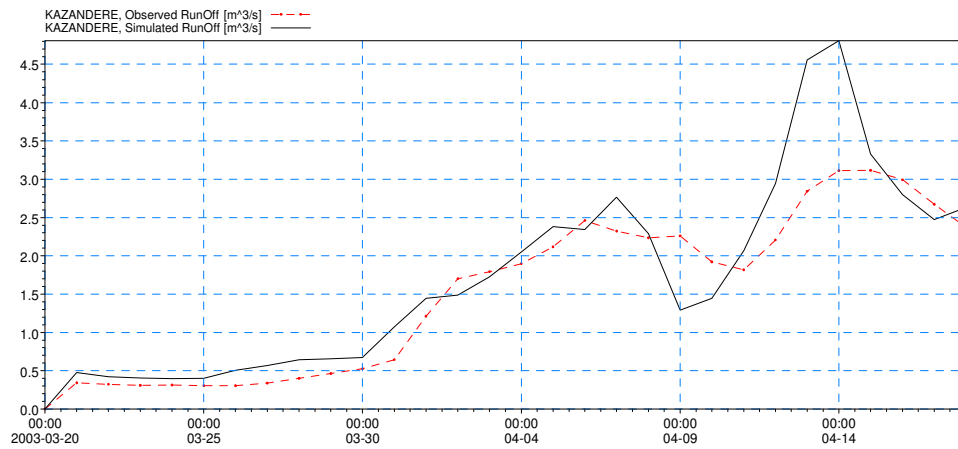
Figure 6.12. Kazandere calibration result graph (20.03.2003 – 18.04.2003)

114
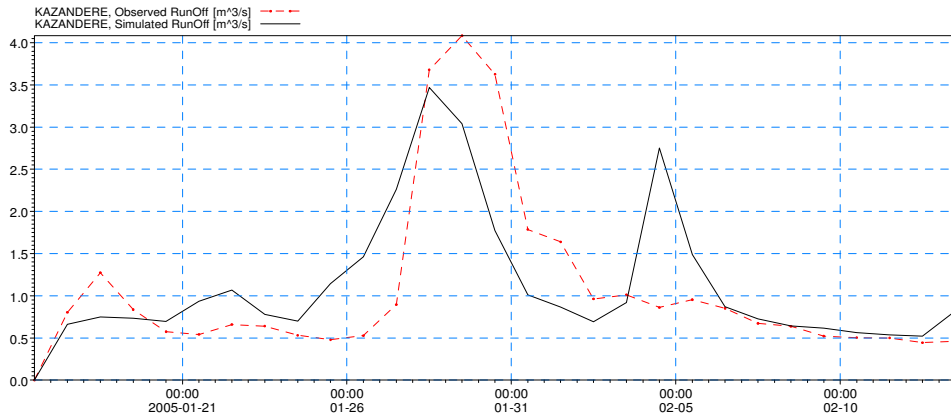
Figure 6.13. Kazandere validation result graph (16.01.2005 – 13.02.2005)
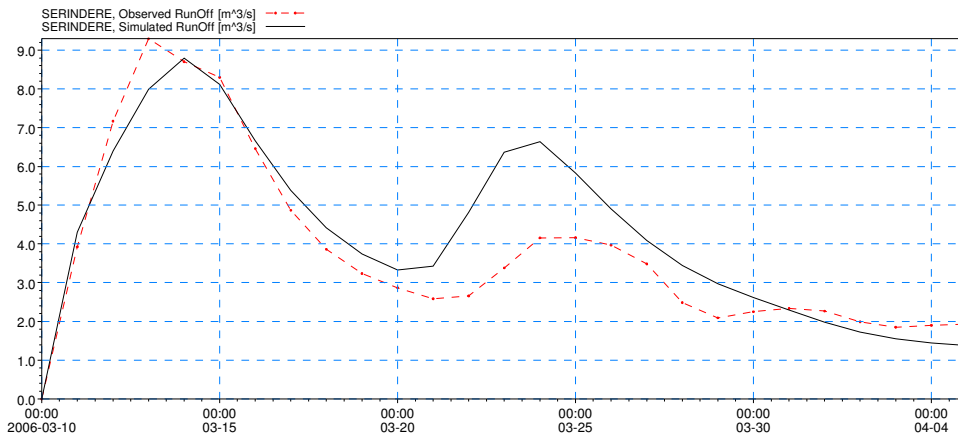
Figure 6.14. Serindere calibration result graph (10.03.2006 – 05.04.2006)
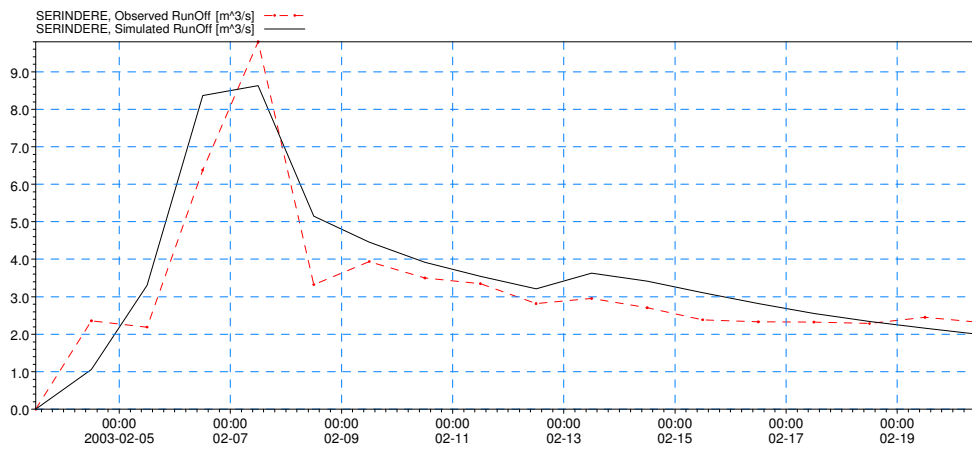
Figure 6.15. Serindere validation result graph (03.02.2003 – 21.02.2003)

115

As seen from the presented graphs, the parameters that are found in the calibration process fits well for the validation process, so these parameters can be recommended for simulation to estimate daily runoffs using Mike11 for Yuvacık sub-catchments.

CHAPTER 7

CONCLUSIONS AND RECOMMENDATIONS

In this study, Mike11 hydrological modeling software with NAM module and UHM module are applied to Yuvacık Basin and model parameters are calibrated. The obtained data are preprocessed by ArcGIS and sub-catchments. River network, hypsometric curves, thiessen polygons are generated by GIS.

In the first part of the study, GIS has been used as an input data for handling hydrological modeling by extracting the drainage area, river network, lag time, slope from DEM by basin preprocessing and processing studies. In the second part of the study, a new methodology for determination of CN that integrates GIS and hydrological modeling together is suggested.

Concerning the data of meteorological variables and model parameters, NAM module and UHM module was used in daily and hourly time steps for snowmelt and rainfall events respectively. The main objective to use two different modules is to have an experience in applying two different modules with different parameter sets for different time scales.

The largest peaks of inflow are observed when the storm events occur due to both snowmelt and rain on snow. The snow starts to accumulate at the mid of December and almost all of the snow reserve melts at the end of March except from the locations at the higher elevations of the basin. Therefore, the simulation of the events is started from the beginning of December and extended to the end of April. Only the NAM module has a built-in snowmelt component, so the snowmelt simulations could not be applied to UHM module. There were data discontinuities for the flow plants of Kazandere and Serindere subbasins between the period 2001-2005 because of the

missing records due to the inconsistencies in water level measurements. Therefore, there are more storm events observed in Kirazdere than that of the other catchments.

New automatic weather stations (RG7 to RG10 and M1 to M3) located at higher elevations (550-1500 m) provide better spatial representation of the precipitation compared to existing rain gage network (RG1 to RG6) which are installed previously by the TWT (at elevations 170-520 m). Spatial distribution of the new stations is better than the existing ones, because existing gages were accumulated around the reservoir, whereas, new stations are scattered inside the basin as much a representative way as possible. Besides, new stations provide temperature, wind and humidity data. Especially air temperature data has crucial importance for the snowmelt modeling studies.

Model efficiency is tested with visual and statistical evaluations. Nash and Sutcliffe model efficiency (NSE) statistical criteria and coefficient of determination (R^2) which are widely used for the model performance evaluation in hydrology is used for the evaluation of the model. Moreover, the results were also analyzed in terms of the percent volume and peak error. The percent volume error is important considering the classical reservoir operation and the percent peak error is important considering floods in the basin.

Statistical analysis yields high goodness of fit for Kirazdere sub-basin the reason may be due to the availability of appropriate modeling data. The model efficiencies are higher than 0.7 at least for half of the events for Kazandere and Serindere. The model efficiency reduces with low flows which is the main issue for Kazandere sub-basin. Either the percent peak and volume percent difference or model efficiency is in the acceptable ranges for almost all simulations. Parameters that are found in the calibration process are tested for their applicability and found to be succesful in the validation process.

The new CN approach by GIS analysis is one way to easily apply the traditional SCS-CN method to areas where saturation excess is an important runoff process and it can be used for improving the reliability of the widely used suite of water quality models based on the traditional SCS-CN method. The new CN method somehow uses the basic form of the traditional SCS-CN method but does not use the tabulated land use and soil class approach to determine potential maximum retention. The only additional data needed are DEM and soil information, which can be obtained from the maps prepared by the governmental organizations in Turkey.

Also an approach for modeling basin hydrology that integrates Hydrological Sensitive Areas (HSAs) concept and hydrological modeling with Mike11 was presented. This kind of approach focuses on the determining the CN value of an event of a catchment and mapping areas that are expected to exhibit similar hydrological response. The spatial distribution of dominant runoff mechanisms and pathways are identified by this approach. This approach for mapping the spatial distribution of runoff mechanisms and components is particularly relevant for water quantity and quality studies, because it forces modelers to quantify the spatial extent of similar hydrological response areas and its characteristics before initiating the modeling process. Also this type of approach is important for the modeling applications in ungauged basins where it is possible to identify spatial extent of the dominant runoff mechanisms.

By using the HSAs the catchment is grouped into regions (cells) that exhibit similar hydrological response and parameterization and calibration of non-existing process is reduced which is physically meaningful. These approach can be applied to any kind of hydrological model which uses the CN approach where the approach focuses on the fundamental part of the catchment that increase awareness of individual sources of runoff, rather than the whole catchment.

The heterogenity of CN can be easily seen with the simulations done by UHM module. The CN found by classical methods do not differ too much, but there is a big

119

difference in CNs which are calculated by event simulations, fractional area and topographic index. The heterogenity of the CN values enables the modeler to define different CN values rather than using one value for the catchment.

The calibrated model parameters should be re-checked with future water year data, and model should be verified. If necessary, model parameters should be updated for better performance of the model runs considering initial soil moisture distribution in the area. Infiltration and soil moisture tests should be conducted in the basin at various soil textures and land use to better define the initial moisture conditions in the model.

Channel routing can be added to the model. Using one of the available routing methods (e.g. kinematic wave, Muskingum) routing parameters can be calibrated and can be used to match time to peak with the observed records.

Moreover, both of the modules combined with a meteorological forecast model can be utilized as a decision support tool to estimate the possible runoff with the recommended parameter set during the real time operation of the dam. The same model is being used in Flood Forecasting Center in DSI and the results of this study would also be helpful for the Turkey Emergency Flood and Earthquake Recovery (TEFER) project model calibration study in the different part of the country which is on going issue in DSI agenda.

REFERENCES

Abbott M., Bathrust J., Cunge J., O'Connell P. and Rasmussen J. (1986) An introduction to the European Hydrological System-Systeme Hydrologique Europeen, "SHE", 2 : modelling system. Journal of Hydrology, 87, 61-77.

Andrieu H., Creutin J.D., Delrieu G., Faure D. (1997), "Use of Weather Radar for the Hydrology of a Mountainous Area. Part I. Radar Measurement Interpretation", Journal of Hydrology, 193: 1-25.

Berry J.K. and Sailor J.K. (1987), "Use of a geographic information systems for storm runoff prediction from small urban watersheds", Environment Management, Vol.11, pp.21-27.

Beven K. J. and Kirkby M. J. (1979), "A physically based variable contributing area model of basin hydrology", Hydrological Sciences Bulletin, 24(1),43-69.

Britannica, (2005), "Encyclopaedia Britannica", Retrieved October 12, 2006, from Encyclopaedia Britannica Online.

Buffo M. And Gonella M. (1999), "Mike11 as a standard tool for the development of the river PO catchment general study", 3rd Software Conference Danish Hydraulic Institute, Denmark.

Chow V. T. (1988), Maidment, D. R., and Mays, L. W.: Applied Hydrology, Mc Graw-Hill, New York

Clark C.D. (1945), "Storage and the Unit Hydrograph", ASCE Transactions, 110, p.1419-1446.

Coskun M., Musaoglu N., Hızal A. (2005), "Prediction of Hydrological Model of Yuvacik Catchment by Using Remote Sensing and GIS Integration", Proceedings of 31st International Symposium on Remote Sensing of Environment, 20-24 June, Saint Petersburg.

Demir H. (2001), "An Application of Rainfall-Runoff on Sohu Basin", M.Sc. Thesis, METU, Dept. Of Geodetic and Geographic Inform. Tech., Ankara.

DHI, (2004), "Mike 11 User & Reference Manual", Danish Hydraulic Institute, Denmark.

DSI Report, (1983) "Izmit-Kirazdere Projesi, Kirazdere Barajı Muhendislik Hidrolojisi Planlama Raporu", Bursa

Einfalt Th., Jensen T. S., Klinting A. (2004), "Combining NWP data, radar data, raingauge data and a hydrological-hydrodynamical model for flood forecasting in Turkey", Proceedings of ERAD, Copernicus GmbH, 6-10 September, Sweden, p. 522–524.

ESRI, (2005), "ArcGIS 9: The Principles of Geostatistical Analysis"; "ArcGIS 9: Exploratory Spatial Data Analysis". ESRI Software Documentation Library.

Gorokhovich Y., Villarini G. (2005), "Application of GIS for processing and establishing the correlation between weather radar reflectivity and precipitation data", Journal of Meteorological Applications, 12:91-99.

GLCF, Global Land Cover Facility, http://glcfapp.umiacs.umd.edu, visited on March 13th, 2006.

Grove M., Harbor J., Engel B. (1998), "Composite vs. Distributed Curve Numbers : Effects on Estimates of Storm Runoff Depths", Journal of American Water Resources Association, Vol.34, No.5, 1015-1023

Hawkins R.H. (1993), "Asymptotic determination of runoff curve numbers from data". Journal of the Irrigation and Drainage Division, American Society of Civil Engineers 119(2): 334–345.

Hawkins R.H. and Ponce, V.M. (1996), "Runoff curve number: Has it reached maturity?", Journal of. Hydrology, Eng. ASCE 1(1), 11–19.

Hewlett J.D., Hibbert A.R. (1967), "Factors affecting the response of small watersheds to precipitation in humid area". In Proceedings International Symposium on Forest Hydrology, Sopper W.E., Lull H.W., Pergamon Press: Oxford; 275–290.

Hjelmfelt A.T. (1991), "Investigation of curve number procedure". Journal of Hydraulics Engineering 117(6): 725–737

Isaaks, E. H., and Srivastava R.M. (1989) "An introduction to applied geostatistics", Oxford University Press, New York.

Jain M. K.,Mishra S.K., Singh V.P. (2006), "Evaluation of AMC-Dependent SCS-CN- based Models Using Watershed Chracteristics", Water Resources Management, 20: 531–552

Jensen N.E., Pedersen L. (2005), "Spatial variability of rainfall: Variations within a single radar pixel", Journal of Atmospheric Research, 77 : 269–277.

Kessler E. and Neas B. (1995), "On Correlation, with Applications to the Radar and Raingauge Measurement of Rainfall", Atmospheric Research, 34:217-229.

Kunstmann H., Stadler C. (2005), "High resolution distributed atmospheric-hydrological modelling for Alpine catchments", Journal of Hydrology, 314:105-124.

Küpçü O. (1996): "Application of GIS to derive SCS Synthetic Unit Hydrograph", METU M. Sc. Thesis, METU Civil Engineering Dept.

Legates D. R. (1999), "Evaluating the Use of "Goodness of Fit" Measures in Hydrologic and Hydroclimatic Model Validation", Water Resources Research, 35:233-241.

Luce C., Tarboton D., Cooley K. (1999), "Sub-grid parameterization of snow distribution for an energy and mass balance snow cover model", Hydrological Process. 13 1921-1933

Maidment D. (1993) "Developing a spatially distributed unit hydrograph by using GIS. In : Applications of GIS in hydrology and water resources (edited by Kovar, K. and Nachtenebel, H.) Proceedings of Vienna conf., April 1993. IAHS publ. no. 211. 181-192.

Maidment D.R. (1996), "Environmental modeling with GIS. In GIS and Environmental Modeling: Progress and Research Issues", GIS World, Inc. Fort Collins, Colorado, 315-323

Mishra S.K. (1998), "Operation of a multipurpose reservoir", Unpublished PhD thesis, University of Roorkee, India.

Mishra S.K., Garg V. (2000), "An SCS-CN-based time distributed model", Journal of Hydrology, Indian Association of Hydrologists: Roorkee, Uttar Pradesh, India.

Mishra S.K., Singh V.P. (1999a), "Another look at the SCS-CN method", Journal of Hydrologic Engineering 4(3): 257–264.

Mishra S.K., Singh V.P. (1999b), "Behaviour of SCS-CN method in spectrum. Proceedings", Hydrologic Modeling, International Conference on Water, Environment, Ecology, Socio-economics, and Health Engineering, Seoul National University, Korea, 18–21 October; 112–117.

Mishra S.K., Kumar S.R., Singh V.P. (1999c), "Calibration and validation of a general infiltration model", Hydrological Processes 13: 1691–1718.

Mishra S.K. and Singh V. P. (2004), "Validity and extension of the SCS-CN method for computing infiltration and rainfall-excess rates", Hydrological processes, No:18: 3323–3345

Mockus V. (1949), "Estimation of Total (Peak Rates of) Surface Runoff for Individual Storms", Exhibit A of Appendix B, Interim Survey Report Grand (Neosho) River Watershed, USDA, 1 December.

Mockus V. 1980. Letter to Orrin Ferris, 5 March, 6 pp. 1964. Reference in Rallison, R.E., "Origin and evolution of the SCS runoff equation", Proceedings, ASCE Symposium on Watershed Management, Boise, Idaho.

Moore D. S. (1991), "Statistics: Concepts and Controversies", 3rd Edition, W. H. Freeman and Compny, New York.

Moore I., Grayson R., Ladson A. (1993), "Digital terrain modelling: a review of hydrological, geomorphological and biological applications. In : Terrain analysis and distributed modelling in hydrology (edited by Beven, K. and Moore, I.)". John Wiley & Sons, Chichester.7-30.

McCuen R. H. (1993): "Microcomputer Applications in Statistical Hydrology", Prentice Hall, New Jersey.

Paşaoğulları O. (2002), "Effect of Scale and Grid Size for Hydrological Modelling", M.Sc. Thesis, METU, Civil Engineering Dept.

Pearson K. (1932), "On a Form of Spurious Correlation Which May Arise When Indices are Used in the Measurements of Organs", Proceedings, Royal Society of London, Vol. 60, 489-502.

Porter J. and McMahon T. (1971) "A model for the simulation of streamflow data from climatic records", Journal of Hydrology, 13, 297-324.

Quinn T., Xing Zhu A., Burt J. E. (2005), "Effects of detailed soil spatial information on watershed modeling across different model scales", International Journal of Applied Earth Observation and Geoinformation, 7 : 324–338.

Raaflaub L.D., Collins M. J. (2005), "The effect of error in gridded digital elevation models on the estimation of topographic parameters" , Environmental Modelling and Software (In Press).

Rallison R. (1980), "Origin and evolution of the SCS runoff equation. In Proceedings of Symposium on Watershed Management", 21–23 July, American Society of Civil Engineers: New York, NY; 912–924.

SCS, (1975), "Soil Conservation Service: Use of storm and watershed characteristics in Synthetic Hydrograph Analysis and Application", U.S. Department of Agriculture, Washington D.C.

SCS. 1956, 1964, 1971, 1985. Hydrology, "National Engineering Handbook", Supplement A, Section 4, Chapter 10 . Soil Conservation Service, USDA: Washington, DC.

Silberstein R.P. (2006), "Hydrological models are so good, do we still need data?", Environmental Modelling and Software, 21 (no. 9): 1340-1352

Steenhuis T.S., Winchell M., Rossing J., Zollweg J.A., Walter M.F. (1995), "SCS runoff equation revisited for variable-source runoff areas". Journal of the Irrigation and Drainage Division, American Society of Civil Engineers 121(3): 234–238.

Şensoy A. (2000), "Spatially Distributed Hydrological Modelling Approach Using Geographic Information Systems", M.Sc. Thesis, METU, Civil Engineering Dept.

Şorman A.A. (1999), "A Remote Sensing and Geographic Information Systems Approach in Hydrological Modelling", M.Sc. Thesis, METU, Civil Engineering Dept.

Şorman A. A. (2005), "Use of Satellite Observed Seasonal Snow Cover in Hydrological Modeling and Snowmelt Runoff Prediction in Upper Euphrates Basin, Turkey", Ph. Doc. Thesis, Civil Engineering Department, METU.

Sutcliffe J.V. and Nash J.E. (1970), "River flow forecasting through conceptual models. Part I: A discussion of principles", Journal of Hydrology, Vol. 10: 282-290.

TEFER (2002), "Turkey Emergency Flood and Earthquake Recovery Project", DSİ.

Usul N., Şorman A.Ü., Akyürek Z., Turan B., Yılmaz M. (2001), "Çoğrafi Bilgi Sistemleri ve Hidrolojik – Hidrolik Model Entegrasyonu ile Taşkın Analizi Pilot Projesi", No: 0007-022-0001, AGÜDOS, METU, Turkey.

Wang X., and Yong Yin Z. (1998), "A comparison of drainage networks derived from digital elevation models at two scales", Journal of Hydrology, 210 : 221–241.

Western A. W., Grayson R. B., Bloschl G. (2002), "Scaling of soil moisture: a hydrologic perspective", Annual Review Earth Planet. Sciences, 30: 149–180.

Wilcox B. P., Rawls W. J., Brakensiek D. L., Wight J. R. (1990), "Predicting Runoff from Rangeland Catchments: A Comparison of Two Models", Water Resources Research, 26:2401-2410.

Willmott C. J. (1981), "On the Validation of Models", Physical Geography, 2:184-194.

Yener M. K. (2006), "Semi-distributed Hydrologic Modeling Studies in Yuvacık Basin", M.Sc. Thesis, METU, Civil Engineering Dept.

Zengin M., Hizal A., Karakas A., Serengil Y., Tugrul D.,Ercan M. (2005), "Planning of the Renewable Natural Resources of the Izmit-Yuvacık Watershed for Water Production(in terms of quality, amount and regime)", Poplar and Fast Growing Forest Trees Research Institute, Izmit, Turkey.

Zhan X., Huang M.L. (2004), "ArcCN-Runoff: an ArcGIS tool for generating curve number and runoff maps" , Environmental Modelling & Software no:19: 875–879

APPENDIX A

OBSERVED AND SIMULATED GRAPHS OF HOURLY EVENTS
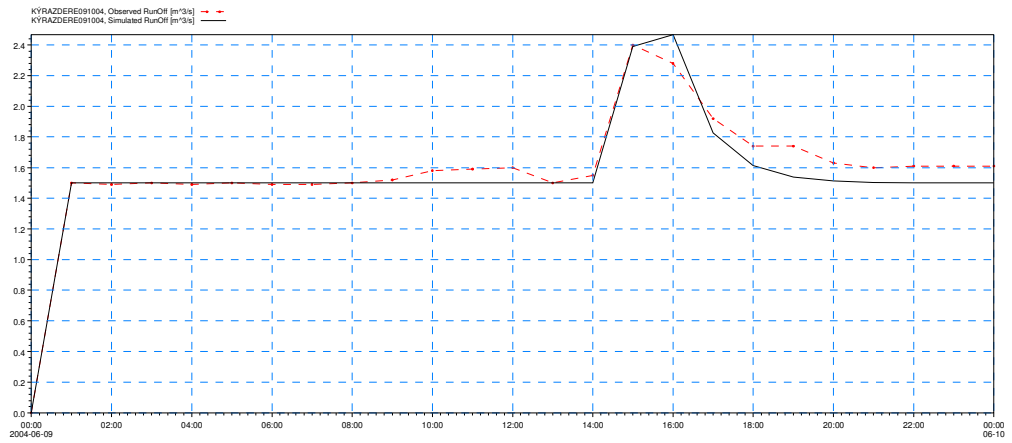
Figure A.1 : Kirazdere hourly simulation graph (09 - 10 June 2004)
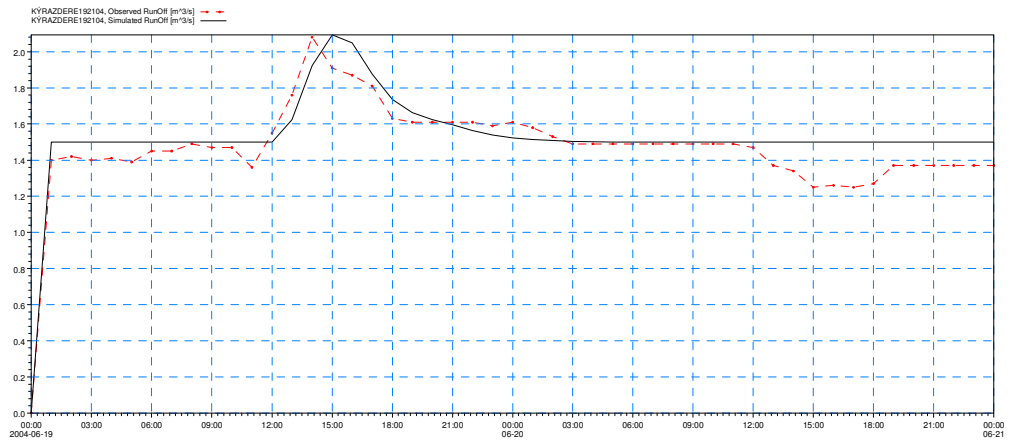
Figure A.2 : Kirazdere hourly simulation graph (19-21 June 2004)
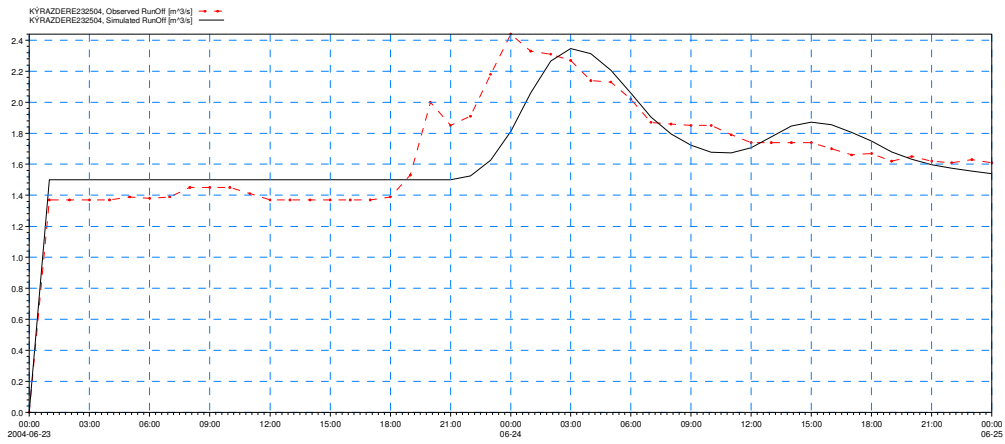
Figure A.3 : Kirazdere hourly simulation graph (23-25 June 2004)
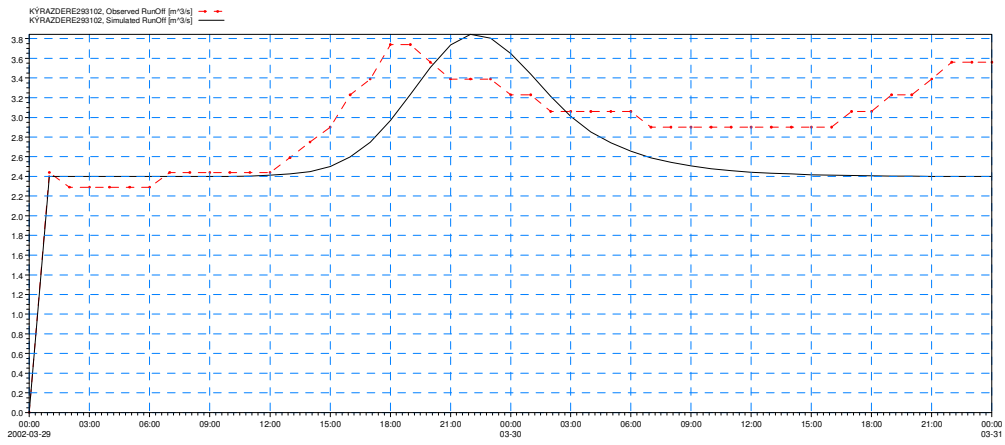
Figure A.4 : Kirazdere hourly simulation graph (29 - 31 March 2002)
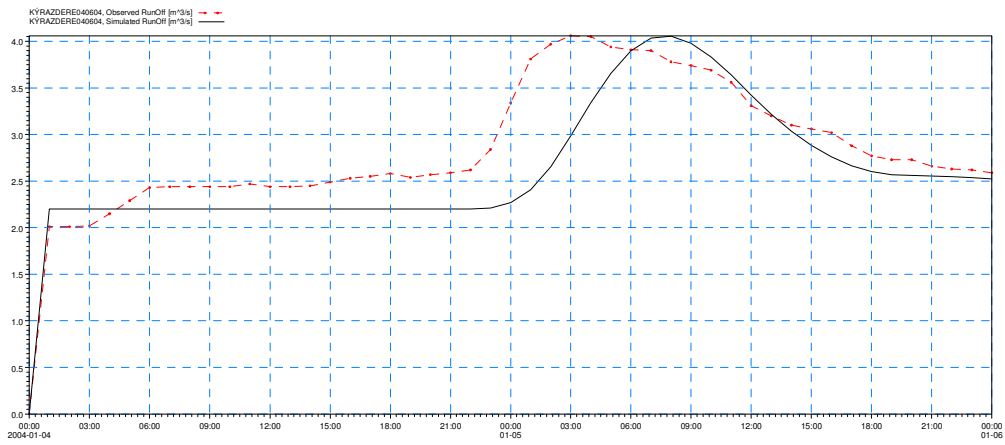
Figure A.5 : Kirazdere hourly simulation graph (04 – 06 January 2004)

130
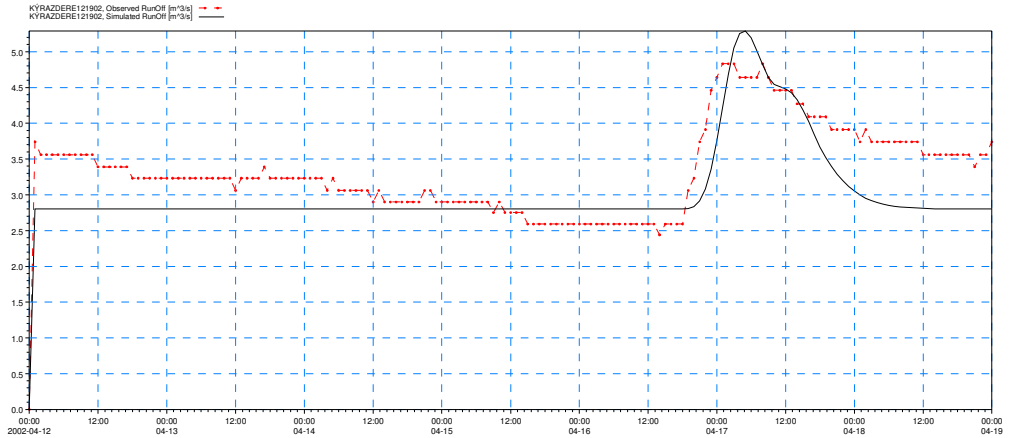
Figure A.6 : Kirazdere hourly simulation graph (12 – 19 April 2002)
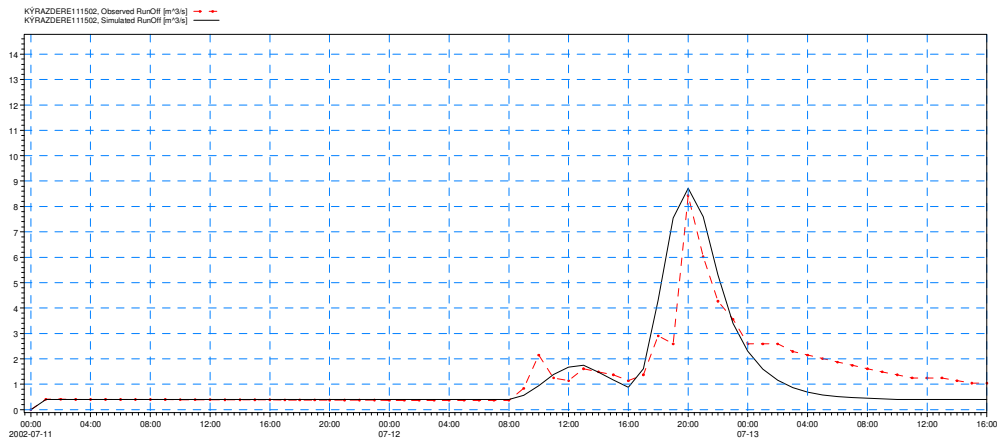
Figure A.7 : Kirazdere hourly simulation graph (11 – 15 July 2002)
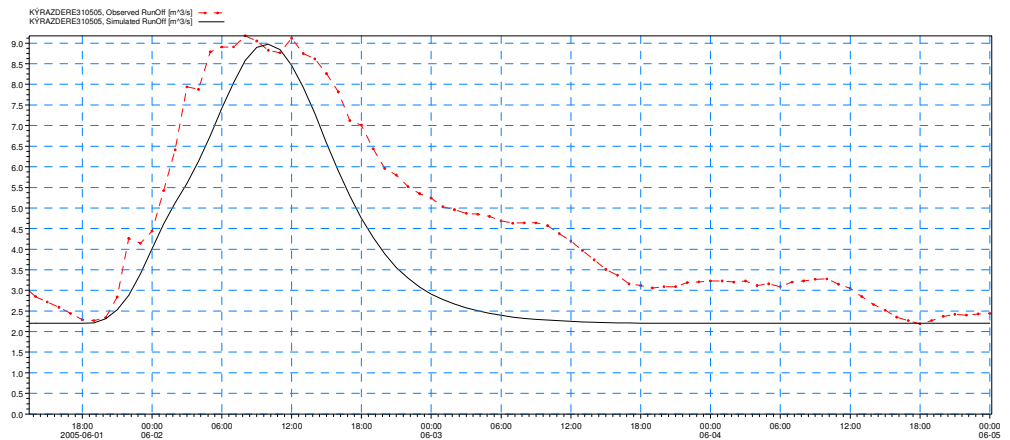
Figure A.8 : Kirazdere hourly simulation graph (31 May – 05 June 2005)
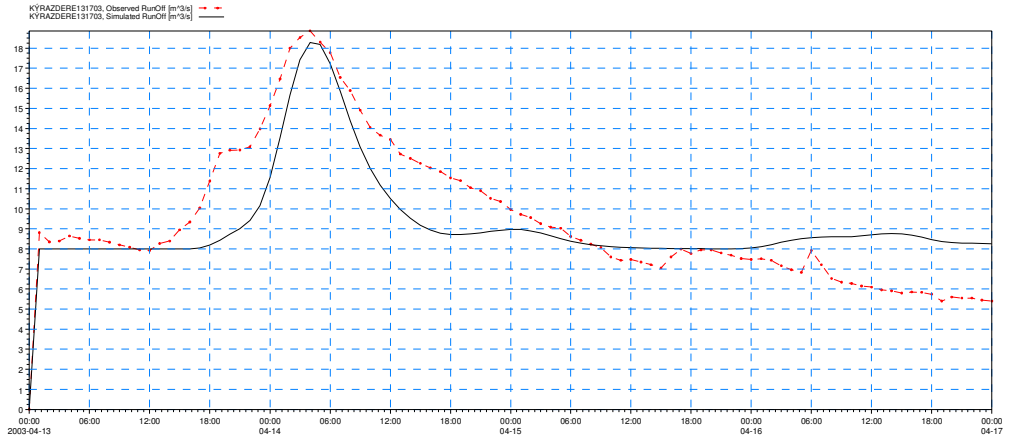
Figure A.9 : Kirazdere hourly simulation graph (13 – 17 April 2003)
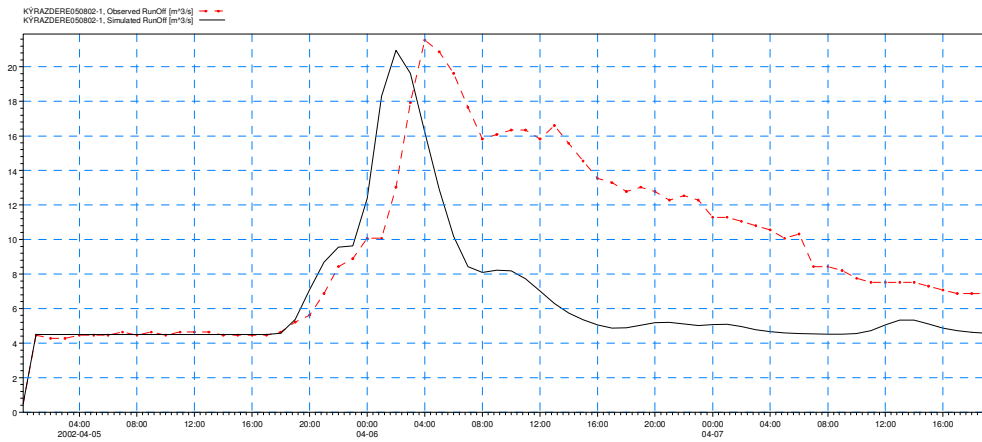
Figure A.10 : Kirazdere hourly simulation graph (05 – 08 April 2002)
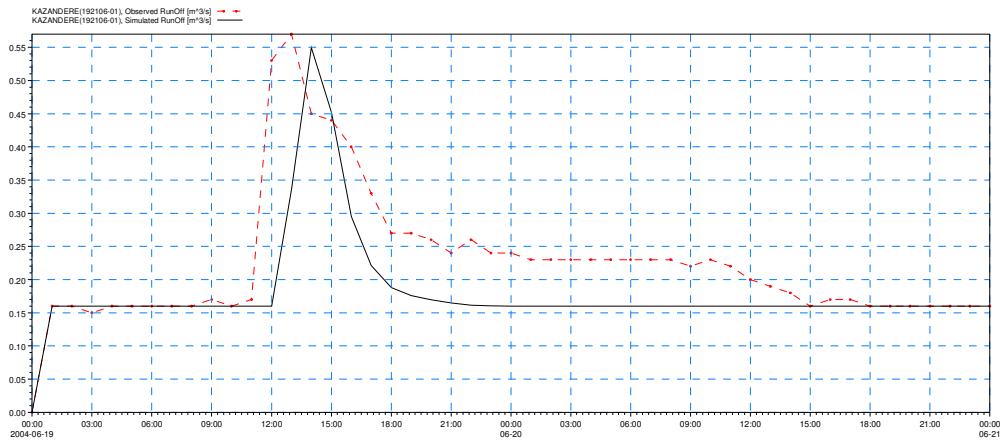
Figure A.11 : Kazandere hourly simulation graph (19 – 21 June 2004)
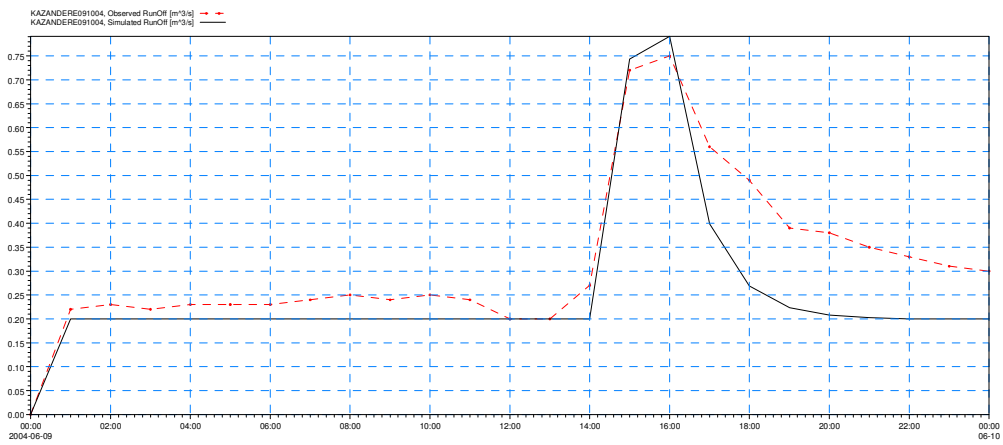
Figure A.12 : Kazandere hourly simulation graph (09 – 10 June 2004)
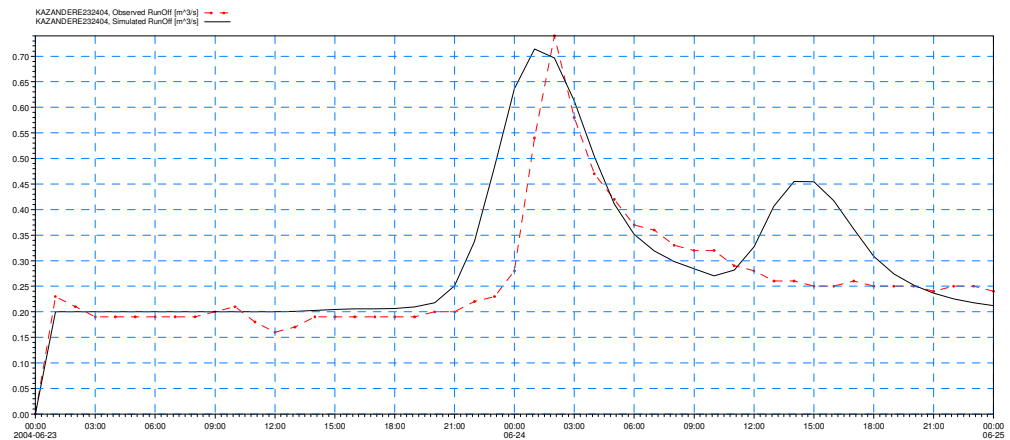
Figure A.13 : Kazandere hourly simulation graph (23 – 25 June 2004)
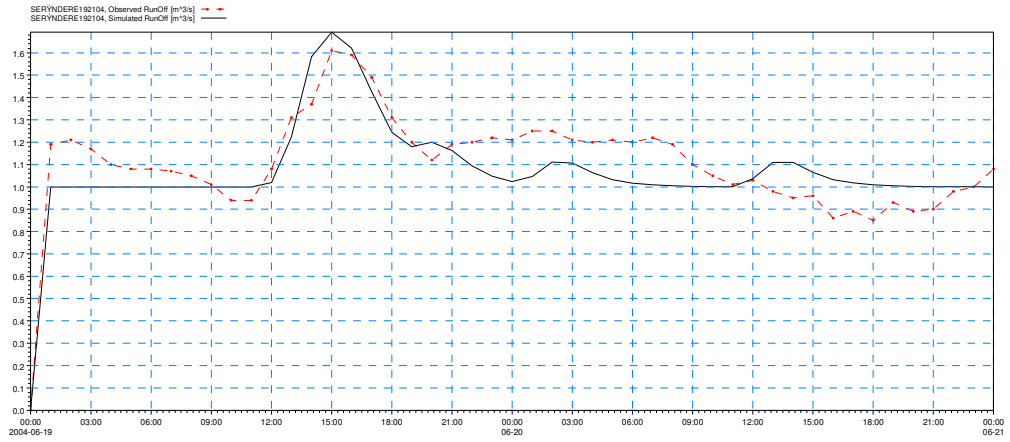
Figure A.14 : Serindere hourly simulation graph (19 - 21 June 2004)
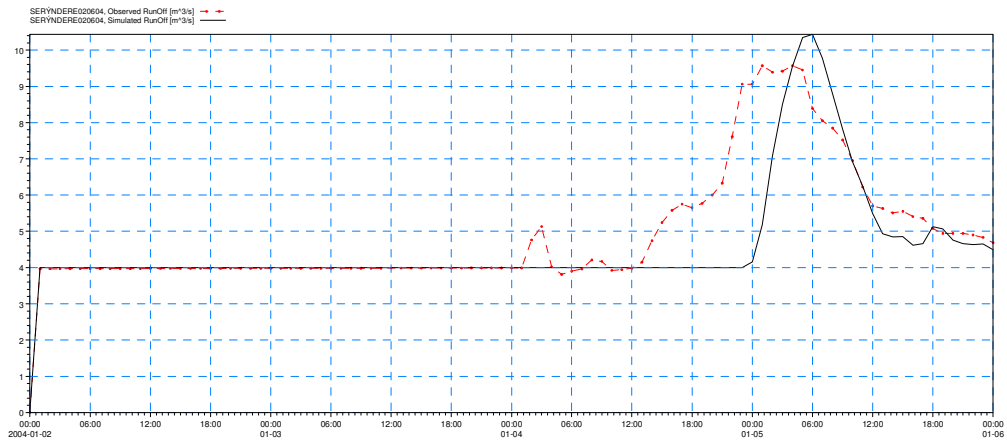
Figure A.15 : Serindere hourly simulation graph (04 – 06 January 2004)
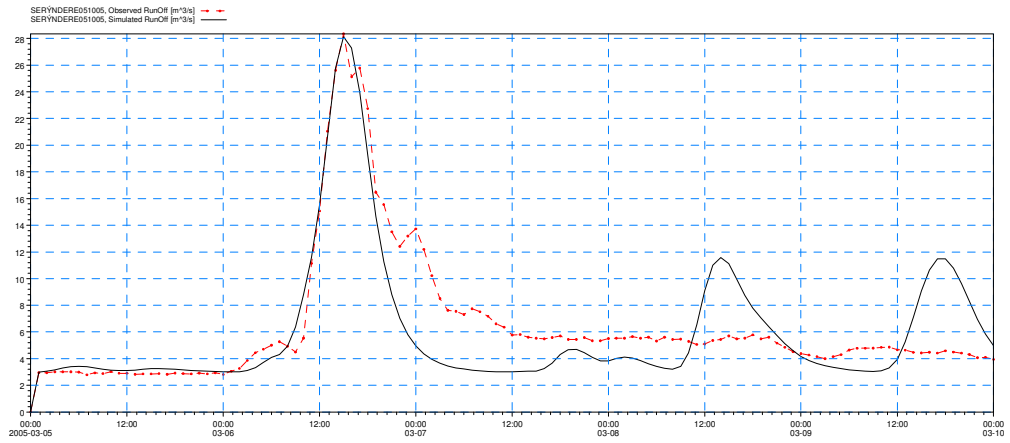
Figure A.16 : Serindere hourly simulation graph (05 – 10 March 2005)

APPENDIX B

OBSERVED AND SIMULATED GRAPHS OF DAILY EVENTS
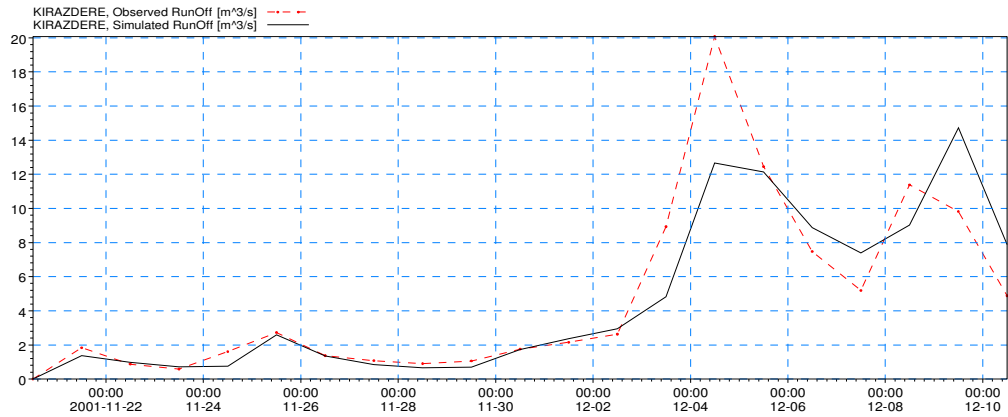
Figure B.1 : Kirazdere calibration result graph (20.11.2001 – 10.12.2001)
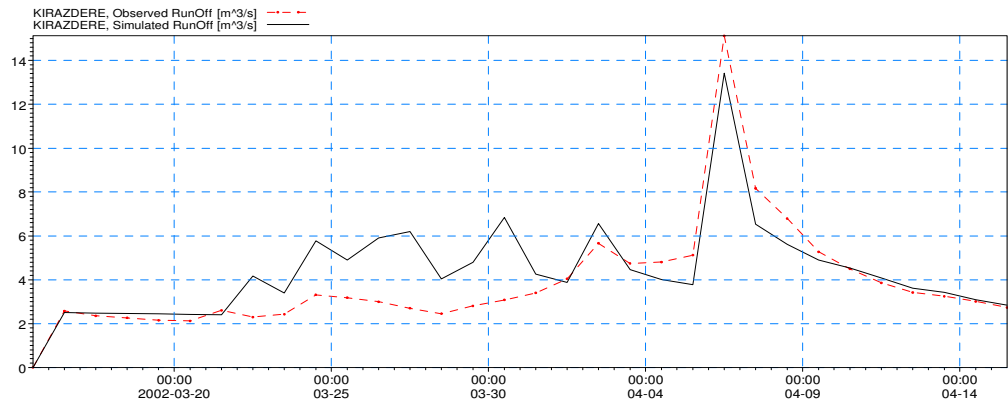
Figure B.2 : Kirazdere calibration result graph (15.03.2002 – 15.04.2002)
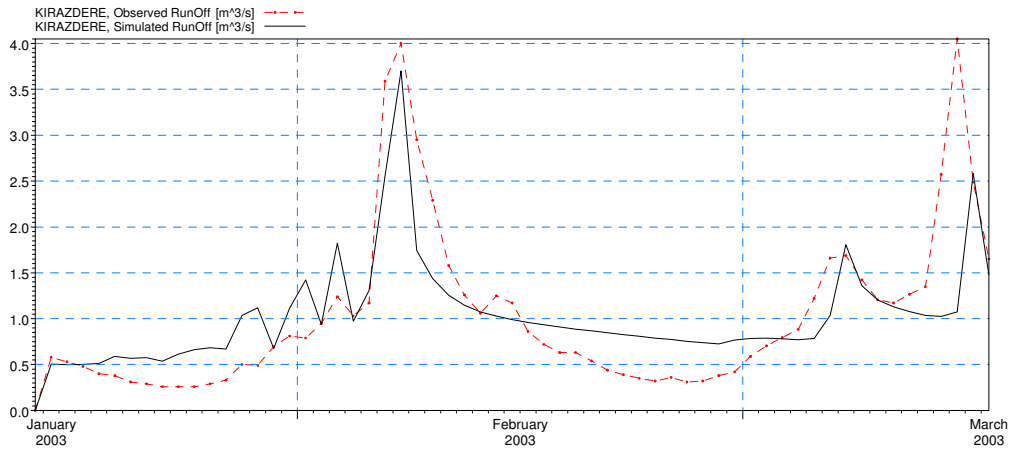
Figure B.3 : Kirazdere calibration result graph (15.01.2003– 16.03.2003)
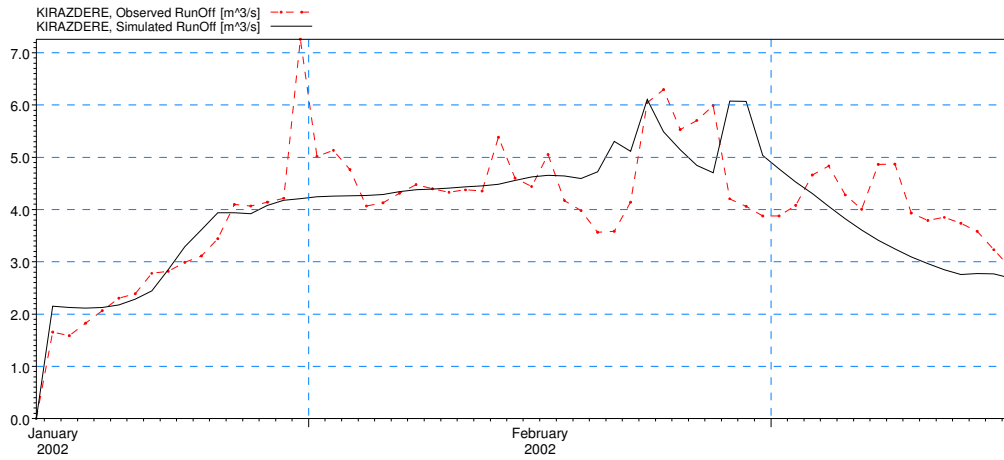
Figure B.4 : Kirazdere calibration result graph (15.01.2002– 15.03.2002)
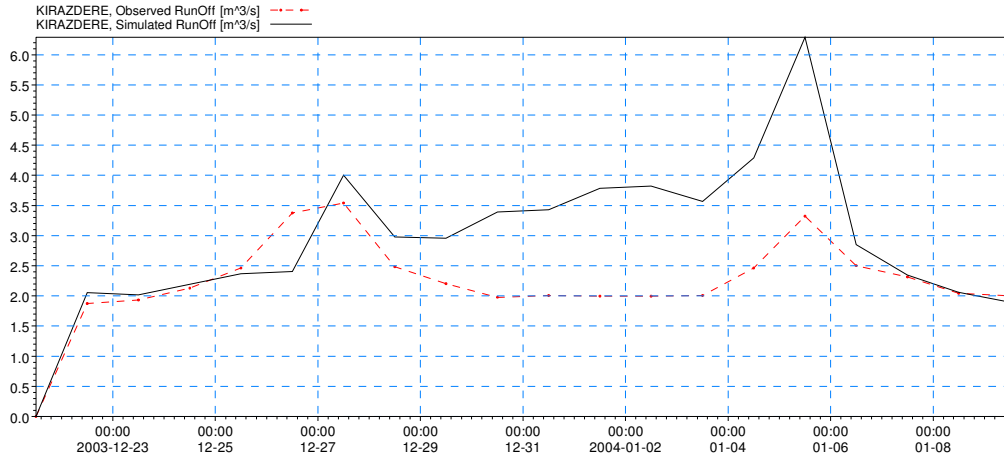
Figure B.5 : Kirazdere validation result graph (15.03.2003– 22.04.2003)
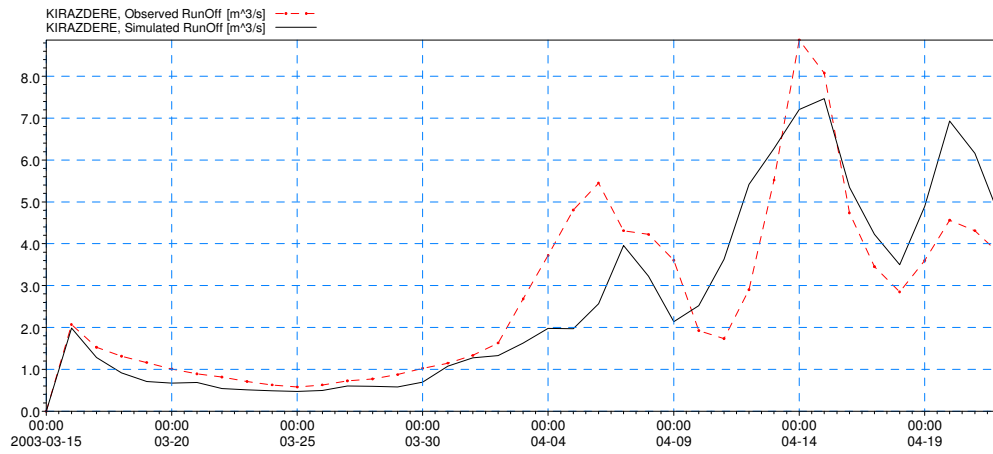
Figure B.6 : Kirazdere calibration result graph (21.12.2003– 09.01.2004)
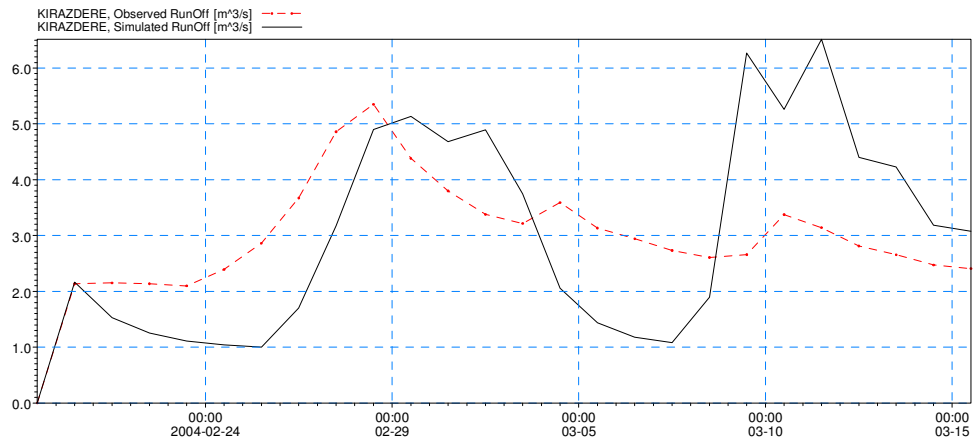
Figure B.7 : Kirazdere calibration result graph (19.02.2004– 15.03.2004)
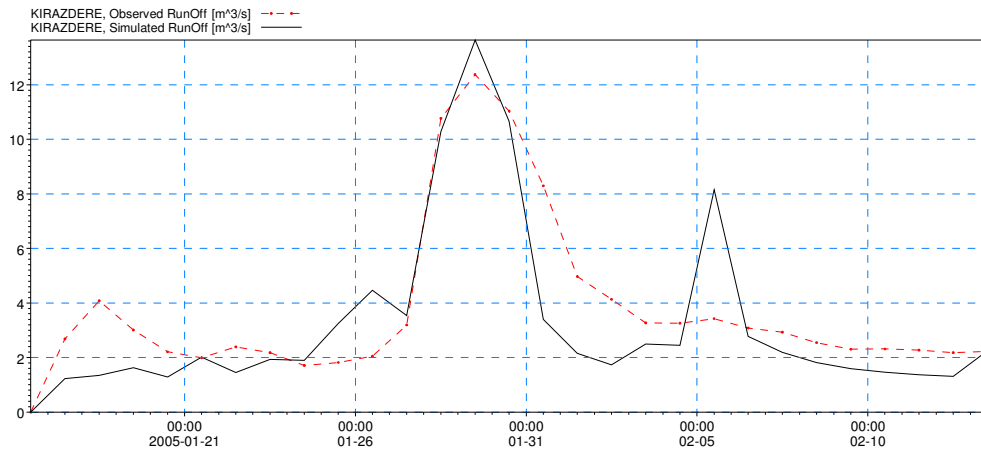
Figure B.8 : Kirazdere validation result graph (16.01.2005– 13.02.2005)
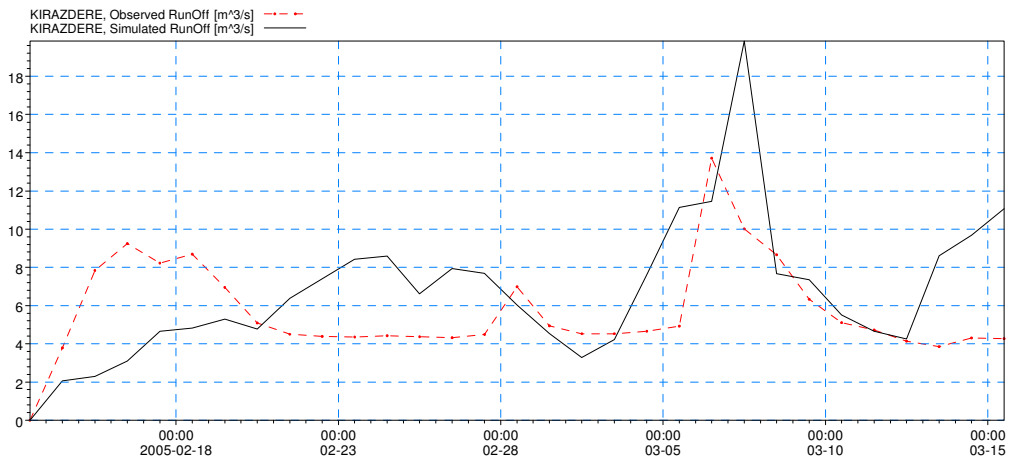
Figure B.9 : Kirazdere validation result graph (13.02.2005– 15.03.2005)
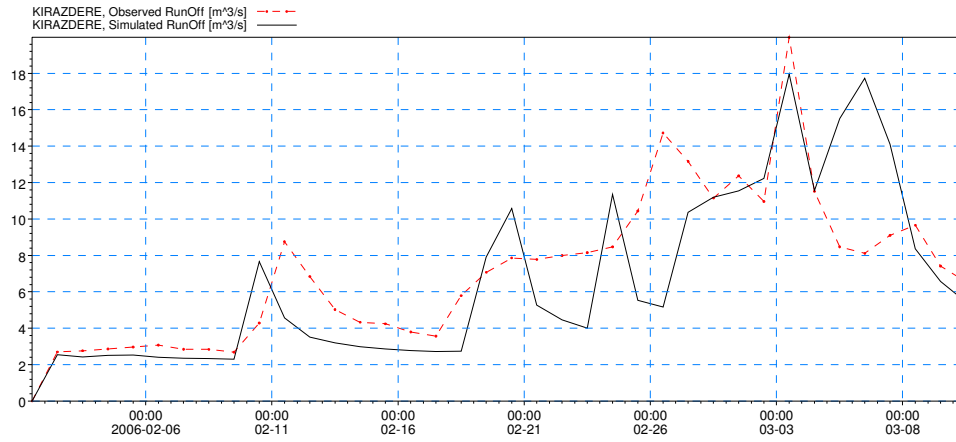
Figure B.10 : Kirazdere validation result graph (01.02.2006– 10.03.2006)
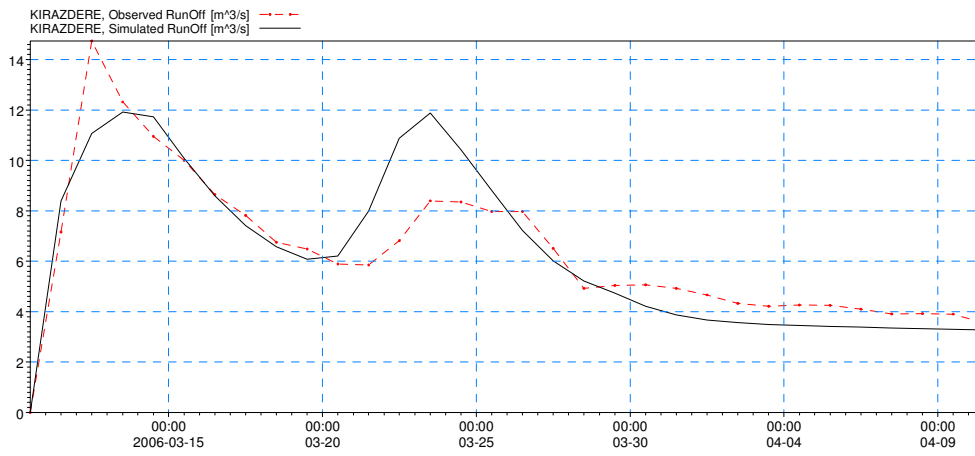
Figure B.11 : Kirazdere validation result graph (10.03.2006– 10.04.2006)
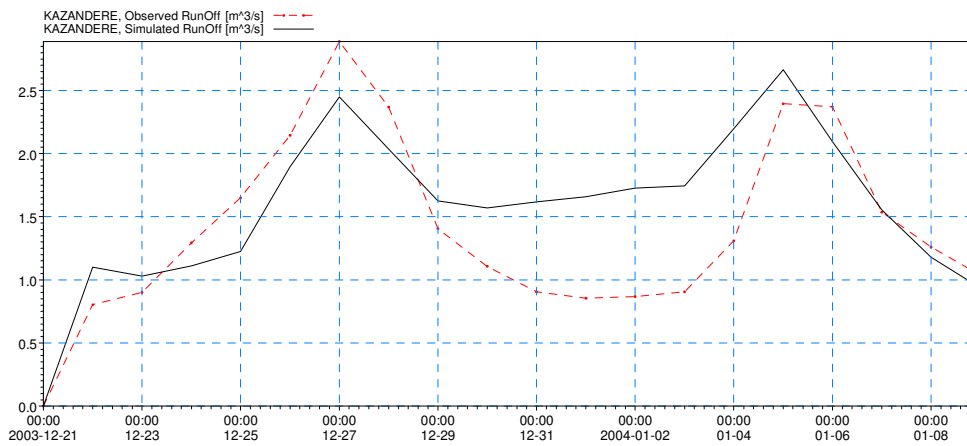
Figure B.12 : Kazandere calibration result graph (21.12.2003– 09.01.2004)
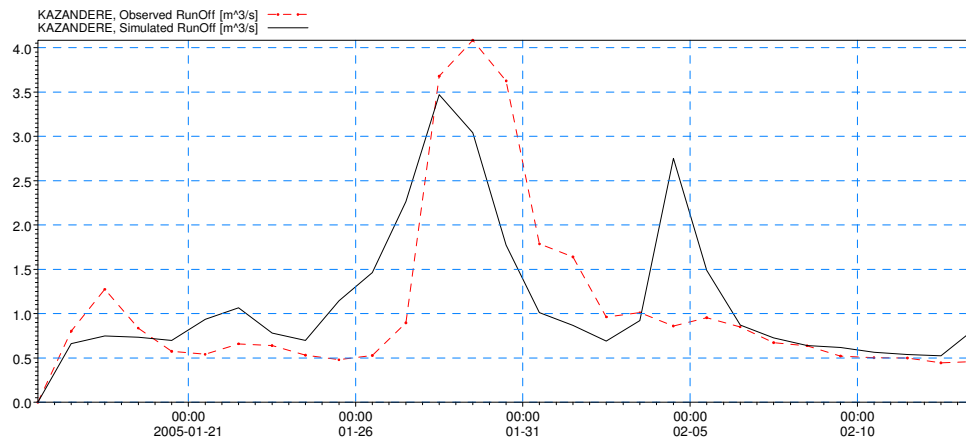
Figure B.13 : Kazandere calibration result graph (16.01.2005– 13.02.2005)
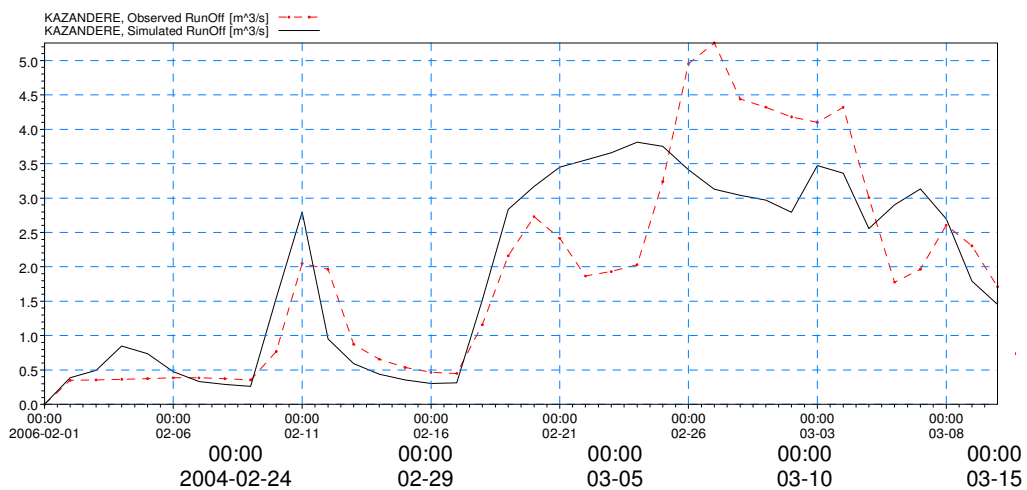
Figure B.14 : Kazandere calibration result graph (19.02.2004-15.03.2004)
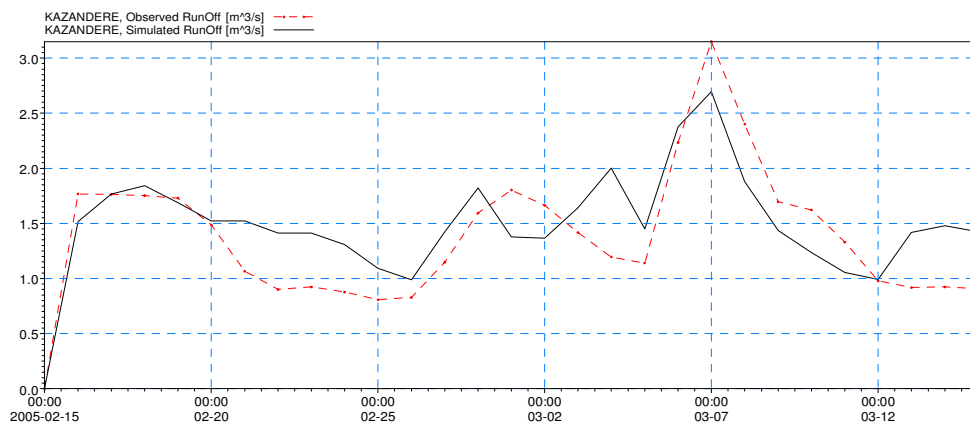
Figure B.15 : Kazandere calibration result graph (13.02.2005– 15.03.2005)

140
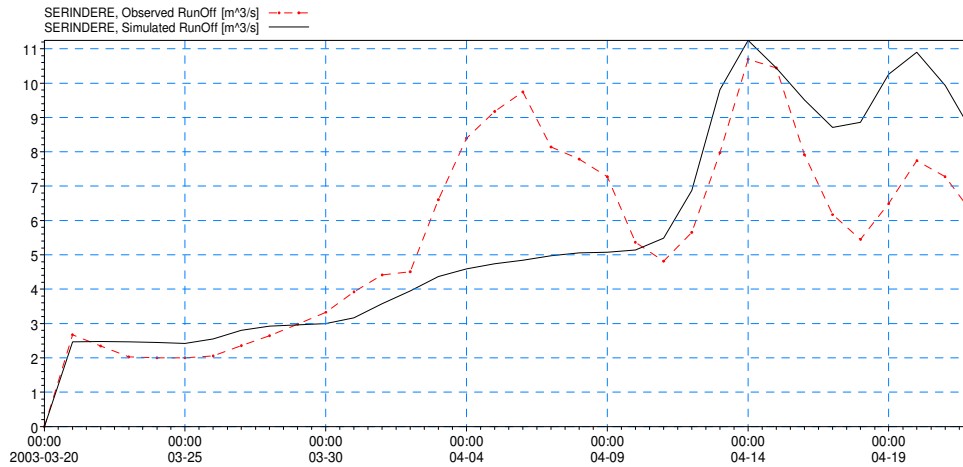
Figure B.16 : Kazandere calibration result graph (01.02.2006– 10.03.2006)
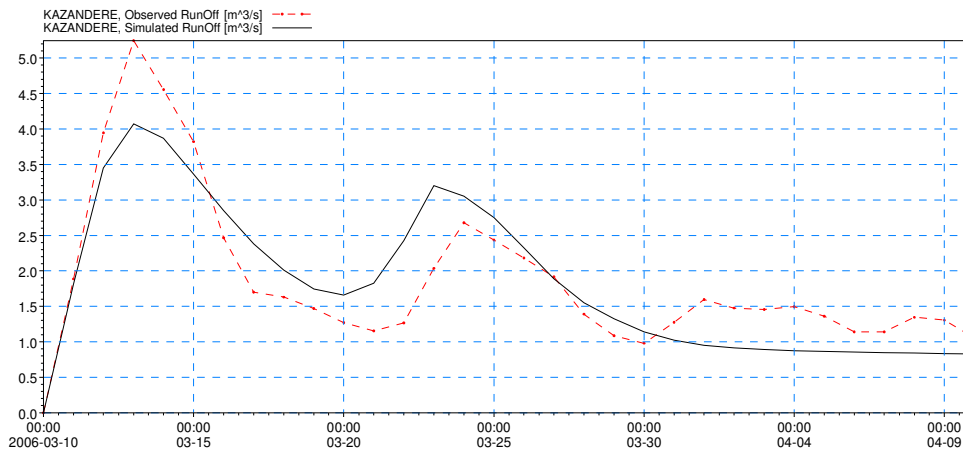
Figure B.17 : Kazandere calibration result graph (10.03.2006 – 05.04.2006)
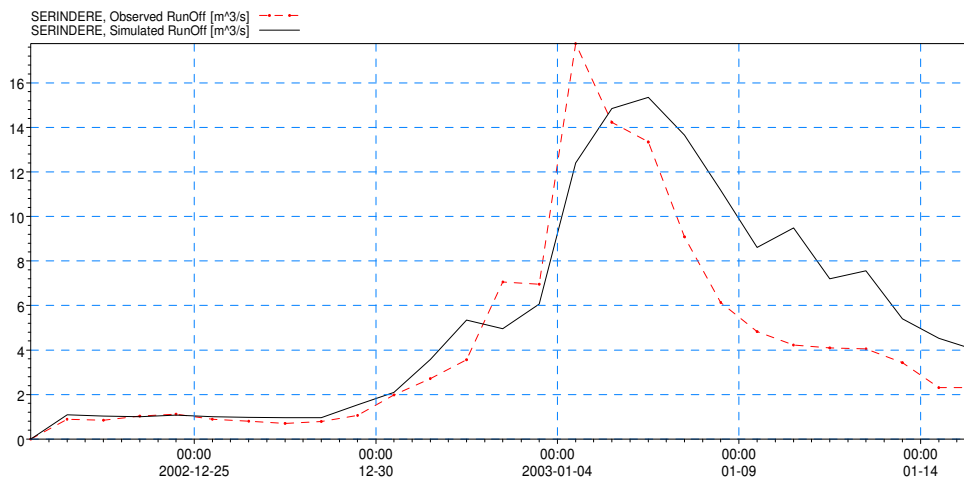
Figure B.18 : Serindere calibration result graph (20.12.2002 – 15.01.2003)
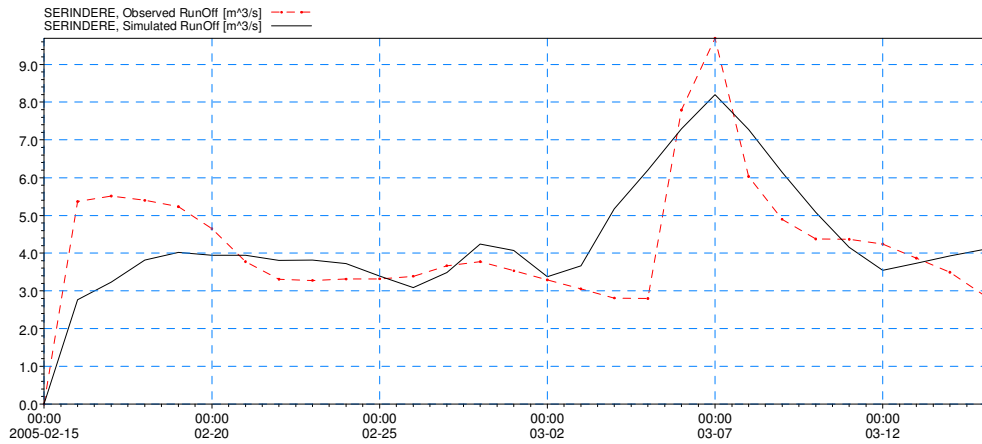
Figure B.19 : Serindere calibration result graph (20.03.2003 – 22.04.2003)
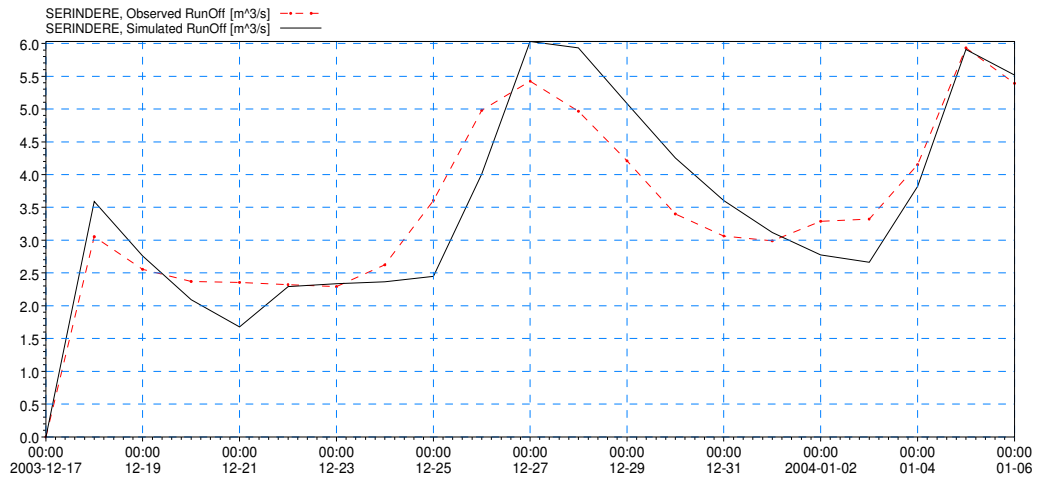
Figure B.20 : Serindere calibration result graph (17.12.2003 – 06.01.2004)
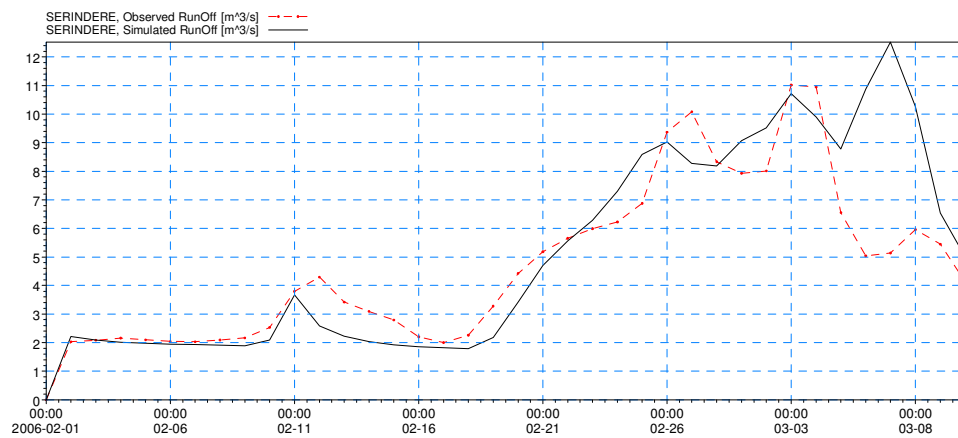
Figure B.21 : Serindere calibration result graph (01.02.2006 – 10.03.2006)

142
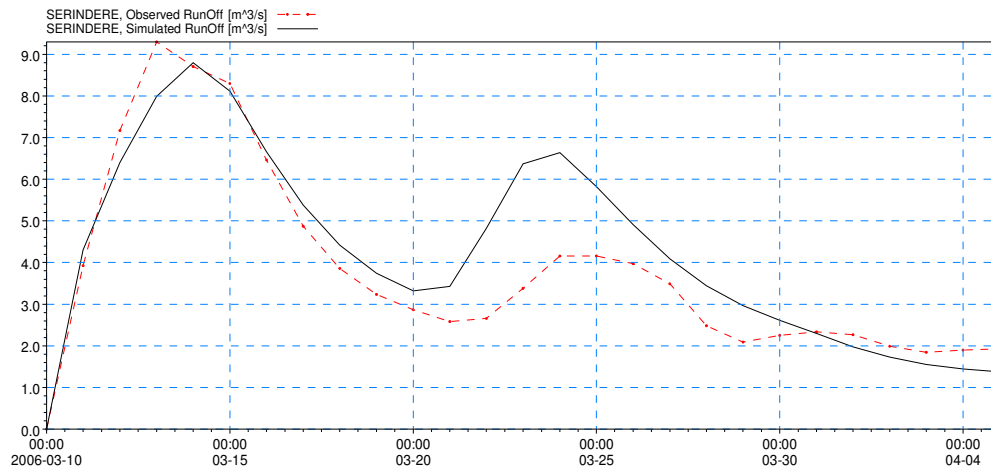
Figure B.22 : Serindere calibration result graph (10.03.2006 – 05.04.2006)

APPENDIX C

PREPARATION OF SIMULATION FILES

Simulations

The input parameters for the Mike 11 is described in chapter 4. In this part, The detailed explanation of preparation of timeseries and simulation files is given.

Timeseries

As explained in fourth chapter, NAM module uses the rainfall, flow, temperature, evaporation values as input. Before starting a new project all of the timeseries of these data must be prepared for the use of model. Model can not use ASCII data directly. Mike 11 uses the file extensions *.dfs0 as the input and the output files. The timeseries can be prepared by different calendar axis such as equidistant calendar axis, non- equidistant calendar axis etc. The example of selecting the time axis is shown in Figure C.1.
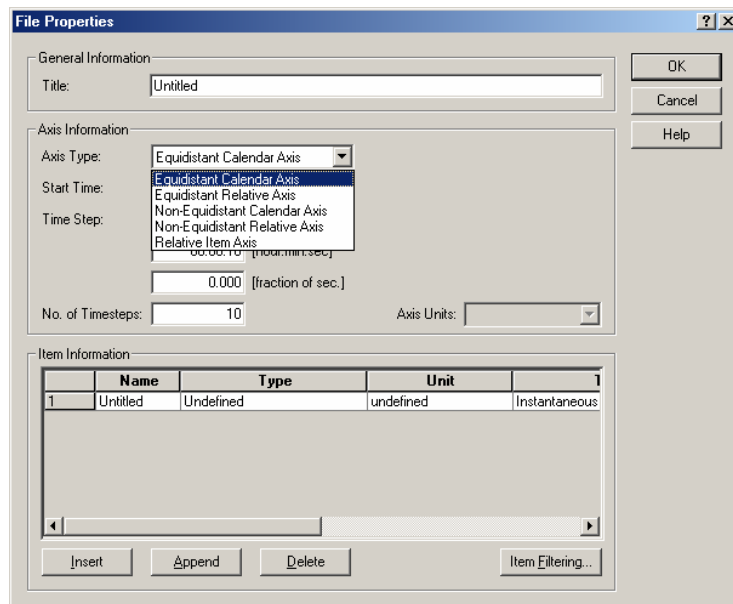
Figure C.1 : An example to form a time series

In the "Item Information" tab, there is one row opened. The type and the unit of the data can be selected from this window. If unit of data does not coincide with the available data, the program give meaningless results.

Simulation editor

Simulation Editor is used to define the modules that will be used. Also it acts like a chainage between the editors so that anyone can use the modules editors without going any other folder. Below is an example from the Kirazdere Runs of water year 2001-2002. As it can be seen from the Figure C.2 that all the modules are included in the simulation editor page. We can select the modules that we will use in the simulation. Here just the "Rainfall-Runoff" is checked.
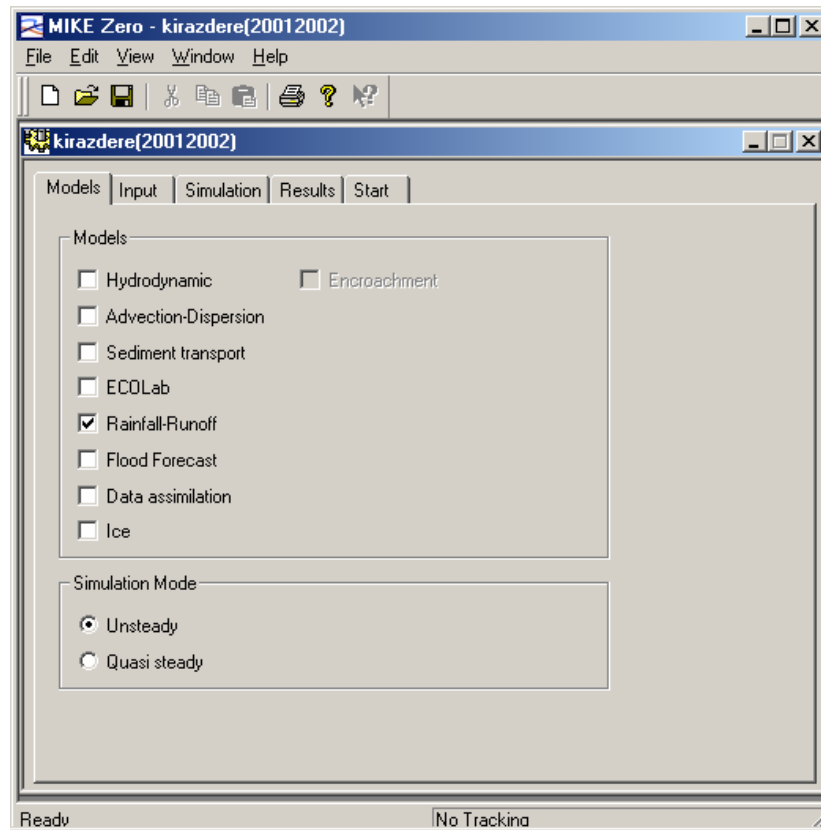
Figure C.2 : Simulation editor

When we click the "Input" Tab bar on the page, we come to a page that we define the locations of our files that will be used in the simulation as shown in Figure C.3.
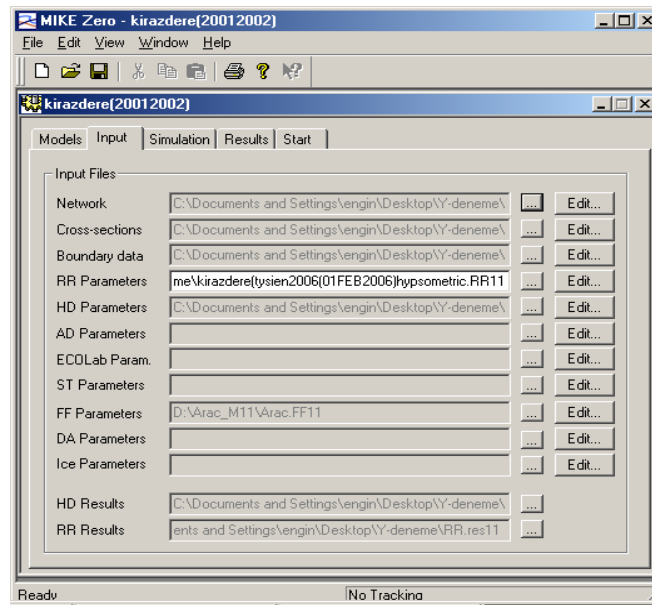
Figure C.3 : Adding the RR parameter file in simulation editor

Simulation editor(Input)

When we click the "Simulation" Tab bar on the page, we come to a page that we define the period, the initial type of condition and the time step of the simulations. The initial type of condition can be given as result file or parameter File. If the result file is checked then the result file of the previous simulations will be used as initial conditions. If the Parameter file is checked then the initial parameters that is defined in the RR Editor are used as initial conditions. Time step depends on our timeseries time step. We can select "Fixed time step" (which is used in this study) as shown in Figure C.4.

146
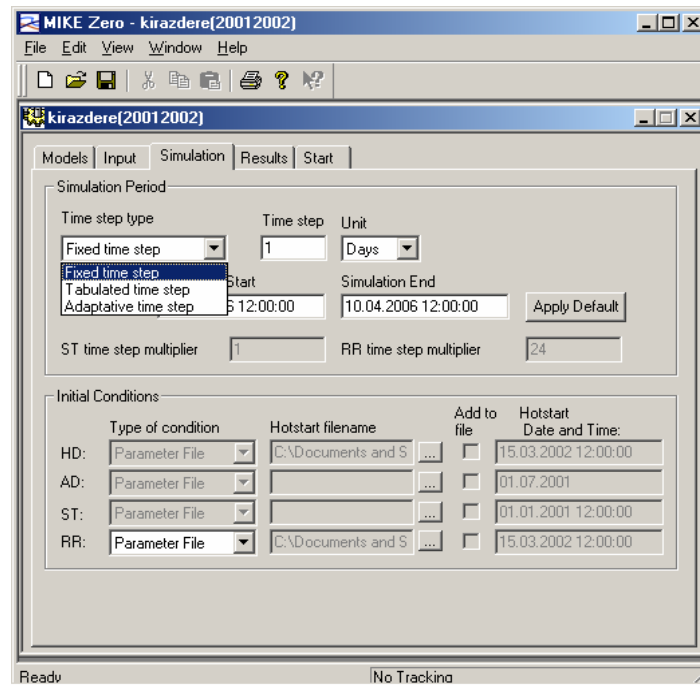
Figure C.4 : Defining the time steps in simulation editor

Rainfall runoff (RR) editor

The Rainfall Runoff Editor (RR-editor) provides the following facilities:

- Input and editing of rainfall-runoff and computational parameters required for rainfall-runoff modelling.

- Specification of timeseries. Time series are specified on the Timeseries page within the Rainfall Runoff Editor. In other Mike 11 modules, the time series input are specified in the boundary file.

- Calculation of weighted rainfall through a weighting of different rainfall stations to obtain basin rainfall.

- Digitizing of basin boundaries and rainfall stations in a graphical display (Basin View) including automatic calculation of basin areas and mean area rainfall weights.

- Presentation of Results. Specification of discharge stations used for calibration and presentation of results.

Simulation

The Rainfall Runoff Editor builds a file containing all the specified data with extension .RR11. Once the basins have been defined and the rainfall-runoff, and the model parameters specified in the rainfall-runoff editor, the Simulation is started from the Mike 11 Run (or simulation) Editor.

- Time step: It is recommended to use a time step not larger than the time step in the rainfall series and not larger than the time constant for routing of overland flow.

Specifying model basins

The basin page is used to prepare the basins to be included in the RR editor as shown in Figure C.5.
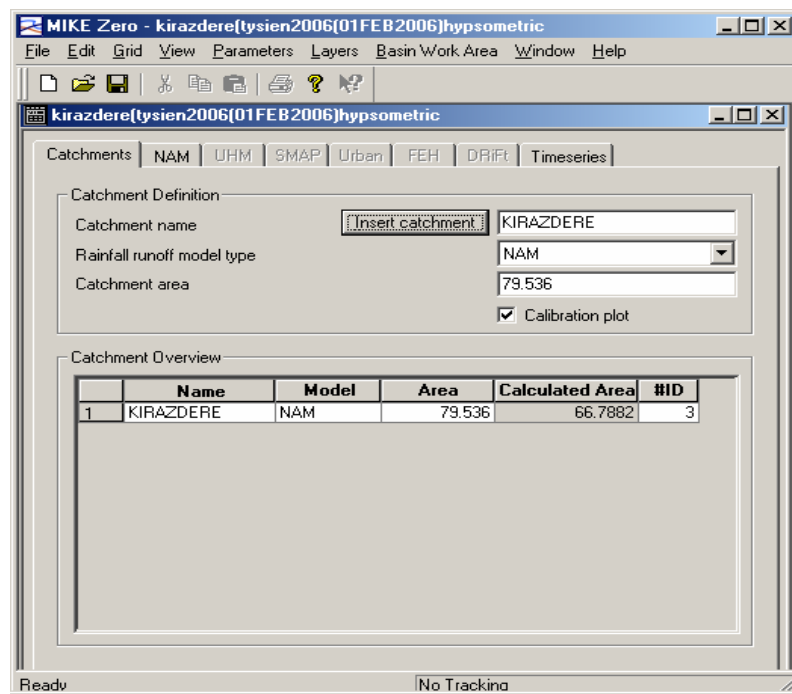
Figure C.5 : Specifying model basins

Inserting basins

New basins are defined via the Insert Basin dialog. The insert basin dialog is automatically activated for the first basin, when creating a new RR- parameter as

shown in Figure C.6. A new RR parameter File is created from the Mike Zero File dialog. Additional basins are defined when pressing the button: Insert basin.

A new basin can be prepared as a copy with parameters from an existing basin or with default parameters . The copy also includes time series from the existing basin.
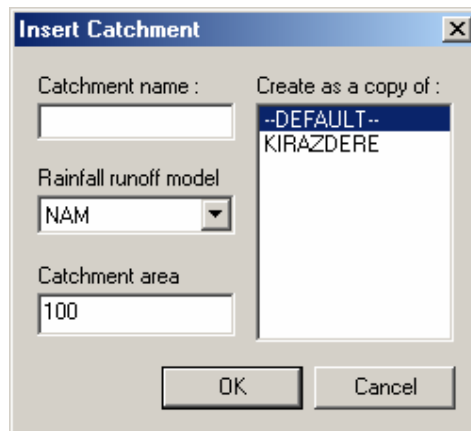
Figure C.6 : Inserting a new basin

Basins definitions

A basin is defined by;

Basin name

Simulations can be carried out for several basins at the same time. The basin name could reflect e.g. the location of the outflow point.

Rainfall runoff model type

The parameters required for each Rainfall-Runoff model type are specified in separate pages in the editor. Following models can be selected. The explanations of the models are given in the first part:

- NAM

- UHM

- SMAP

- Urban

- Combined

Basin area

Defined as the upstream area at the outflow point from a basin.

Calibration plot

A calibration plot will automatically be prepared for basins, where the time series for observed discharge have been specified on the Time series Page and the selection of calibration plot has been ticked off. The calibration can be loaded from the Plot composed and is saved in the subdirectory RRCalibration.

Calculated areas

The Calculated area shown in the Basin Overview is based on the digitized basin boundaries in the Graphical display. The calculated area is activated when the Basin View has been selected. The Basin Area is shown in the edit fields for Area and Calculated Area, when transferring a basin from the Basin View to the basin page. The Area which is used in the model calculation can afterwards be modified manually.

After the selection of the model that will be used, the selected model tab bar is automatically activated. From the activated tab bar, in this study NAM model", you can define the parameter where the definitions of the parameters are given in the first part. Figure C.7 is an example from the study basin Kirazdere.
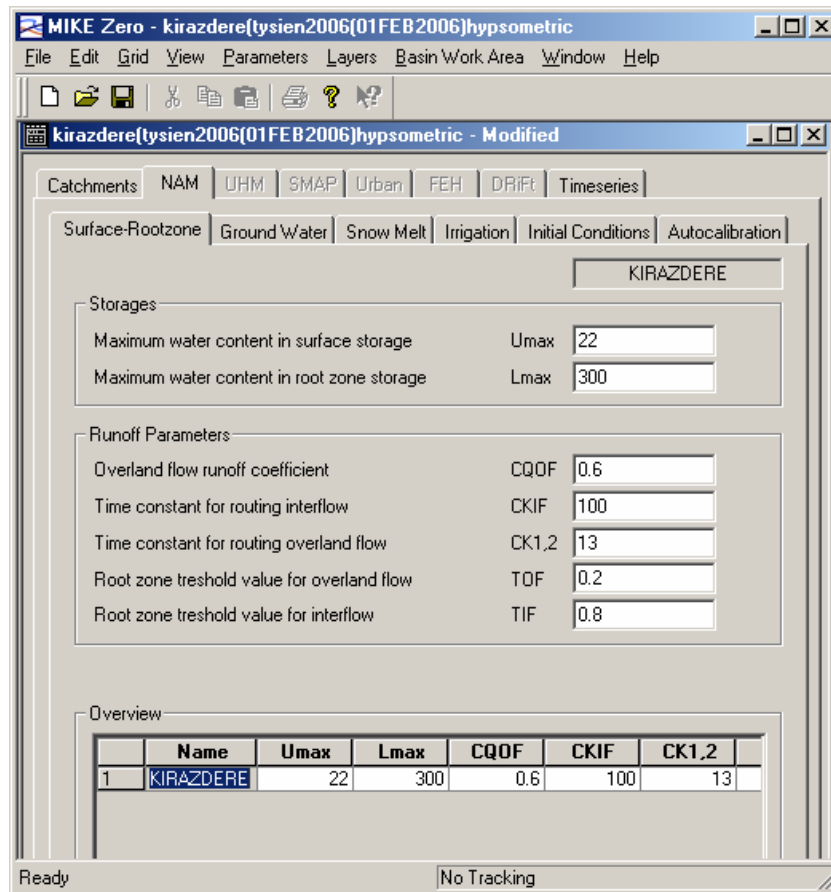
Figure C.7 : Parameters window of RR editor

In the "Ground water" tab bar, the definition of the parameters is possible. The "Snow Melt" tab bar is used to define the parameters for the snow melt as shown in Figure C.8. In Yuvacık Dam Basin the snow melt is very effective in the runoff , so it is activated in this study.
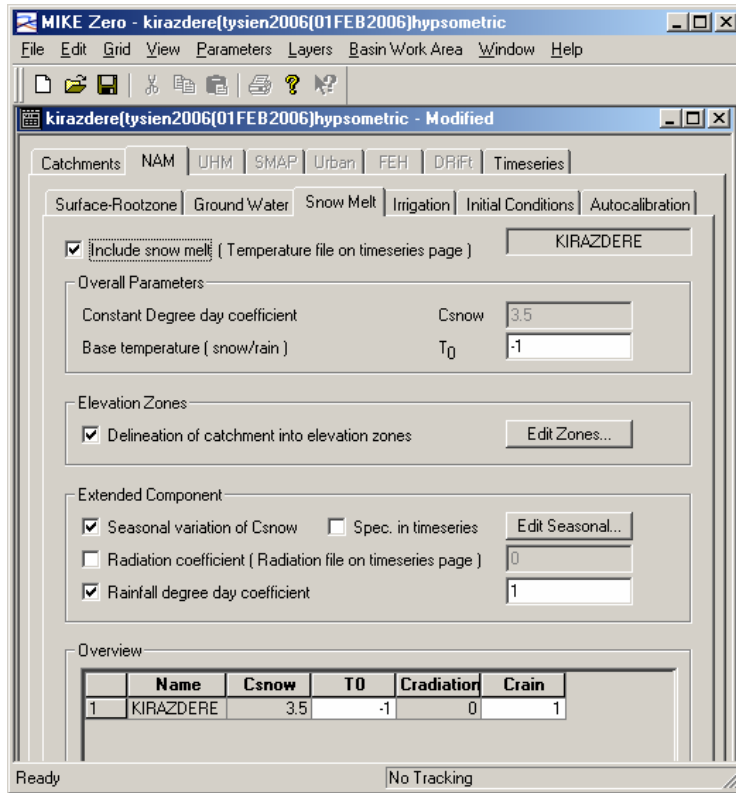
Figure C.8 : Snow melt parameters window

The detailed description of all of the parameters are given in the first part of this report. When the "Delineation of Basin into elevation zones" is checked, below is an example from the activation. In this study the Kirazdere basin is divided into three elevation zones as shown in Figure C.9.

Figure C.9 : Elevation zones of Kirazdere

Also when the "Seasonal variation of Csnow" is checked, the variation of Csnow can be defined monthly. As it can be seen from the Figure C.10, Csnow values increase in winter time and decrease in summer time. Depending on the period of the simulation of interest, the model use the related Csnow value.

Figure C.10 : Seasonal variation of snow melt for Kirazdere basin

If there is any effect of Irrigation in the basin then the "Irrigation " tab bar is activated. But in this study it is not used.

The "Initial Conditions" tab bar is used to define the initial conditions parameters for the simulation as shown in Figure C.11. This values are used when the "Parameter file" is selected in the Simulation Editor. In most of the hydrological models, the definition of the snow depth is not an easy task so there is an option to define the initial snow depth as snow water equivalent value. Figure C.12 is an example for defining the initial snow value.
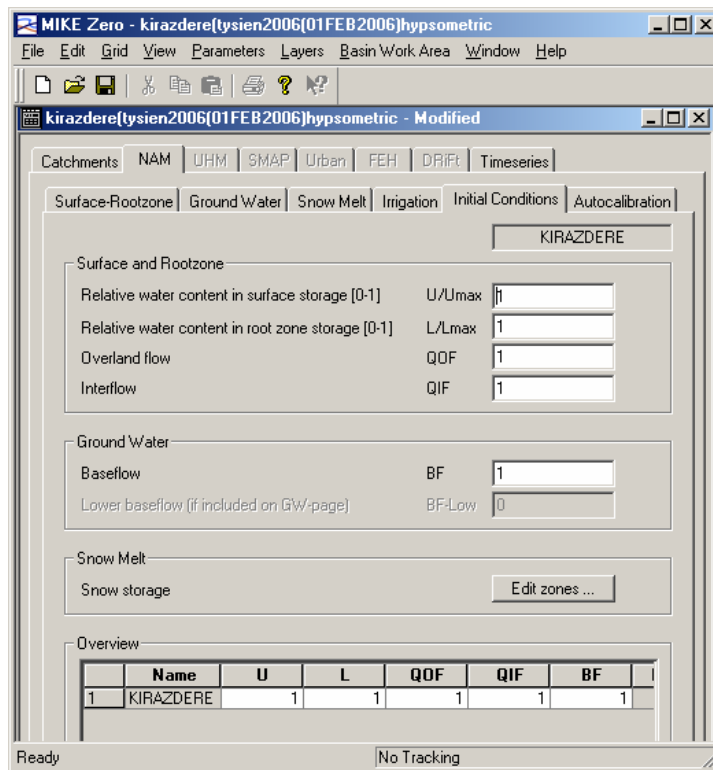
Figure C.11 : Defining the Initial conditions for the simulation

154
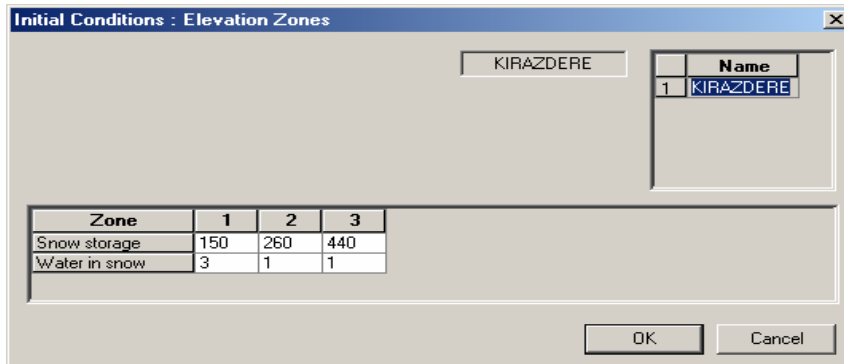
Figure C.12 : Initial snow water equivalent for elevation zones

The "Autocalibration" tab bar is used if the autocalibration process will be applied to the parameters. For running the autocalibration process the observed data must be available and defined in the timeseries.

In the above "Timeseries" tab bar in the RR editor window, the definition of the files which are as timeseries is given. The timeseries page serves two purposes: Input of time series and calculation of weighted time series. The temperature timeseries is a must if any snow melt component is defined. Also the observed data timeseries must be defined if any autocalibration process is applied. Figure C.13 is an example of the timeseries of Kirazdere basin.
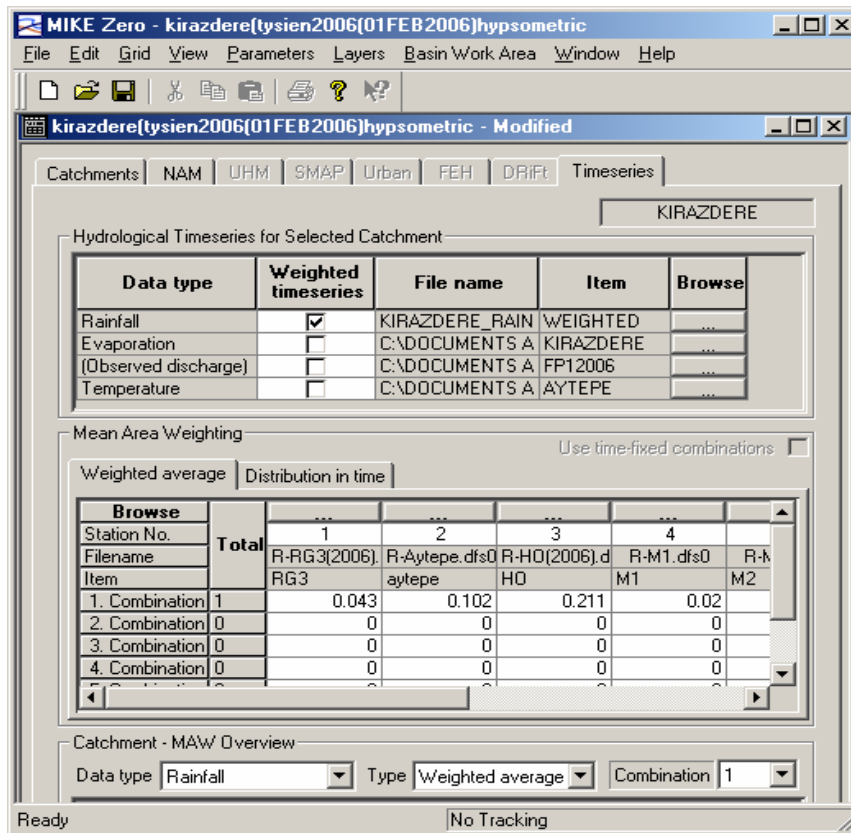
Figure C.13 : Defining the timeseries for the simulation

Input of time series

The input time series for the rainfall-runoff simulations are specified on this page. The time series are used as boundary data to a Mike 11 simulation.

Calculation of weighted time series

This calculation usually needs only be made once. Once the calculation is made the result are stored in time series that can be used for subsequent rainfall-runoff modelling runs. If the rainfall data, weights or number of basins changes the calculation must be repeated.

The Mean Areal Weighting calculation can be performed in two ways.

1- Directly within the Rainfall Runoff Editor. From the top toolbar menu select Basin Work Area and the Calculate mean precipitation. The calculation is made without requiring a model run.

2- During a simulation. A new simulation is started in the Simulation Editor:

If the weighted time series is ticked, the Mean Area weighting calculation is carried out as part of the model run.

It is recommended to use option 1.This will ensure that the available periods of the input files known in the simulations editor.

After having calculated the weighted time series once the calculation can be disconnected when removing the tick mark for weighted time series.

Mean area weighting

Weighted average combinations

Where complete time series for all stations are available for the entire period of interest only one weight combination is required. Where data is missing from one or more stations during the period of interest different weight combinations can be specified for different combinations of missing data.

It is not necessary to specify weight combinations for all possible combinations of missing stations. For each calculation, the Mean Area Weighting algorithm will identify estimate weights which best represent the actual combination of missing data. In most cases only one set of weights need to be specified. The Mean Area Weighting algorithm will automatically redistribute weights from missing stations equally to the stations with data.

Alternatively, the user may specify the weight to be used for specific combination of missing data. For each such basin, a suitable weight should be specified for the reporting stations and a weight of "-1.0" given for the non-reporting station(s), including missing data.

Distribution in time

If data is available from stations reporting at different frequencies, e.g. both daily and hourly stations, the Distribution in time of the average basin rainfall may be determined using a weighted average of the high-frequency stations. You may, for example, use all daily and hourly stations to determine the daily mean rainfall over the basin and subsequently use the hourly stations to the distribute (desegregate) this

daily rainfall in time. Different weight combinations for different cases of missing values may be applied also to this calculation of the distribution in time.

Results view applications

Model generates two Rainfall Runoff Result files. The first result file contains simulated runoff and net precipitation. The second, additional result file (RRAdd) contains time series of all calculated variables, such as the moisture contents in all storages, the baseflow etc., and can be very useful during model calibration. The results of the simulation can be generated in two formats, either as RES11 or DFS0 file type. The format of the result file should be selected before running the simulation. Three facilities are available to plot and analyze the results of a rainfall-runoff simulation:

1. MikeView. To apply MikeView for result analysis during calibration, use RES11 as result file type. Plot layouts can be generated (and saved) in MikeView for comparing simulated and observed flow while displaying e.g. the Root Zone storage variation, the snow storage, the rainfall etc.

2. MikeZero time series editor. The time series editor can also be used to view and compare simulated and measured results and to export results to e.g. a spreadsheet for further processing. The result file should then be given a DFS0 extension.

3. MikeZero plot composer. The MikeZero Plot composer, which also uses DFS0 files, is suitable for arranging final plots for presentation in reports and can also be used in the calibration procedure.

Summarized output

Mike 11 generates as standard a Table with yearly summarized values of simulated discharge. The Table is stored as the text file "RRStat.txt" in the current simulation directory. The Table is extended with observed discharge for catchments, where the time series for observed discharge have been specified on the Timeseries Page. This includes a comparison between observed and simulated discharge with calculation of the water balance error and the coefficient of determination.

The output from a NAM catchment is extended with summarized values from other components in the total water balance for a catchment. Figure C.14 shows an example on the content of summarized information about Kirazdere simulation for the period of Feb 01- Apr 10, 2006
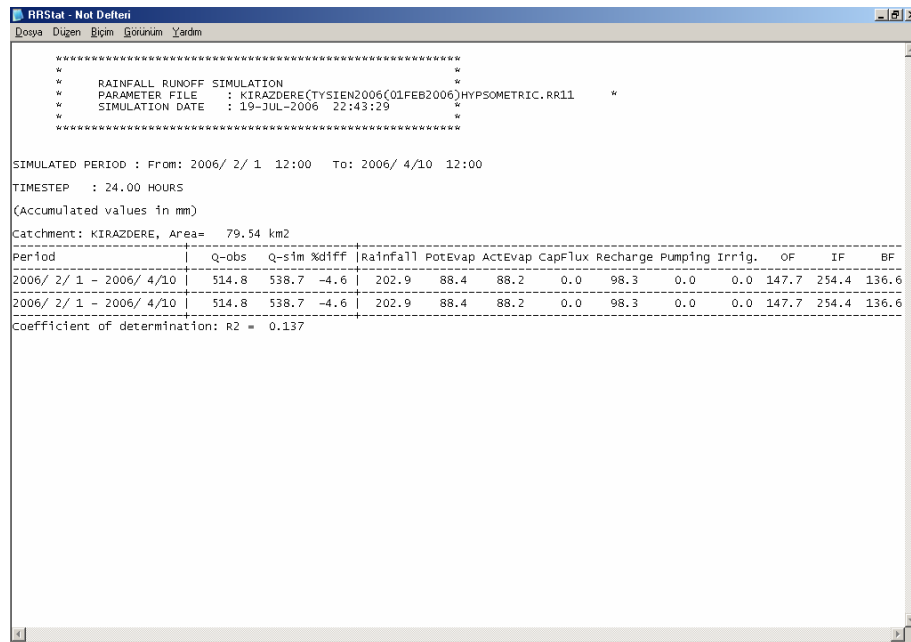

Figure C.14 : Example of summarized information

Calibration plot

A calibration plot will automatically be prepared for catchments, where the time series for observed discharge have been specified on the Time series Page and the selection of calibration plot has been ticked off on the catchment page. The calibration can be loaded from the Plot composed and is saved in the subdirectory RRCalibration with the file name: Catchment- name.plc. The time series in these plots are also available in DFS0 format in the subdirectory RRcalibration with the file name: Catchmentname. dfs0. The plot shows following results (an example for the result file is shown in Figure C.15 for the period February 01- April 10, 2006 for Kirazdere catchment)

159
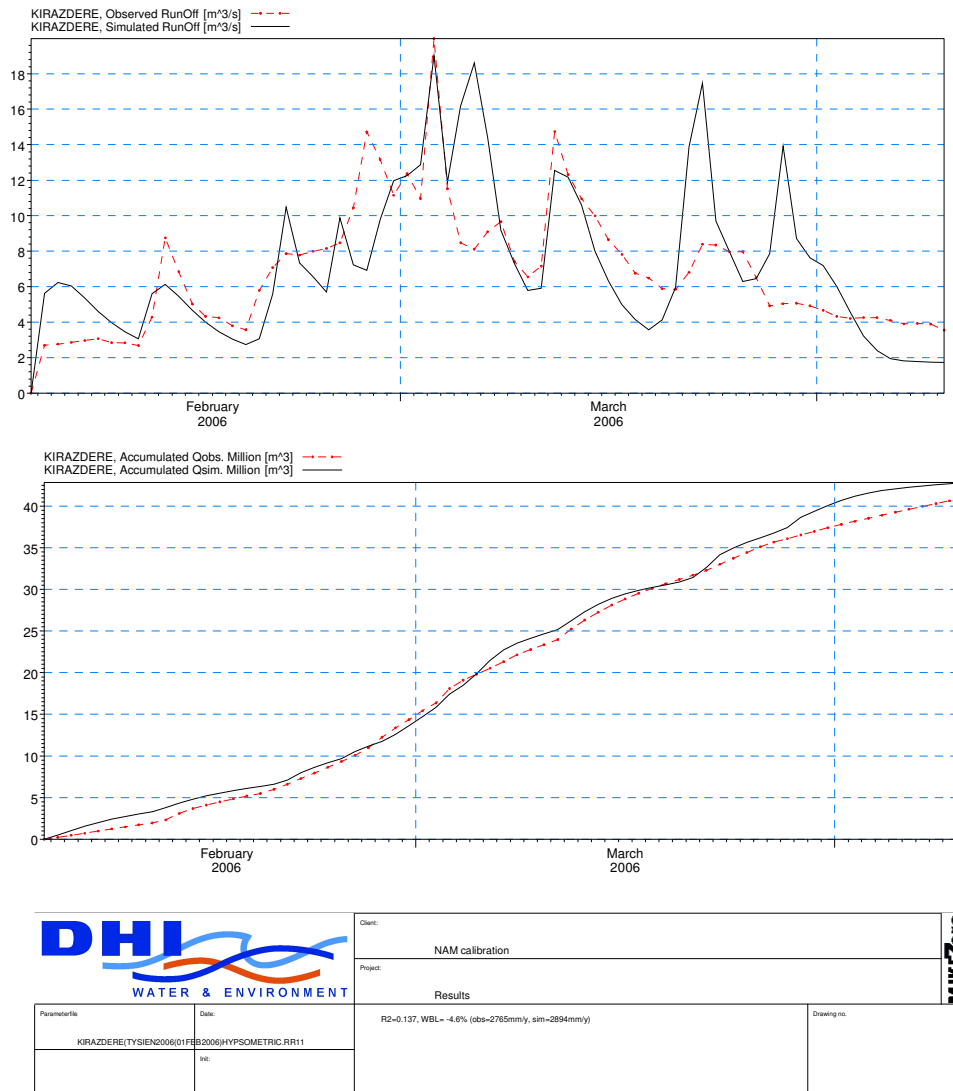
Figure C.15 : Example of a result file

The below items can be seen in the calibration plot window.

– Comparison between observed and simulated discharge.

– Comparison between accumulated series for observed and simulated discharge.

- Values for water balance error and coefficient of determination.

AIR TEMPERATURE LAPSE RATE COMPARISON GRAPHS
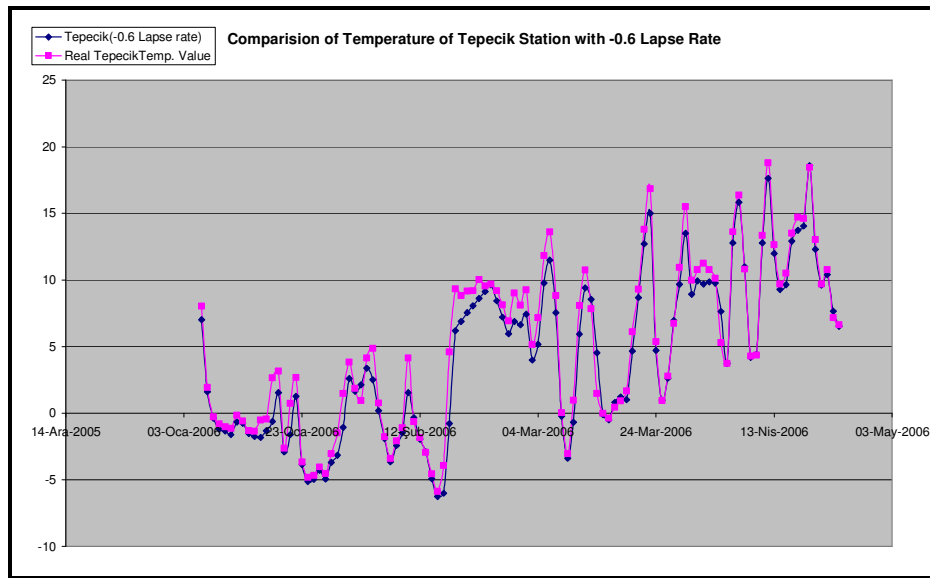
Figure D.1 : Comparison of the real air and lapse rate modified temperature for RG7
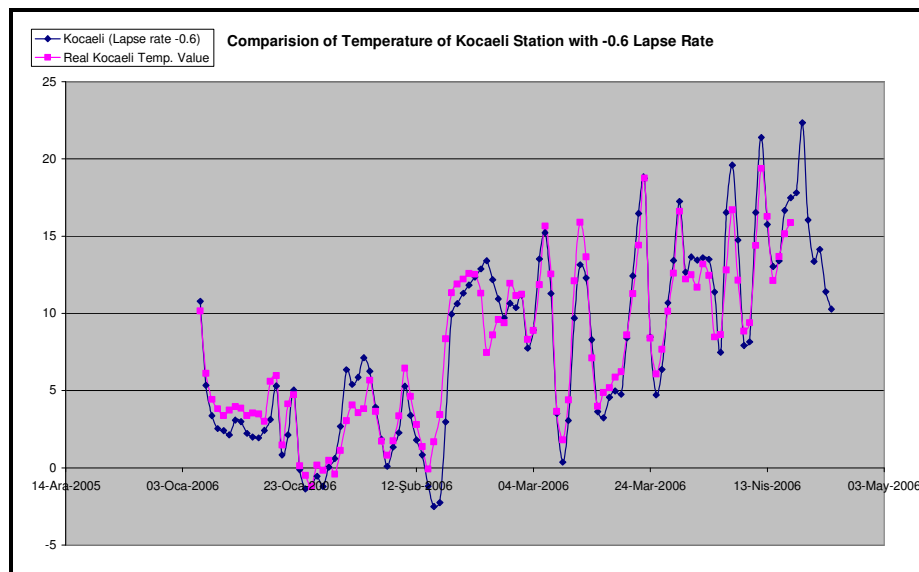
Figure D.2 : Comparison of the real air and lapse rate modified temperature for KE
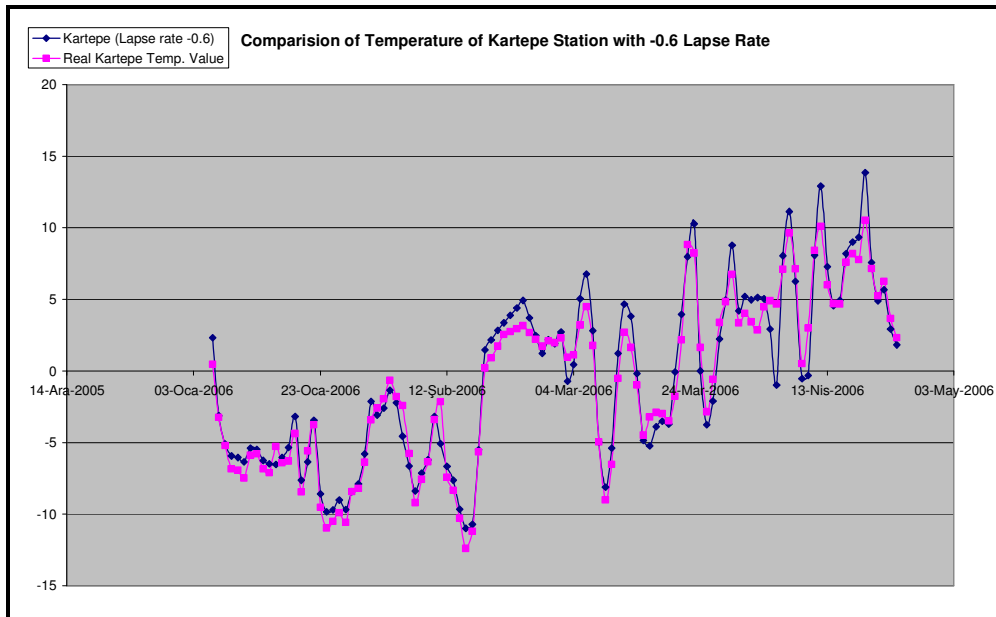
Figure D.3 : Comparison of the real air and lapse rate modified temperature for
RG10
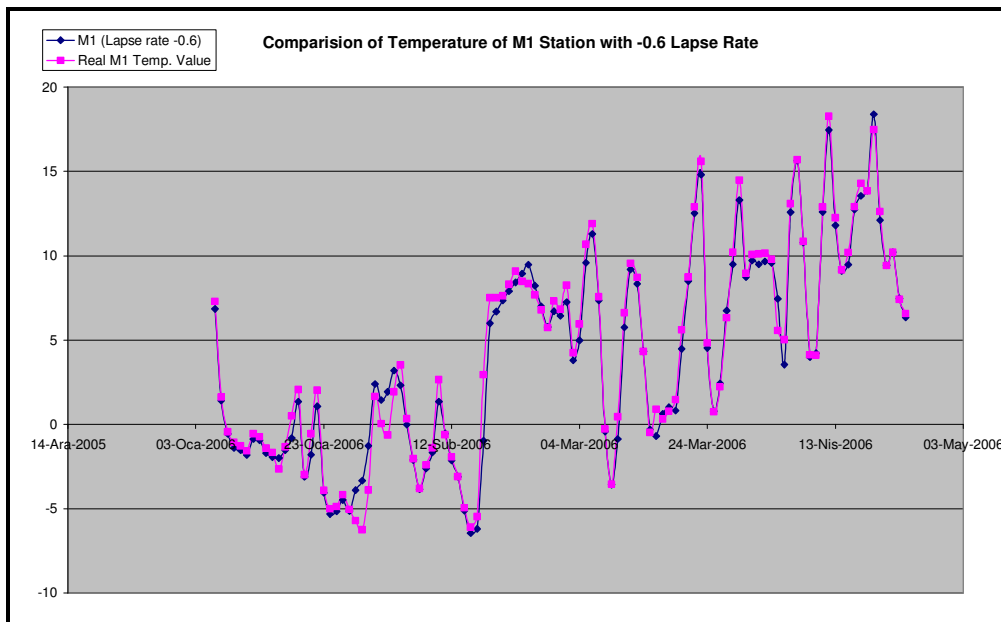
Figure D.4 : Comparison of the real air and lapse rate modified temperature for M1

162
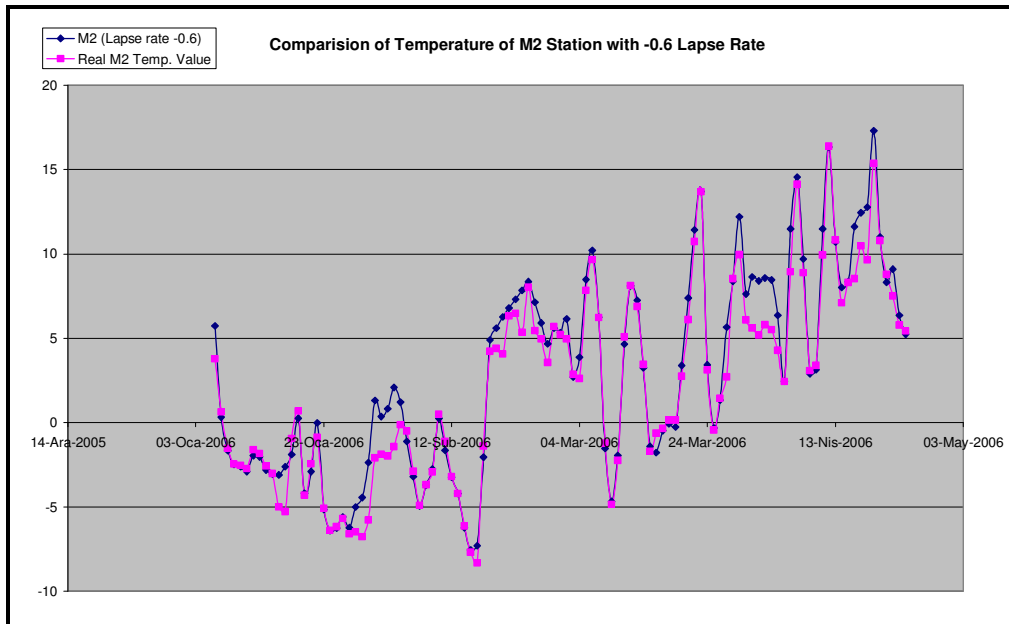
Figure D.5 : Comparison of the real air and lapse rate modified temperature for M2
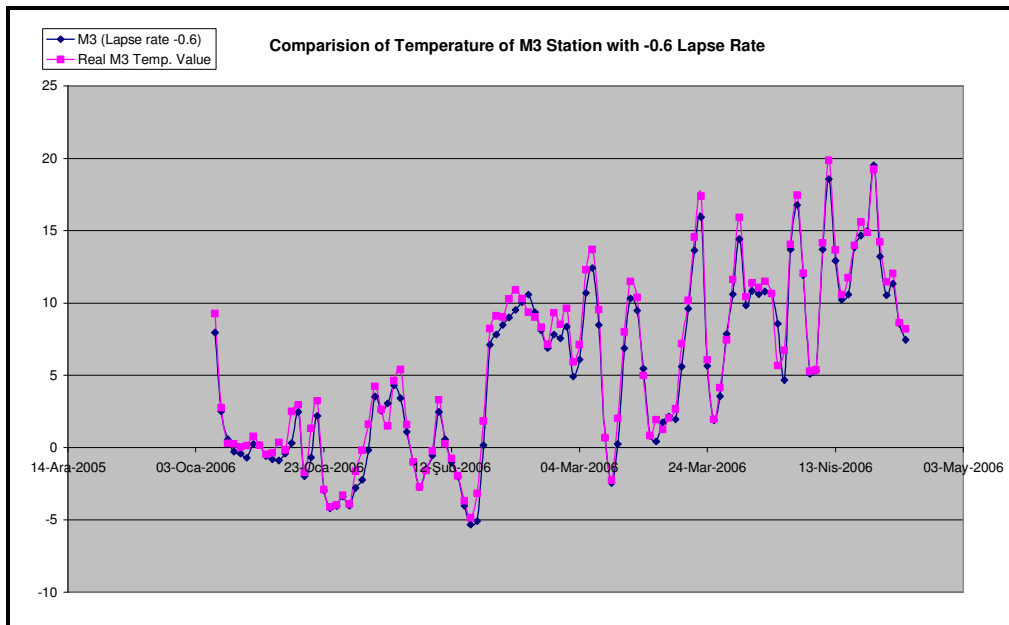

Figure D.6 : Comparison of the real air and lapse rate modified temperature for M3